

LIBRARY OF  
CHARLES A. PARKER

NOAA Technical Memorandum OMPA-3



---

A GEOCHEMICAL AND SEDIMENTOLOGICAL  
STUDY OF THE DREDGED MATERIAL DEPOSIT  
IN THE NEW YORK BIGHT

R. Dayal  
M.G. Heaton  
M. Fuhrmann  
I. W. Duedall

Boulder, Colorado  
February 1981

---

**noaa**

NATIONAL OCEANIC AND  
ATMOSPHERIC ADMINISTRATION

Office of Marine  
Pollution Assessment

Final Report

Submitted to  
Marine Ecosystems Analysis (MESA)  
National Oceanic and Atmospheric Administration  
Stony Brook, New York 11794

DISCLAIMER

The National Oceanic and Atmospheric Administration (NOAA) does not approve, recommend, or endorse any proprietary product or proprietary material mentioned in this publication. No reference shall be made to NOAA or to this publication furnished by NOAA in any advertising or sales promotion which would indicate or imply that NOAA approves, recommends, or endorses any proprietary product or proprietary material mentioned herein, or which has as its purpose an intent to cause directly or indirectly the advertised product to be used or purchased because of this publication.

## CONTENTS

	<u>Page</u>
Abstract .....	xi
1. INTRODUCTION.....	1
2. SAMPLING AND METHODOLOGY.....	4
2.1 Field Sampling.....	4
<u>2.1.1 Vibracoring Cruise.....</u>	4
<u>2.1.2 Interstitial Water Chemistry Cruise.....</u>	7
2.2 Methodology.....	9
<u>2.2.1 Core Processing.....</u>	9
<u>2.2.2 Water Content and Bulk Density.....</u>	11
<u>2.2.3 Combustible Organic Matter.....</u>	12
<u>2.2.4 Total Metal Analysis.....</u>	12
<u>2.2.5 Interstitial Metal Analysis.....</u>	16
<u>2.2.6 Sedimentological Analyses.....</u>	18
3. DREDGED MATERIAL INPUTS TO THE BIGHT.....	22
3.1 Source Areas.....	22
3.2 Volume and Mass Estimates.....	22
3.3 Dredged Material Characteristics.....	27
3.4 Metal Inputs.....	28
4. DEPOSITIONAL RECORD.....	28
4.1 Bathymetry.....	31
<u>4.1.1 1936 Survey.....</u>	31
<u>4.1.2 1973 Survey.....</u>	33
<u>4.1.3 1978 Survey.....</u>	33
<u>4.1.4 Cross-sectional Profiles.....</u>	34
<u>4.1.5 Net Bathymetric Changes.....</u>	34
<u>4.1.6 Sedimentation Rates.....</u>	36
<u>4.1.7 Volume and Mass Estimates.....</u>	38

	<u>Page</u>
4.2 Description of Sediment Types.....	39
<u>4.2.1 Black Mud.....</u>	42
<u>4.2.2 Clay Types.....</u>	47
<u>4.2.3 Greensand.....</u>	50
<u>4.2.4 Coarse Sands.....</u>	54
<u>4.2.5 Artifact Material.....</u>	60
4.3 Gravel/Sand/Mud Depth Profiles.....	61
4.4 Overall Stratigraphy.....	70
4.5 Sedimentary Processes.....	72
<u>4.5.1 Large-Scale Sediment Differentiation.....</u>	73
<u>4.5.2 Sand Incursion.....</u>	90
4.6 Geochemical Depositional Record.....	94
<u>4.6.1 Depth Distributions of Metals and Organic           Matter.....</u>	94
<u>4.6.2 Intracore Variability in Metal Concentrations.....</u>	111
<u>4.6.3 Metal Enrichments in Coastal Deposits.....</u>	114
<u>4.6.4 Geochemical Correlations.....</u>	116
<u>4.6.5 Depositional Record of Metal Inputs.....</u>	128
<u>4.6.6 Interstitial Water Chemistry.....</u>	133
<u>4.6.7 Stratigraphy.....</u>	146
5. MASS BALANCE OF DREDGED MATERIAL AND ASSOCIATED METALS....	155
5.1 Dredged Material.....	155
5.2 Trace Metals.....	157
6. GEOCHEMICAL CONSEQUENCES OF DREDGED MATERIAL DUMPING.....	161
7. CONCLUSIONS.....	162
8. ACKNOWLEDGEMENTS.....	165
9. REFERENCES.....	166
Appendix A. WATER CONTENT, BULK DENSITY, AND BULK POROSITY PROFILES.....	172

LIST OF TABLES

<u>Table No.</u>		<u>Page</u>
1	Schedule and location of vibracores collected at the Dredged Material Dumpsite, New York Bight.....	6
2	Schedule and location of gravity cores for use in the sampling of interstitial water.....	10
3	Summary of atomic absorption methods for bulk and interstitial metal analyses.....	15
4	Precision of bulk metal analyses using atomic absorption.....	17
5	Precision of interstitial water analyses using atomic absorption.....	19
6	Estimates of amounts of material dredged and dumped at the mud dumpsite during the period 1936-78.....	26
7	Average metal concentrations in dredged material sediments based on published data.....	29
8	Estimates of metal inputs from sources areas, via dredged material dumping, to the mud dumpsite.....	30
9	Rates of dredged material accumulation at the dumpsite.....	37
10	Estimates of amounts of accumulated material in the deposit during the period 1936-78.....	40
11	An overview of the major sediment types observed in the dredged material deposit.....	41
12	Mean composition, standard deviation, coefficient of variation, and the compositional range for the sediment cores collected in the New York Bight.....	74
13	Range of metal concentrations and organic matter in sediment cores from the dredged material deposit.....	100
14	Average concentrations of metals and organic matter and their enrichments in dredged material deposit..	103

<u>Table No.</u>		<u>Page</u>
15	Mean, standard deviation and range of concentrations (calculated on a gravel free basis) for dredged material and natural sediment in the cores collected at the dumpsite, New York Bight.....	112
16	Metal enrichments in coastal sediment deposits.....	115
17	Interelement correlation coefficients in dredged material deposit sediments.....	117
18	Correlation coefficients between metals and organic matter and mud content in dredged material deposit sediments.....	118
19	Anthropogenic inputs of metals and organic matter associated with dredged materials dumped in New York Bight during the periods 1936-73 and 1973-78..	129
20	Interstitial concentrations of iron, manganese, and zinc in cores 4I, 6I, 8I, and 9I.....	132
21	Estimates of the diagenetic flux of dissolved Fe, Mn, and Zn in dredged material sediments, New York Bight.....	143
22	Estimates of dredged material dumped during the period 1936-78 and material present in the deposit.	156
23	Average metal concentrations of dredged material derived from the source areas and from the deposit.	158
24	Comparison of mass and rates of metal inputs associated with dredged material dumping during 1973-78 with the metal inputs based on the depositional record.....	159

## LIST OF FIGURES

<u>Figure No.</u>		<u>Page</u>
1	Map of the New York Bight showing the various dumpsites.....	3
2	The general study area of the dumpsite, showing the two sampling transects I and II and the vibracoring stations.....	5
3	The photographs show the vibracorer being deployed: (a) vibratory head attached to the core barrel; and (b) a core being brought on board vessel.....	8
4	Dredging areas and dredged material dumpsite.....	23
5	The annual volumes of material dumped at the mud dumpsite for the period 1930-1978 based on reported federal dredging projects. Private dredging estimates are not involved.....	24
6	Bathymetric surveys of the study area: (a) 1936 survey; (b) 1973 survey; and (c) 1978 survey.....	32
7	Cross-sectional profiles of the deposit, based on the 1936, 1973, and 1978 surveys, along the transects A, B, and C as shown in Figure 2.....	35
8	Ternary plot showing the relative percentages of gravel, sand, and mud contents of all core samples analyzed.....	43
9	Color photograph showing sections of core 3.....	44
10	Gravel fraction of black mud in dredged material sediments: (a) shell fragments in core 6 at 650 cm depth; (b) coal in core 7 at 10 cm depth; and (c) iron flakes in core 9 at 15 cm depth.....	46
11	Color photograph showing a massive bed of gray clay in sections OA, AB, and BC of core 1.....	49
12	A section of the gray clay bed in core 1, containing a sand ball.....	51
13	A peel section of core 10 showing the burrowed texture observed in the greensand bed.....	52

<u>Figure No.</u>		<u>Page</u>
14	Color photograph showing a greensand bed in section FG of core 4.....	53
15	Color photograph showing black mud at the surface overlying white, gravelly sand in core 7.....	56
16	Gravel fraction of four sandy sediment types from cores 4, 7, and 10: (a) core 7 at 70 cm depth; (b) core 4 at 510 cm depth; (c) core 10 at 240 cm depth; and (d) echinoderm assemblage observed in the white sand present in core 4 at 330 cm depth...	57
17	Color photograph showing dredged material at top of section OA of core 10 underlain by fine grained white sand.....	58
18	Color photograph showing sections CD, DE, and EF represent 3 meters of natural sandy sediment observed below the dredged material/natural sediment boundary in core 4.....	59
19	Artifact material observed in core 9.....	62
20	Artifact material found in the dredged spoils at the dumpsite: (a) in core 9 at 5 cm depth; (b) in core 3 at 620 cm depth; (c) in core 9 at 460 cm depth; and (d) in core 2 at 270 cm depth.....	20
21	Artifact material observed in the dredged spoil sediment: (a) the fragmented, fossilized remains of a crab; (b) industrially shaped mica flakes.....	64
22	Depth distribution profiles of gravel, sand, and mud in cores 1, 2, 3, 4, 5.....	65
23	Depth distribution profiles of gravel, sand, and mud in cores 6, 7, 8, 9, and 10.....	66
24	Cross-sectional profile of the study area along the two transects I and II, illustrating the lithology of the deposit.....	71
25	Statistical variations about the mean value of gravel and mud fractions in each core, based on 95% confidence intervals.....	76

<u>Figure No.</u>		<u>Page</u>
26	Color photograph showing distinct textural features in sections OA, AB, and BC of core 6: (A) varved red clay; (B) clay galls; (C) massive bedding; (D) graded bedding; and (E) laminated bedding.....	78
27	Contact prints of x-radiographs of the top six meters of core 6.....	79
28	Histograms showing the frequency of occurrence of beds of various thicknesses in cores 2, 3, and 6 within the dredged material deposit: (a) frequency of occurrence of beds varying in thickness from 0-5 to 25-30 cm; and (b) a breakdown of the first three intervals given in (a) into bed thicknesses varying from 0-1 to 14-15 cm.....	82
29	Plots of mean grain size versus standard deviation for dredged material deposit sediments: (a) for all samples analyzed; (b) for samples from core 10; (c) for samples from core 4; and (d) for samples from core 6.....	84
30	Two sections of core 6, showing the laminated sediment structure.....	86
31	Prints of x-radiographs of the lower sections of core 6.....	87
32	Prints of x-radiographs of the upper sections of core 4.....	88
33	Prints of x-radiographs of the lower sections of core 4.....	89
34	Typical interlayered sand and mud texture observed in dredged material in core 9.....	91
35	Sections EF and FG of core 6.....	92
36	Depth distribution profiles of metals and organic matter: (a) core 1; (b) core 2.....	95
37	Depth distribution profiles of metals and organic matter: (a) core 3; (b) core 4.....	96
38	Depth distribution profiles of metals and organic matter: (a) core 5; (b) core 6.....	97

<u>Figure No.</u>		<u>Page</u>
39	Depth distribution profiles of metals and organic matter: (a) core 7; (b) core 8.....	98
40	Depth distribution profiles of metals and organic matter: (a) core 9; (b) core 10.....	99
41	Total iron-trace metals correlation plots.....	120
42	Total manganese-trace metals correlation plots.....	121
43	Interelement correlation plots.....	122
44	Interelement correlation plots.....	123
45	Organic matter (LOI) metals correlation plots....	124
46	Mud-metals correlation plots.....	125
47	Depth distributions of interstitial iron, manganese, and zinc in dredged material deposit cores: (a) core 4I (b) core 6I; (c) core 8I; and core 9I.....	134
48	Cross-sectional profile of the deposit along the northwest-southeast transects showing the textural stratigraphy.....	147
49	Cross-sectional profile of the deposit along the northwest-southeast transects showing the metal stratigraphy.....	148

## ABSTRACT

Geochemical and sedimentological investigations of the dredged material deposit reveal that the sediments are composed of a wide variety of sediment types which can be classified as quartz and glauconitic sands, muds, sandy muds, gravel intermixed with muds, and artifact material such as coal and fly ash, wood, slag, metal flakes, glass, etc. Fine grained, black sandy mud is characteristic of dredged material. Glauconitic sand and gravelly quartzose sand are typical of the natural sediment underlying the deposit and in surrounding areas.

The spatial distributions of heavy metals such as Pb, Cu, Ag, Hg, Cd, Fe, and Mn in the dredged material deposit exhibit highly variable and considerably elevated concentrations over those observed in sediment outside the deposit and in underlying natural sediment. Compared to metal enrichments reported for other coastal deposits, the enrichments observed in dredged material sediments are orders of magnitude greater. The calculated rates and magnitudes of sediment and metal inputs to the New York Bight, via dredged material dumping, are found to be orders of magnitude higher than those reported for other naturally deposited coastal sediments.

A mass balance of total inputs to the dumpsite via dredged material dumping with inputs estimated from the depositional record for the period 1973-78 indicates that, although most of the dumped material is present in the deposit, most metals are lost from the system in varying degrees either during the dumping process or following deposition of the dumped material.

Pore water data indicate a sediment derived flux of dissolved Fe, Mn, and Zn to the overlying water column. Other metals, such as Cd and Hg, were present at undetectably low concentrations in pore waters, indicating that their benthic flux is very small or practically negligible.

Sedimentological data indicate that large scale differentiation of sediment takes place at the dumpsite. Laminated sediments and discrete beds of variable thickness are typical of the central part of the deposit which receives the bulk of direct dumping. In contrast, fine grained sediments, presumably derived from the center of dumping activity, are characteristic of the fringes of the deposit. In addition, sand, derived from surrounding areas, has been brought to the fringes of the deposit as storm entrained sediment and represents as much as 8% of the entire volume of the deposit.

An overall stratigraphy of the deposit, defining the natural sediment basement and the various horizons of anthropogenic materials, has been developed.



## 1. INTRODUCTION

The most prominent sedimentological feature of the New York Bight is the dredged material deposit, centered in the Bight apex approximately 8 km east of the New Jersey coast. The deposit has a peak elevation of 14 meters and covers an area of 36 km<sup>2</sup> (Freeland and Merrill, 1977). The cumulative effect of the continual disposal of dredged material since at least 1900 is this unique topographic feature in the Bight apex. On an annual basis, the dumpsite receives approximately  $4.5 \times 10^6$  m<sup>3</sup> of material dredged principally from the New York Harbor. This amount is three times greater than the annual sediment load carried by the Hudson River to the harbor area (Meade, 1972; Panuzio, 1965). The total mass of material contained in the deposit corresponds to approximately 250 times the annual sediment discharge of the Hudson River (Panuzio, 1965). When compared to the total annual load of suspended sediment delivered by rivers to the entire east coast of the United States (Meade, 1972), the dredged material deposit has a mass that is ten times greater.

To further evaluate the magnitude of dredged material dumping, in terms of sediment and metal inputs, it is essential to compare the dredged material input with natural sediment accumulation in a coastal area. The deposition of dredged material essentially represents an accelerated sedimentation process, in terms of mass and time, similar to episodic sedimentation periodically interrupted by some accumulation of natural sediment. The difference, however, lies in the fact that

deposition of dredged material is highly localized in time and space whereas episodic deposition, such that occurs under flood conditions, involves accumulation of homogeneously dispersed material over a large area in a relatively longer period of time.

The sediments discharged at the mud dumpsite have been primarily dredged from the Hudson River, particularly from around the dockage areas and from the channels of the inner Harbor, with smaller volumes taken from the Newark Bay and Raritan River areas (Conner *et al.*, 1979). In addition, other types of material have been dumped in the Bight apex and their dumpsites are shown in Figure 1. Much of the sediment in the harbor areas has been contaminated with toxic metals and hydrocarbons, frequently as a result of raw sewage disposal and wastewater discharges into these waters (Gross, 1970; Mueller *et al.*, 1976; Conner *et al.*, 1979). Therefore, associated with dredged material dumping is the injection of toxic metals into the New York Bight at rates proportional to the frequency of the dump events and the mass and metal loading of the disposed material.

In terms of time and space, the disposal of dredged material in the New York Bight represents perhaps the largest and most concentrated anthropogenic inputs of toxic metals to a coastal environment. The resultant dredged material deposit represents a sedimentary record of the dumping activities for the last 100 years or so with respect to rates and magnitudes of dumped material and the associated toxic metals.

The primary objectives of our investigation were: (1) to identify the metal contaminants and their spatial distributions in the dredged

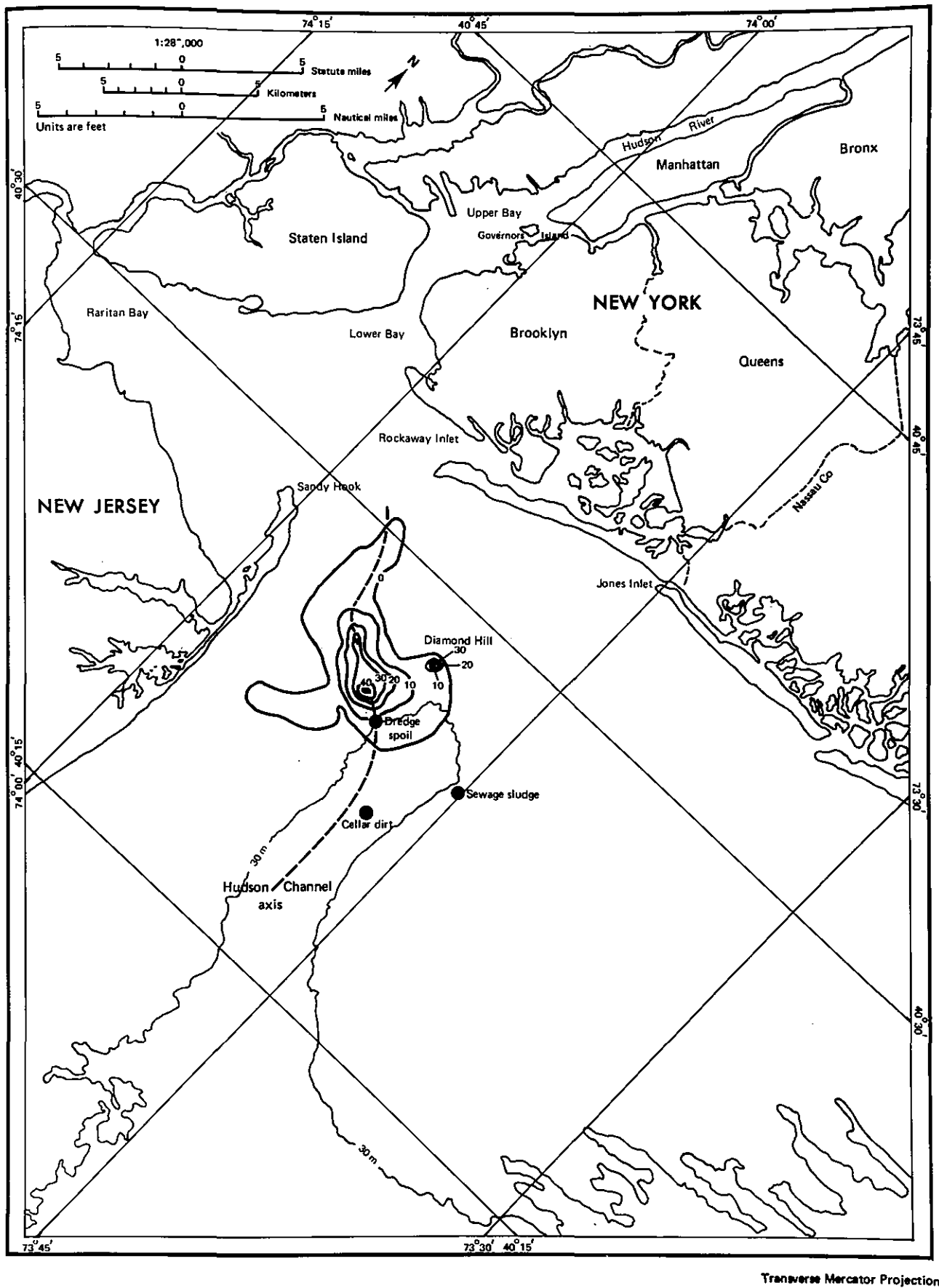


Figure 1. Map of the New York Bight showing the various dumpsites (after Gross, 1976).

material deposit; (2) to determine the volume and mass of material deposited in the pile; (3) to develop a stratigraphic record of the deposit, defining the natural sediment basement; (4) to estimate the sediment and metal inputs to the Bight based on bathymetric changes and metal profiles observed in the deposit; (5) to define the lithology of the cores, describing the sediment types and the sedimentary structures observed in the deposit; (6) to determine the sedimentary processes that account for the observed distribution of the sediment types in the deposit; and (7) to evaluate the diagenetic remobilization of toxic metals in the deposit and their subsequent release to the overlying water column.

## 2. SAMPLING AND METHODOLOGY

### 2.1 Field Sampling

#### 2.1.1 Vibracoring Cruise

Ten vibracores, varying in length from 3.0 to 8.4 m were collected at the study site at stations located on two transects intersecting at the apex of the dredged material dumpsite (Figure 2). Information on the vibracores collected in the study area is summarized in Table 1. The coring was contracted to Ocean Seismic Survey, Inc. of Norwood, New Jersey. Coring was performed during three days, May 30 to June 1, 1978, aboard the R/V ATLANTIC TWIN. Each station was fixed by navigation with a Motorola Mini-ranger unit.

The vibracorer consists of a steel pipe with plastic liner (9 cm i.d.) which is essentially hammered into the sediment by a pile driver

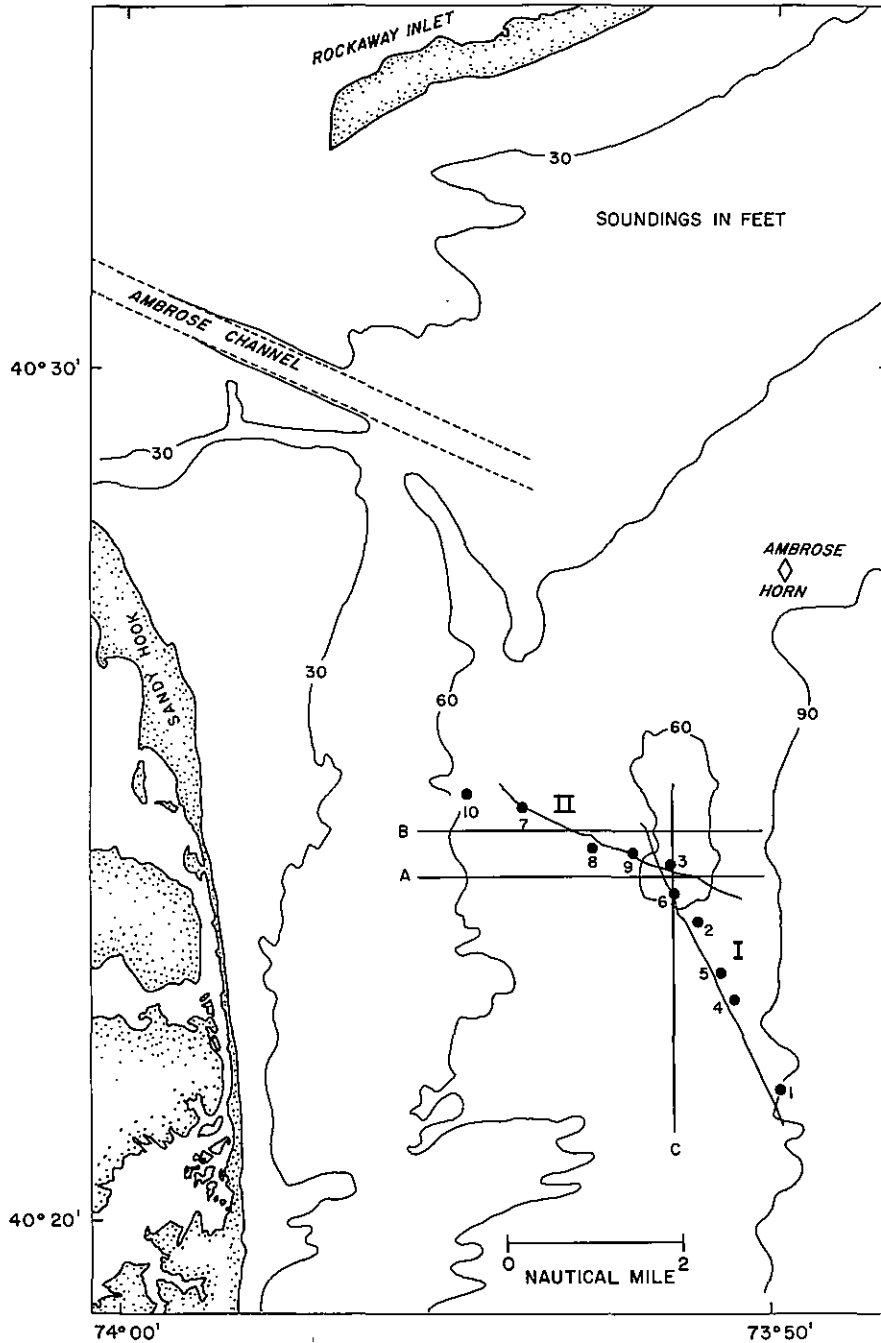


Figure 2. The general study area of the dumpsite, showing the two sampling transects I and II and the vibracoring stations as indicated by black circles. Cross-sectional profiles of the deposit along the transects A, B and C are given in Figure 7.

Table 1. Schedule and location of vibracores collected at the Dredged Material Dumpsite, New York Bight.<sup>1</sup>

Station No.	Date Collected	Water Depth (m)	Length of Core (m)	Latitude <sup>2</sup>	Longitude <sup>2</sup>
1	5/31/78	28.0	5.7	40°21.50'N	73°50.30'W
2	5/31/78	17.4	6.6	23.58'	51.45'
3	5/30/78	16.8	7.9	24.25'	51.80
4	5/31/78	26.5	7.6	22.58'	50.95'
5	5/31/78	22.3	5.4	22.98'	51.13'
6	5/30/78	15.9	8.4	23.95'	51.75'
7	6/01/78	23.8	3.0	24.97'	54.00'
8	6/01/78	24.1	4.6	24.47'	52.97'
9	6/01/78	21.0	6.1	24.40'	52.39'
10	6/01/78	20.7	3.2	25.18'	54.83'

<sup>1</sup>The cores were collected from the R/V ATLANTIC TWIN operated by Ocean Seismic Survey, New Jersey.

<sup>2</sup>Provided by Motorola Mini-Ranger<sup>R</sup> with Loran C backup.

located on top of the core assembly. The corer is supported on the sediment surface by a pyramid-shaped metal framework through the center of which was mounted an I-beam along which slid the core barrel (Figure 3). Affixed to the top of the barrel was the pneumatically powered vibratory head. The cored material was retained in a four inch plastic core liner. During the coring operation penetrometer records were obtained. This mechanism consisted of a chain driven potentiometer which read out on a recorder on deck. Each foot of penetration was displayed as a single line crossing the tape. Penetration was read off in feet per second.

On occasion short cores were recovered on the first attempt. In these cases a new core liner was fitted to the barrel. But instead of repeating the entire length of the corer, water was pumped down the barrel "jetting" through the sediment to the level where previous recovery had stopped. The water jet was then stopped and pneumatic coring resumed.

After the corer was brought on board and the liner was withdrawn from the barrel the two ends were immediately capped. The liner and cored material were cut into one meter sections, capped, labeled, and stored in a vertical position. After this cruise the meter lengths were returned to MSRC and refrigerated prior to further subsectioning.

#### 2.1.2 Interstitial Water Chemistry Cruise

Gravity cores for sampling of interstitial waters were taken as close as possible to the original vibracoring stations. Four gravity

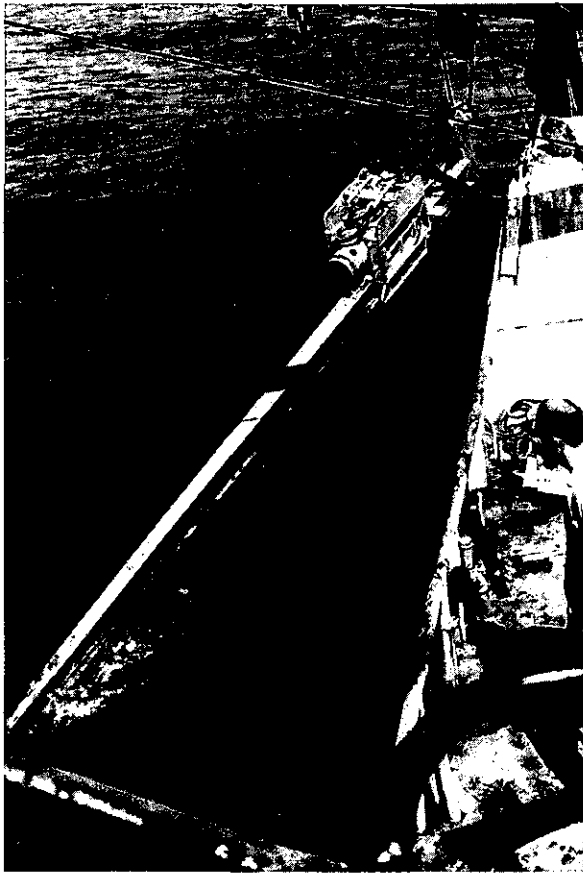


*Figure 3. The photographs show the vibracorer being deployed: (a) vibratory head attached to the core barrel; and (b) a core being brought on board vessel.*

cores were collected during a four day cruise, 26-29 March 1979, aboard the NOAA R/V KELEZ. Navigation was provided by Raydist while Loran C was used to locate the original stations. Station locations, water depths, and core lengths are listed in Table 2.

Interstitial water was extracted from the sediment samples on board the research vessel. Immediately following retrieval, the core in its plastic liner (6.7 cm i.d.) was placed in a nitrogen-filled glove bag in a controlled temperature room. Sediment sections were extruded and loaded into Reeburgh-type sediment squeezers (Reeburgh, 1967). Nitrogen gas, gradually elevated to 120 psi, was used to pressurize the squeezers and force the interstitial water through a 0.45  $\mu\text{m}$  Nucleopore membrane filter. All samples and apparatus remained in the glove bag under nitrogen until most of the interstitial water was removed (Troup *et al.*, 1974; Bray *et al.*, 1973). Squeezing temperatures were maintained within  $\pm 3.5^\circ\text{C}$  of *in situ* bottom temperatures which ranged between  $4.5^\circ$  and  $6.0^\circ\text{C}$ . Seven to ten interstitial water samples were collected from each of four cores retrieved at stations 4, 6, 8, and 9 (Table 2). Samples were preserved by acidification with high purity Ultrex<sup>R</sup> nitric acid and refrigerated until analyzed.

## 2.2 Methodology

### 2.2.1 Core Processing

In the laboratory, the vibracores were bisected longitudinally with a circular saw which had been adjusted to allow the tungsten carbide blade to cut only the plastic core liner. The sediment itself

Table 2. Schedule and location of gravity cores for use in the sampling of interstitial water.<sup>1</sup>

Station No. <sup>2</sup>	Date Collected	Water Depth (m)	Length of Core (cm)	Latitude	Longitude
4I	3/27/79	25.0	40	40°22.55'N	73°50.90'W
6I	3/28/79	15.1	54	23.98'	51.75'
8I	3/27/79	24.6	78	24.65'	52.90'
9I	3/29/79	21.2	36	24.40'	52.35'

<sup>1</sup>The cores were collected from the R/V G.B. KELEZ.

<sup>2</sup>The gravity cores were taken at stations 4, 6, 8, 9. At these stations, vibracores were also collected from the R/V ATLANTIC TWIN as described in Table 1.

was separated into the two longitudinal sections with a plastic spatula. The two halves provided identical samples for detailed geochemical and sedimentological analyses. The cores were immediately photographed and color-coded and general sediment types were described.

### 2.2.2 Water Content and Bulk Density

For determination of bulk density and percent water the wet sediment section was placed in a pre-weighed, acid washed beaker and compressed so that air pockets were removed. A 30 ml syringe (with the tip removed, forming a cylinder) was pressed into the sediment until full to the 30 ml mark. After checking to see that no voids were present, the sample was extruded into another pre-weighed beaker and the mass of wet sediment immediately determined. Bulk density was then calculated by dividing the mass of wet sediment by its bulk volume.

The entire sample was then weighed and heated at 85°C to constant mass. The water content was calculated from the dry and wet masses of the sample as percent water.

Porosity, the fraction of the sediment volume occupied by water, was calculated from the relation (Berner, 1971)

$$\phi = \frac{Wd_s}{Wd_s + (1-W)d_w} \quad (1)$$

where

$W$  = weight percent water (net weight/100)

$d_s$  = average density of sediment particles (2.7 g/cm<sup>3</sup>)

$d_w$  = density of interstitial water (1.03 g/cm<sup>3</sup>).

Bulk density precision analysis was performed in replicate on four samples of different sediment types. Coefficients of variation ranged from 0.3 to 1.7% with no apparent relationship to grain size.

### 2.2.3 Combustible Organic Matter

Subsamples of the dried and finely ground sediments used for total metal analyses were weighed and combusted at 550°C for five hours, allowed to cool in a dessicator to room temperature and reweighed. Percent weight loss on ignition (LOI) was calculated and is reported as percent combustible organic matter. This analysis is easily performed and has been found to correlate well with total carbon by dry combustion in CO<sub>2</sub> - free oxygen at 1500°C followed by gasometric analysis of the evolved CO<sub>2</sub> (Gross, 1970). To obtain an estimate of total carbon, the LOI value is divided by a factor of 1.8 to 1.9 (Jackson, 1958). High clay content in sediment may cause a positive error in the analysis due to water trapped in the clay lattice during drying and released during combustion (Gross, 1971).

Determination of precision for this measurement was performed on replicate subsamples used for total metal precision determinations described later. Each subsample was combusted and the results compared. Coefficients of variation were found to be in the range of 0.3 to 5%.

### 2.2.4 Total Metal Analysis

Sample Preparation. Sediment samples for geochemical analyses were carefully removed with a plastic spatula from the center of the

core to avoid potentially contaminated material which may have come in contact with the saw blade. These samples, generally taken at 10 cm intervals, were double sealed in plastic bags and refrigerated prior to analysis. Actual geochemical analysis was performed at 30 cm intervals with greater detail in many instances.

Dried sediment samples were sieved through 2 mm nitex screen to remove the > 2 mm gravel fraction. The gravel-free fraction was ground to an approximately uniform grain size in an alumina-ceramic container. The ground sample was carefully homogenized and subsampled for analysis.

Sediment Digestion. Ten mL each of concentrated reagent grade HCl and HNO<sub>3</sub> were slowly added to a 3 to 10 g sediment sample contained in a Bel-Art<sup>R</sup> polyethylene bottle. The loosely capped bottle was placed on an 85°C (± 3°C) sand bath in a fume hood for about four hours. The digest was then vacuum filtered, while still hot through an acid-washed Gelman Type A glass fiber filter into a 50 mL volumetric flask. The bottle and filter were rinsed with small quantities of HCl and deionized distilled water which, after passing through the filter, were added to the volumetric flask. The digest solution and rinses were then brought to volume with deionized distilled water. The solutions were transferred to polyethylene bottles and placed in a refrigerator for storage prior to analysis.

This method has been found to be superior to the H<sub>2</sub>SO<sub>4</sub> - HCl method, specifically for Pb, where precipitation of PbSO<sub>4</sub> causes loss of Pb during filtration (Anderson, 1974). The HNO<sub>3</sub> - HCl and HNO<sub>3</sub> methods have been questioned for determination of Hg in soils (Ure and Shand, 1974) and

other materials (Reimers *et al.*, 1973) due to the volatility of Hg. However, Hoover *et al.* (1971) found recoveries using a similar method to be 95 to 102% in Hg spiked samples. It was determined that the HNO<sub>3</sub> - HCl method was preferred and that the number of samples precluded using a separate digestion for Hg alone.

Leachate Metal Analysis. The acid digests were analyzed for Fe, Mn, Pb, Cu, Cd, and Ag by direct aspiration of the sample into the air/acetylene flame of a Perkin-Elmer Model 403 atomic absorption spectrophotometer (AAS). Samples found to be outside the linear range were diluted. Standards were serial dilutions of Fisher Scientific atomic absorption standards.

Hg determinations were performed by the cold vapor technique using the Perkin-Elmer MHS-10 Mercury/Hydride System attached to the Perkin-Elmer Model 403 AAS. In this procedure (Perkin-Elmer Corp., 1978) Hg<sup>2+</sup> present in the acid sample solution is reduced to atomic Hg<sup>0</sup> by a 1% NaOH/3% NaBH<sub>4</sub> reductant solution and flushed out of the reaction vessel with nitrogen gas. The vapor passes through a quartz tube through which the spectrophotometer beam is focused. Absorption recorded is proportional to the quantity of total Hg in the sample. Standards were serial dilutions of Fisher Scientific atomic absorption standards preserved with 1.5% Ultrex<sup>R</sup> HNO<sub>3</sub> and a few drops of 5% KMnO<sub>4</sub>. Standards and reductant solution were prepared daily. The reader is referred to Table 3 for a summary of transition metal analyses.

Precision of the total metal analysis was determined by homogenizing the dried < 2 mm sediment fraction and analyzing four subsamples of

Table 3. Summary of atomic absorption methods for bulk and interstitial metal analyses.

Metal	Wave Length (nm)	Method
Total Fe	248.3	Flame AAS <sup>1</sup>
Total Mn	279.5	Flame AAS
Total Pb	283.3	Flame AAS
Total Cu	324.7	Flame AAS
Total Cd	228.8	Flame AAS
Total Pb	329.1	Flame AAS
Total Hg	253.6	Cold Vapor AAS
Interstitial Fe	248.3	Flame AAS
Interstitial Mn	279.5	Flame AAS
Interstitial Cd	228.8	Flameless AAS
Interstitial Hg	253.6	Cold Vapor AAS

<sup>1</sup>Atomic absorption spectroscopy.

the same core section. This was repeated for four separate core sections with differing grain size characteristics. The subsamples were ground, digested and analyzed and the resulting concentrations compared statistically. Precision of this analysis was generally better than 4% (Table 4). Greater error was observed for Cu and Pb in one sample (core 3, 620-630 cm) which contained what appeared to be flakes of oxidized metal.

#### 2.2.5 Interstitial Metal Analysis

Analysis of interstitial waters for Fe and Mn was accomplished by direct aspiration of the sample into the air/acetylene flame of a Perkin-Elmer Model 403 atomic absorption spectrophotometer with a background corrector. Some samples required dilution.

Since Zn concentrations varied over a wide range, the samples were analyzed by both flame and flameless techniques on the Perkin-Elmer Model 5000 spectrophotometer. Samples containing Zn concentrations greater than about 12 ppb were analyzed using the air/acetylene flame with scale expansion and background correction. Samples containing less than about 12 ppb Zn were analyzed by the method of additions using the HGA 500 attached to the Model 5000 spectrophotometer with background correction.

Analysis for Cd and Cu were performed by flameless techniques with the HGA 500 attached to the model 5000 spectrophotometer with background correction. Since concentrations of both these metals were in the low ppb range, interferences were strong in the seawater matrix and error in the analyses were large despite the use of the method of additions.

Table 4. Precision of bulk metal analyses using atomic absorption.

Metal	Sample No. <sup>1</sup>	Mean Concentration	Coefficient of Variation (%) <sup>2</sup>
Fe	3-620	4.1%	0.7
	4-230	2.2	3.9
	9-520	3.2	2.5
	9-450	3.7	0.5
Mn	3-620	381 ppm	1.9
	4-230	135	0.5
	9-520	545	0.4
	9-450	393	0.7
Pb	3-620	570 ppm	6.9
	4-230	55	0.3
	9-520	9	0.1
	9-450	229	1.7
Cu	3-620	745 ppm	1.7
	4-230	63	1.2
	9-520	17	3.6
	9-450	150	0.8
Cd	3-620	3.8 ppm	1.6
	4-230	1.0	0.3
	9-520	<0.2	-
	9-450	1.2	4.3
Ag	3-620	4.9 ppm	2.0
	4-230	1.2	0.3
	9-520	<0.2	-
	9-450	2.4	3.3
Hg	3-620	3.2 ppm	3.1
	4-230	1.0	0.3
	9-520	<0.2	-
	9-450	4.4	3.1

<sup>1</sup>Four different sediment types were considered for precision determinations.

<sup>2</sup>The precision values are based on four determinations of each sample.

For Hg, the cold vapor method was employed using the MHS-10 unit attached to the Model 403 spectrophotometer with background correction. Potassium permanganate was added to the samples to promote oxidation of dissolved organics.

All standard were dilutions of Fisher Scientific Atomic Absorption Standards. Precision of the analyses is given in Table 5.

### 2.2.6 Sedimentological Analyses

Core Logging. The cut surfaces of the core sections were scraped clean, examined and logged for sediment texture and color. The Munsell Soil Color chart was used as a color reference. Immediately after logging, the cores were color photographed with Kodak Ektachrome II film under sunlight. Kodak Color Control Patches (Kodak Publication 9-13) were included in each photograph to show the veracity of color reproduction in each photograph. Before any sampling was done the cut surfaces of the cored material were again carefully scraped, frequently revealing fine layering and laminations which were obscured in the wet cores. Sections of particular interest were again photographed, in close up, with Kodak Plus-X black and white film.

X-radiography. Two cores, from stations 4 and 6, were x-radiographed at Brookhaven National Laboratory using a Fedrex 300 x-ray unit. The film used was Dupont Cronex NDT 55 with two minute exposure times (150 KVP, 4 amperes). The x-radiographs were photographically reduced to a smaller size and contact printed.

Peel Sections. Peels of certain sections of the cores were made in order to both preserve the form of the material and to develop a

Table 5. Precision of interstitial water analyses using atomic absorption.

Metal	Method	Mean Concentration	Coefficient of Variation (%) <sup>1</sup>
Fe	Flame	1.1 ppm	1.4
		4.2	1.1
Mn	Flame	1.0 ppm	1.0
		2.6	0.8
Zn	Flame	81 ppb	1.7
		20	2.7
		48	1.0
Zn	Flameless	12 ppb	10.7
		7	2.2
		11	3.4

<sup>1</sup>Precision values are based on five determinations of each sample.

three dimensional view of the overall texture within the core sections. The method used was a modification of that outlined by Hezeen and Johnson (*in* Bouma, 1969). Elmer's Glue-all was spread over the section to be preserved to a thickness of about one-eighth of an inch. This was allowed to soak in for two to five minutes. When necessary another lighter coating was applied followed by a coarsely woven stiff fabric which was pressed into the glue. A third coating was spread onto the top of the fabric. After drying for at least 48 hours the edges of the cloth were separated from the liner with a razor blade and the peel gently lifted from the core. The peel was then mounted on a strip of plywood, labeled and sprayed four times with laquer in order to adhere loose grains. Black and white photographs were made of the peel sections.

Grain Size Analysis. Samples were taken at each distinct layer of sediment within the cores, as well as at certain small lenses of interest. Each sample was a two centimeter wide section removed from the core. These were labeled, logged, dried and then split with a Soil Test Microsplitter<sup>R</sup> into two samples.

One split of each sample weighing 10 to 20 g was used for grain size analysis. All samples were dried, weighed, and soaked overnight in 50 ml of 2% Calgon solution and then sonified for 10 seconds. Immediately after sonification, the samples were separated into gravel, sand, and mud fractions by wet sieving. The gravel and sand fractions were dried and weighed. The mud fraction was retained for further size analysis. The gravel was further differentiated by sieving through -2 $\phi$  (4 mm) and -1.5 $\phi$  (3 mm) screens.

The sand fraction was subsequently split and analyzed with a Rapid Sediment Analyzer. This device consists of a large settling tube which has two outlets spaced one meter apart. These are connected by tubing to a pressure transducer, which in turn, is coupled to an amplifier/recorder. By measuring the changes of hydrostatic pressure at the sensor outlet as sediment falls through the column and comparing these changes to fall time it is possible to rapidly determine the frequency percent/size distribution for the sand fraction.

The mud fraction was analyzed by the hydrometer method (modified after Royse, 1970) using the *Nanographic Chart for the Solution of Stokes Law* by Soil Test Inc. A computer program was used to plot a cumulative frequency vs. grain size curve on a probability plot, simultaneously calculating Folk's (1974) statistics of mean, skewness, kurtosis, and standard deviation.

Oxidizable Carbon. One split of each sample was used for the determination of oxidizable organic content (Royse, 1970). Samples weighing approximately two grams were placed in weighed flasks. This sediment was digested at room temperature with an excess of 30% hydrogen peroxide. After the initial reaction had diminished the volume was brought to 50 ml. The reaction was allowed to continue for at least 24 hours. The samples were then rinsed with distilled water and set aside to settle. After decanting and oven drying for 24 hours at 85°C, the samples were reweighed. In some cases where the reaction was incomplete H<sub>2</sub>O<sub>2</sub> was again added after the sample had been dried. This particular method was chosen because there is a large body of data for the New York Bight which were obtained by this method (A. Cook, personal communication).

### 3. DREDGED MATERIAL INPUTS TO THE BIGHT

For a quantitative evaluation of the impact of dredged material dumping in the New York Bight, it is essential to have a knowledge of the input parameters. For this purpose, available records of the Corps of Engineers dredged material dumping projects in the New York Bight were examined. Data were compiled on the bulk volume and mass estimates of material dredged from the principal dredging sites, the bulk volume and mass of dredged material dumped annually at the mud dumpsite, and the trace metal composition of the dredged material. These data were used to calculate estimates of inputs by volume and mass of material and the associated metals dumped.

#### 3.1 Source Areas

The sediments discharged at the mud dumpsite have been primarily dredged from the Hudson River Estuary, particularly from around the dockage areas and from the channels of the inner Harbor, with smaller volumes taken from the Newark Bay and Raritan River areas (Conner *et al.*, 1979). The general area contributing dredged material to the mud dumpsite is shown in Figure 4.

#### 3.2 Volume and Mass Estimates

The quantity of dredged material disposed at the mud dumpsite has fluctuated widely in the past. This is shown in Figure 5 which depicts the total volume of dredged material (federal projects) dumped annually at the site. During the period 1941 to 1946 (World War II), the dredged material was dumped in the harbor or in landfills; no dumping took place at the dumpsite. However, just prior to that period and again after it, the volume of disposed material peaked at more than  $6 \times 10^6$  m<sup>3</sup>/yr.

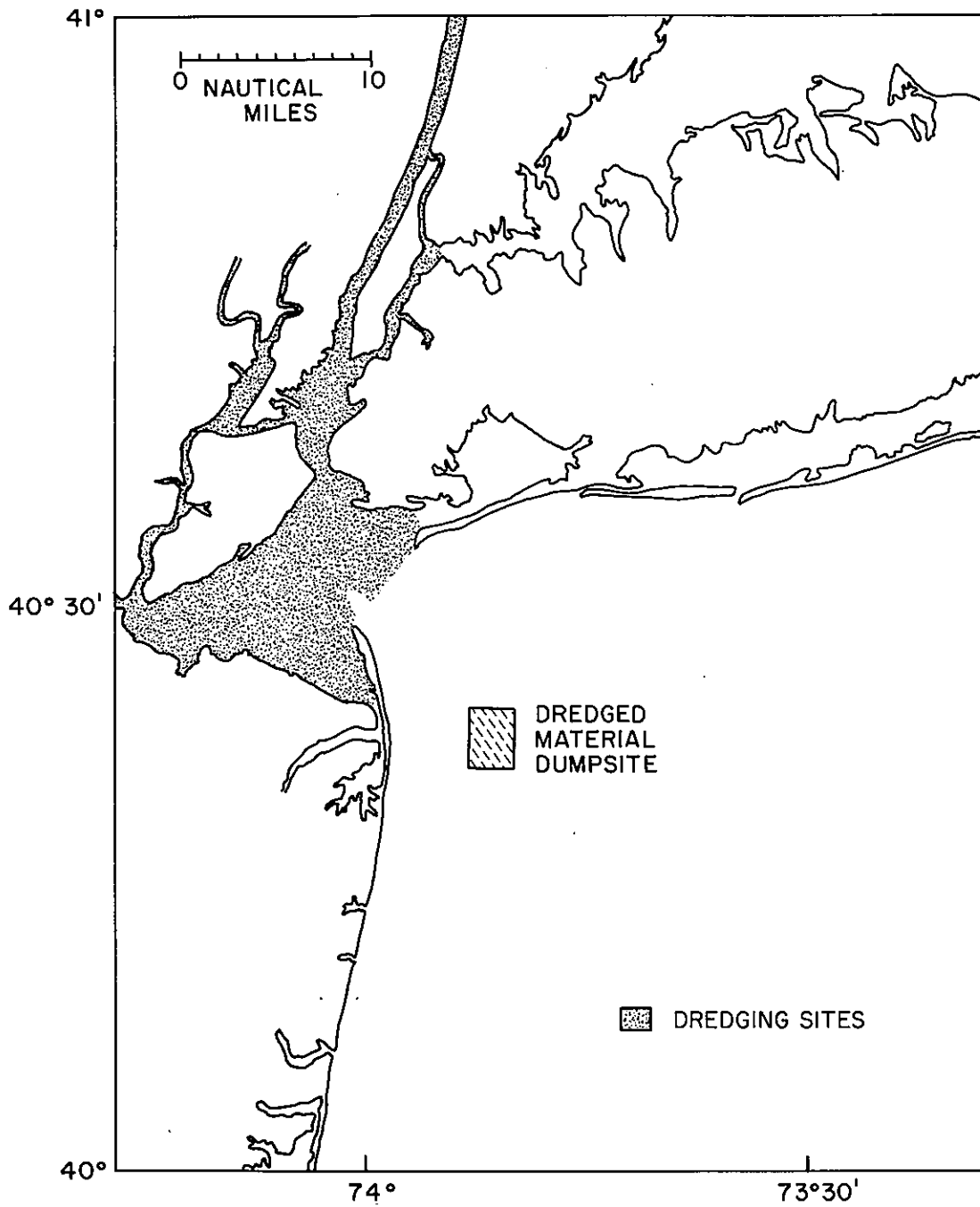


Figure 4. Dredging areas and dredged material dumpsite.



Figure 5. The annual volumes of material dumped at the mud dumpsite for the period 1930-1978 based on reported federal dredging projects. Private dredging estimates are not involved.

The year of the greatest annual discharge was 1973 when over  $9 \times 10^6 \text{ m}^3$  were disposed of at the mud dumpsite. A total volume of  $208 \times 10^6 \text{ m}^3$  of dredged material was dumped at the site during the period 1936-1978. Approximately  $156 \times 10^6 \text{ m}^3$  were dumped between 1936 and 1973 and  $52 \times 10^6 \text{ m}^3$  between 1973 and 1978. These figures correspond to an average annual rate of dumping of  $4.9 \times 10^6 \text{ m}^3/\text{yr}$ .

The figures given above represent the COE estimates based on: (1) estimates of individual barge and hopper loads; and (2) estimates of the volume of sediment removed from specific sites through pre- and post-dredging bathymetric surveys. The data provided by the COE represent only federal dredging projects. Conner *et al.* (1979) provide data for 1970 through 1976 which differentiates between federal and private dredging projects, showing that private projects contribute 24% of the volume dredged. We, therefore, have used the ratio of the volume of federal to private dredging to estimate the total volume of material dumped. Estimates of total bulk volume of dredged material deposited at the dumpsite during the period 1936-78 are given in Table 6. Also included in Table 6 are the average annual rates of dumping during this period.

To obtain estimates of the mass of material dumped, we used an average bulk density value of  $1.2 \text{ g/cm}^3$  based on the range of 1.1 to  $1.3 \text{ g/cm}^3$  reported for New York Harbor sediments and dredged material in the hoppers (Gross, 1970; Mueller *et al.*, 1976). A value of  $270 \times 10^{12} \text{ g}$  was obtained for the total wet mass of material dumped at the site during 1936-78. To calculate the total dry mass of material deposited, the average water content was taken as 50% of the

Table 6. Estimates of amounts of material dredged and dumped at the mud dumpsite during the period 1936-78.

Dumping Period	Total Amount Dumped			Amount Dumped Annually		
	Bulk Volume <sup>1</sup> (10 <sup>6</sup> m <sup>3</sup> )	Bulk Mass <sup>2</sup> (10 <sup>12</sup> g)	Dry Mass <sup>3</sup> (10 <sup>12</sup> g)	Bulk Volume (10 <sup>6</sup> m <sup>3</sup> /yr)	Bulk Mass (10 <sup>12</sup> g/yr)	Dry Mass (10 <sup>12</sup> g/yr)
1973-78 (5 years)	52.0	62.4	31.2	10.4	12.5	6.2
1936-73 (37 years)	156.0	187.2	93.6	4.2	5.1	2.5
1936-78 (42 years)	208.0	249.6	124.8	4.9	5.9	2.9

<sup>1</sup>Estimates based on dredged material dumping records compiled by Conner *et al.* (1979).

<sup>2</sup>Calculated from bulk volume data using a bulk density value of 1.2 gm/cm<sup>3</sup>.

<sup>3</sup>Calculated from bulk mass data using a value of 50% by weight for the average water content of dredged material.

total bulk weight of the harbor or dredged material sediments. This gave a value of  $135 \times 10^{12}$  g for the total dry mass deposited during the same period. These estimates, along with the annual rates of dumping of the mass of dredged material during the period 1936-78, are compiled in Table 6.

### 3.3 Dredged Material Characteristics

Mud is by far the most common material dumped, appropriately, on the mud dumpsite. Actually, much of this material would not strictly be described as mud according to the grain size classifications but is an "eyeball" classification made at the time of dredging. Another is "coarse-grained" material. According to COE dumping records (Conner *et al.*, 1979) for the period of 1970-74, this category consisted of sand, gravel, granular material and blasted rock. During these five years  $\approx 0.52 \times 10^6$  m<sup>3</sup> of coarse grained material were discharged at the site.

Artifact material incorporates the COE classifications of sludge, spent caustic soda, steam ash, concrete, chemical wastes, effluent wastes and iron oxide (Conner *et al.*, 1979). Significant amounts of coal ash were dumped in the New York Bight for many years. According to Gross (1972), an average amount of  $0.1 \times 10^6$  tons were dumped annually during the period 1960-68. In the 1970's, however, the amount dumped was not significant. It should be noted that many of these materials are present in the sediments of the harbor area (Panuzio, 1965; Olsen *et al.*, 1978) and are therefore also present within the category of mud.

### 3.4 Metal Inputs

To estimate the inputs of certain metals associated with the dredged material dumped at the site, average metal concentrations reported for the source area sediments were used. Conner *et al.* (1979) have reported the average concentrations of Cu, Cr, Pb, Ni, Hg, and Cd in dredged material sampled from the dredge hoppers (Table 7). Also included in Table 7 are averaged concentrations of Fe, Mn, and Zn in New York Harbor and Hudson River sediments reported by Williams *et al.* (1978).

Estimates of total metal inputs, through dredged material disposal, to the New York Bight derived from the dredging sites are given in Table 8. The annual rate of metal inputs for the period 1936-78 are also included in Table 8.

## 4. DEPOSITIONAL RECORD

The geochemical and sedimentological characteristics of the dredged material deposit are presented in this section. Estimates of bulk volume and mass of material present in the deposit and rates of material accumulation for the period 1936-78 have been calculated using the 1936, 1973, and 1978 bathymetric surveys. These surveys also provide an insight into the evolution of the deposit over a period of time. Other sections include the spatial distributions of metals and organic matter in the deposit and the enrichments of metals in dredged material relative to the underlying natural sediment. Discussion of the sediment

Table 7. Average metal concentrations in dredged material sediments based on published data.

Metal	Average Concentration (ppm)	Reference
Fe	35000	Williams <i>et al.</i> (1978) <sup>1</sup>
Mn	420	" "
Zn	550	" "
Cu	180	Conner <i>et al.</i> (1979) <sup>2</sup>
Cr	140	" "
Pb	134	" "
Ni	73	" "
Hg	4.5	" "
Cd	3.6	" "

<sup>1</sup>Metals analyzed in sediment sampled from the dredging sites such as New York Harbor and Hudson River.

<sup>2</sup>Metals analyzed in dredged material sampled from the dredge hoppers.

Table 8. Estimates of metal inputs from sources areas, via dredged material dumping, to the mud dumpsite.

Metal	Total Metal Inputs (g)			Annual Metal Inputs (g/yr)		
	1936-78	1936-73	1973-78	1936-78	1936-73	1973-78
Fe	$4.72 \times 10^{12}$	$3.54 \times 10^{12}$	$1.18 \times 10^{12}$	$11.2 \times 10^{10}$	$9.6 \times 10^{10}$	$23.6 \times 10^{10}$
Mn	$5.68 \times 10^{10}$	$4.26 \times 10^{10}$	$1.42 \times 10^{10}$	$13.5 \times 10^8$	$11.5 \times 10^8$	$28.4 \times 10^8$
Cu	$2.44 \times 10^{10}$	$1.83 \times 10^{10}$	$0.61 \times 10^{10}$	$5.8 \times 10^8$	$4.9 \times 10^8$	$12.2 \times 10^8$
Pb	$18.10 \times 10^9$	$13.60 \times 10^9$	$4.50 \times 10^9$	$4.3 \times 10^8$	$3.7 \times 10^8$	$9.0 \times 10^8$
Hg	$6.08 \times 10^8$	$4.56 \times 10^8$	$1.52 \times 10^8$	$14.5 \times 10^6$	$12.3 \times 10^6$	$30.4 \times 10^6$
Cd	$4.87 \times 10^8$	$3.65 \times 10^8$	$1.22 \times 10^8$	$11.6 \times 10^6$	$9.9 \times 10^6$	$24.4 \times 10^6$

<sup>1</sup>Based on inputs of dredged material, estimated from dumping records, and average metal concentrations reported in Table 7.

properties of the deposit includes the spatial distributions of different sediment types present in the deposit, emphasizing the sedimentary structures and processes associated with dredged material dumping. Statistical grain size parameters were evaluated to distinguish between natural sediment and dumped material in the deposit and to further clarify the sedimentary processes occurring at the dumpsite. Based on the sedimentary record, inputs of sediment and metals to the dumpsite have been estimated for the period 1936-78. Pore water chemistry results are presented, with a discussion of the benthic processes that control the transfer of dissolved metals across the sediment/water interface. Fluxes of dissolved Fe, Mn and Zn have been estimated to evaluate the magnitude of the benthic fluxes of these metals. Finally, a stratigraphy of the deposit has been established based on characteristic sedimentological and geochemical features observed in the cores.

#### 4.1 Bathymetry

The most dynamic aspects of the New York Bight dredged material dumpsite are its size and shape. The evolution of the deposit is recorded in the bathymetric charts of the area based on surveys made in 1936, 1973 and 1978 (Figure 6). The 1936 and 1973 charts are after Freeland and Merrill (1977) and the June 1978 survey (Figure 6c) was supplied by Dennis Suszkowski of the Corps of Engineers (COE) New York District Office. All soundings are corrected to mean low water.

##### 4.1.1 1936 Survey

The 1936 survey (Figure 6a) shows an area of the New York Bight that was modified by dumping only since 1845 on the northern

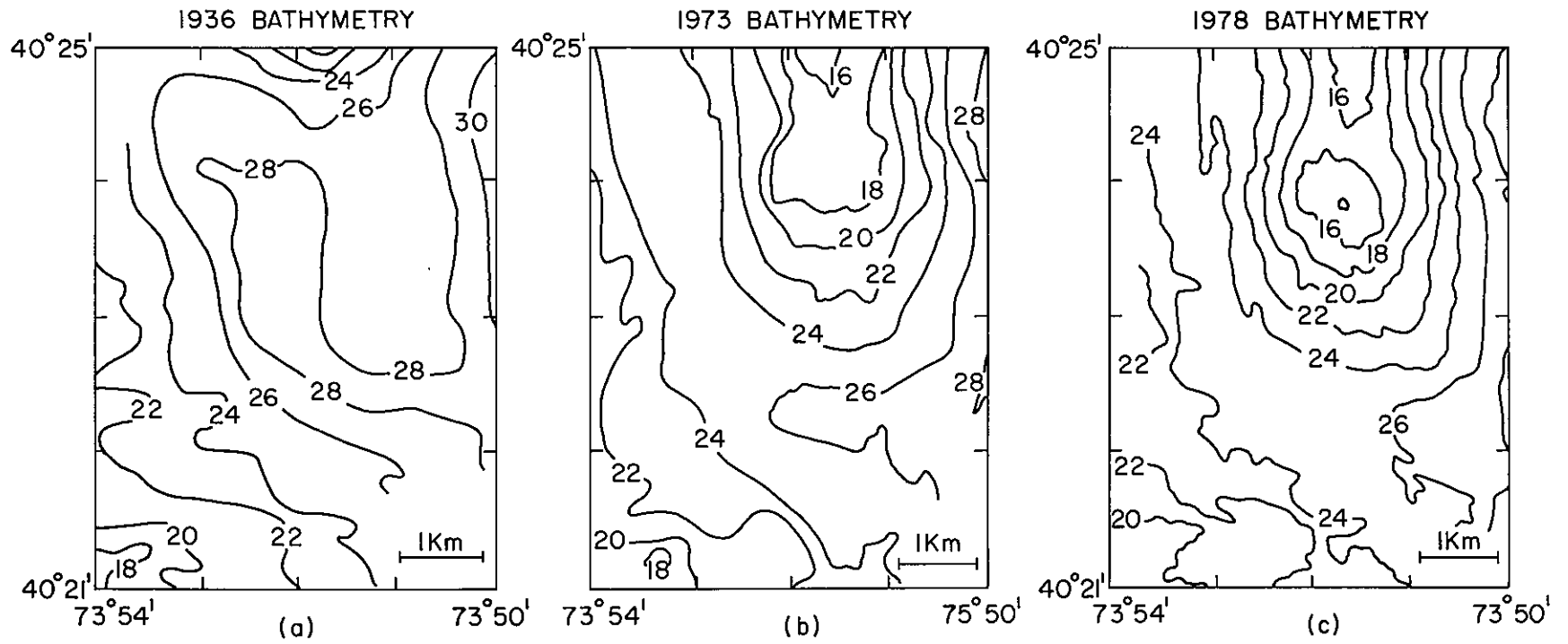


Figure 6. Bathymetric surveys of the study area: (a) 1936 survey; (b) 1973 survey; and (c) 1978 survey.

periphery of the study area (Freeland and Merrill, 1977). The continual disposal of material here since 1845 has formed a distinct submarine mound (Williams and Duane, 1974; Freeland and Swift, 1978). It was roughly circular in form with a diameter of about 2 km and a maximum elevation of 8 m. The remainder of the area was dominated by a gently sloping tongue-like trough delineated by the 28 m isobath. This trough projects to the northwest from the relatively straight 30 m contour that lies to the east of the site. It appears that dumping may have begun to fill in the trough resulting in the southerly extending lobe of the 26 m isobath found in the center of the area. In the southeastern corner of the study area the observed shoaling is related to the Shrewsbury Rocks found to the south of the site.

#### 4.1.2 1973 Survey

Figure 6b is the bathymetric chart for the 1973 COE Survey (Freeland and Merrill, 1977). It shows a broad, elongated hill which has risen to a minimum depth of 16 m. It was approximately 3.5 km long and 3 km wide, within the study area. The steepest slope on the flank of the pile was found on the northeastern side of the site where a 10 m change in depth occurred over a distance of 1 km. A small trough was found south of the deposit at the 26 m isobath. The 38 m isobath was located just at the eastern edge of the study site. Slight shoaling was present in the southwest corner.

#### 4.1.3 1978 Survey

Figure 6c depicts the bathymetry of the 1978 COE survey (D. Suszkowski, personal communication). This is a more detailed survey than those of

earlier years. There are two peaks of the deposit that are 16 m in depth and one point which is only 14 m. The deposit has prograded to the south and has filled in much of the trough at the 26 m isobath. The most steeply sloped section of the site is on the eastern side of the deposit at transect A with a gradient of 8 m per km. There is shoaling in the southwest corner.

#### 4.1.4 Cross-sectional Profiles

Figure 7 shows cross-sections of the pile along the transects A, B, and C shown in Figure 2. The cross-sectional profiles of the dredged material deposit along the three transects are shown for the three survey years. Transect A runs from west to east at  $40^{\circ}24'N$ . Transect B also traverses the deposit from west to east but at  $40^{\circ}24.5'W$ . Transect C presents a longitudinal cross-section of the pile running at  $73^{\circ}51.5'W$ . The cross-hatched regions of Figure 7 indicate erosion.

#### 4.1.5 Net Bathymetric Changes

1973-1978 Period. Between 1973 and 1978 little change occurred in the overall shape of the dredged material deposit. There was, however, an accumulation of as much as 4 m of material on the southern and western slopes of the pile. The maximum sedimentation rate was, therefore, approximately 0.8 m per year. As a result of this accumulation, the minimum depth reached 14 m at two points. On the eastern side of the pile, it appears that some erosion took place at a rate of approximately 0.2 m per year.

In Figure 7a, 2 m of material were added to the top of the deposit which had become more rounded in form. Near the top on the western

# BATHYMETRIC PROFILES

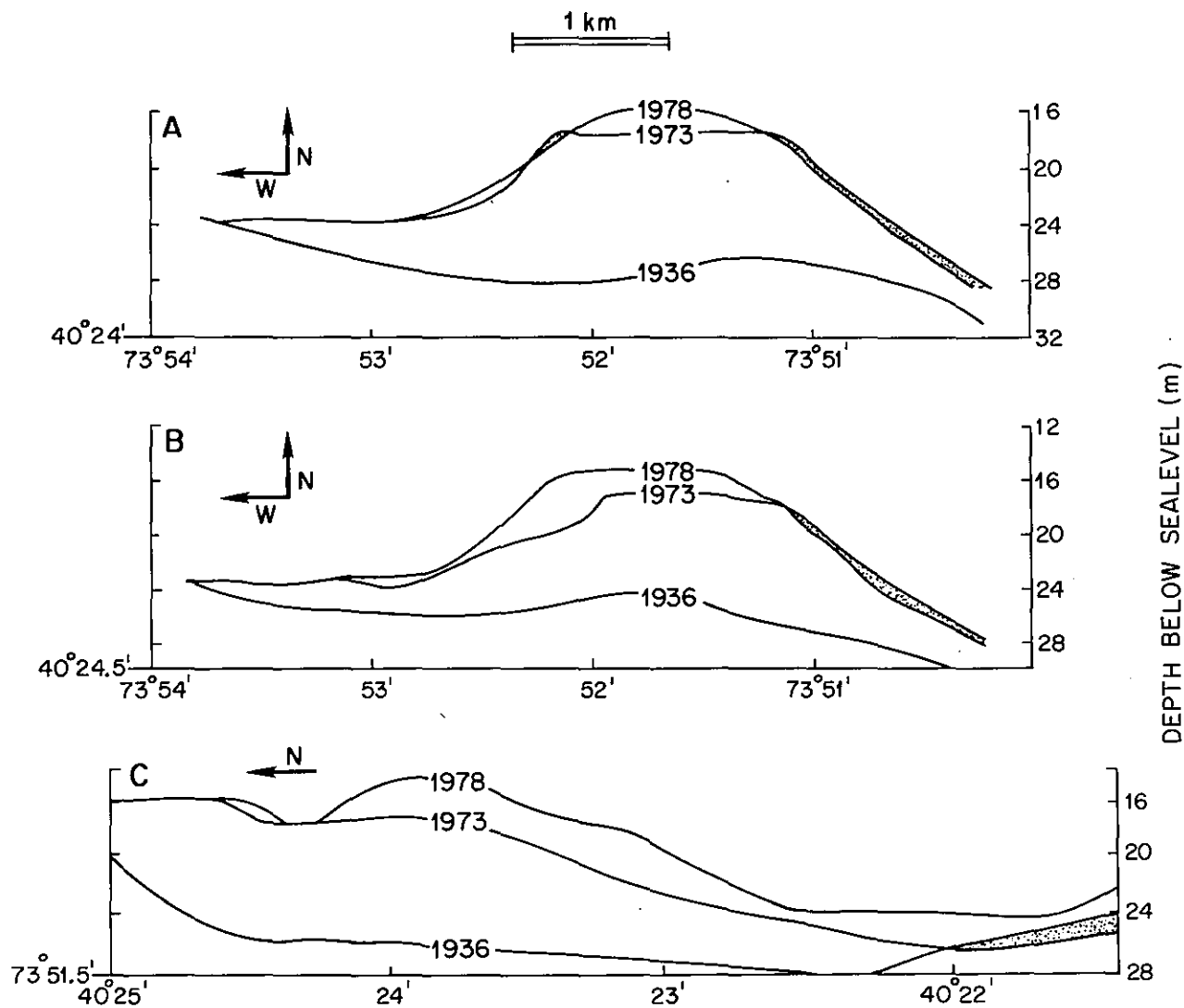


Figure 7. Cross-sectional profiles of the deposit, based on the 1936, 1973 and 1978 surveys, along the transects A, B and C as shown in Figure 2. Shaded areas indicate erosion. The vertical scale corresponds to the depth below sealevel (MLW) in meters.

slope there was a small amount of erosion with some deposition of material just below it. It is not known whether the bathymetry for the two survey years are accurate enough to detect such subtle changes, but it appears that a slump event occurred at this point.

Figure 7b shows accumulation of a maximum of 4 m of material on the western slope of the mud dump. There were also approximately 2 m added to the top of the pile. To the east as much as 1 m was eroded from the deposit.

Figure 7c shows that most of the accumulation took place along the southern slope of the deposit, with little addition of material in the north. This is to be expected since the dumpsite has recently been moved slightly to the south. A net change chart of the site, prepared by the COE for the period between 1973 and 1978 (Freeland and Merrill, 1977), shows that significant amounts of dredged material have been dumped to the west of the site. It also revealed that there were areas of erosion on the north and east slopes of the deposit.

A trough appeared at 40°24.4'N, between the areas of little change and the area slightly farther to the south, where there was intense deposition. On the southern slope an elongated deposit of as much as 4 m thickness formed where the 1973 profile dropped off. There was 2 to 3 m infilling of the trough along the southern perimeter.

#### 4.1.6 Sedimentation Rates

Sedimentation rates, as calculated for the coring stations, based on 1936, 1973 and 1978 surveys are listed in Table 9. Comparison of

Table 9. Rates of dredged material accumulation at the dumpsite.<sup>1</sup>

Core No.	Station Location	Sedimentation Rate (cm/yr)		
		1973-78	1936-73	1936-78 <sup>2</sup>
6	Pile apex	60	45	47
3	Pile apex	42	41	41
9	Top of northwest slope	11	13	13
8	Base of northwest slope	6	6	6
2	Top of southeast slope	36	14	16
5	Middle of southeast slope	40	6	11
4	Base of southeast slope	20	4	6

<sup>1</sup>Based on the 1936, 1973, and 1978 bathymetric charts.

<sup>2</sup>The total amount of dredged material observed in the cores agrees with the amount deposited based on estimates from the 1936 and 1978 bathymetric charts.

the sedimentation rates at different stations on the pile for the period 1936-78 show that the deposit apex has been the site of heaviest dumping during the period 1936-78. Lowest sedimentation rates were observed for station 8, located at the base of the northwest slope. Downslope stations, cores 2, 4, and 5, located on the southeast slope also exhibited low sedimentation rates for the period 1936-73. For the recent 1973-78 dumping period, however, the sedimentation rates at these stations are higher than those for the 1936-73 period by a factor of 3, 5, and 7, respectively, indicating that in recent times the dumping took place on the southeast slope of the deposit. This is also evident from higher sedimentation rates for the 1973-78 period at stations 2 and 6, located on the southeast slope, as compared with the pre-1973 rates. Stations 3, 8, and 9, located on the northwest slope, however, do not reveal significant differences in sedimentation rates for the two time periods.

As expected, the sedimentation rates for the period 1936-78 are comparable to those estimated for 1936-73, the period during which most of the dumping took place.

#### 4.1.7 Volume and Mass Estimates

Estimates of bulk volume of dredged material accumulated at the mud dumpsite during the period 1936-78 were obtained from the net changes observed in the bathymetric charts based on surveys conducted in 1936, 1973, and 1978. The bulk density for accumulated material in the deposit was determined for over 500 samples of the cores taken

in this study. The average bulk density of these samples, excluding the natural basement sediment, was found to be  $1.7 \text{ g/cm}^3$ . It is unknown how much compaction was caused by the vibracoring. This bulk density figure was applied to the bulk volumes to obtain bulk mass estimates. Dry mass estimates were obtained from bulk mass values using an average water content of 31% by weight for dredged material determined in this study for the same samples. Estimates of bulk volume, bulk mass, and dry mass of material deposited at the site since 1936 are given in Table 10.

Table 10 shows that the annual accumulation rates of dredged material vary from  $1.8 \times 10^{12} \text{ g/yr}$  for the period 1973-78 to  $2.9 \times 10^{12} \text{ g/yr}$  for 1936-73; the overall rate for the period 1936-78 being  $2.4 \times 10^{12} \text{ g/yr}$ .

#### 4.2 Description of Sediment Types

Four major sediment types were found in the cores taken at the dredged material dumpsite. These were: (1) black mud and black sandy mud; (2) yellow and white coarse grained sands; (3) red and gray plastic clays; and (4) glauconitic sand (greensand). These sediment types were classified according to their color, grain size, and mineralogy. Significant quantities of artifact material such as coal and cinders were associated with the black mud. All of the aforementioned sediments are briefly described and discussed below.

An overview of the major diagnostic parameters that define the observed sediment classes is given in Table 11. It includes information

Table 10. Estimates of amounts of accumulated material in the deposit during the period 1936-78.

Dumping Period	Accumulated Material			Annual Accumulation		
	Bulk Volume <sup>1</sup> (10 <sup>6</sup> m <sup>3</sup> )	Bulk Mass <sup>2</sup> (10 <sup>12</sup> g)	Dry Mass <sup>3</sup> (10 <sup>12</sup> g)	Bulk Volume (10 <sup>6</sup> m/yr)	Bulk Mass (10 <sup>12</sup> g/yr)	Dry Mass (10 <sup>12</sup> g/yr)
1973-78 (5 years)	27.0	45.9	31.7	5.4	9.2	1.8
1936-73 (37 years)	93.0	158.1	109.1	2.5	4.3	2.9
1936-78 (42 years)	120.0	204.0	140.8	2.9	4.9	3.4

<sup>1</sup>Based on bathymetric surveys conducted in 1936, 1973, and 1978.

<sup>2</sup>Calculated from bulk volume estimates using a bulk density of 1.7 gm/cm<sup>3</sup> for deposited dredged material.

<sup>3</sup>Calculated from bulk mass estimates using a value of 31% by weight for the average water content of dredged material.

Table 11. An overview of the major sediment types observed in the dredged material deposit.

Sediment Type	Description	Range of Values (%)			Mean $\phi$	Sorting $\phi$	Skewness	Kurtosis	Organics (%)	Munsell Color Code	Inferred Origin
		Gravel	Sand	Mud							
Black Mud and Black Sandy Mud	Black, medium to fine silt, poorly sorted, fine skewed. Ranges to fine sand or gravelly, sandy mud.	0-35	0-50	40-100	6.3	1.5-2.0	-0.001- -0.85	=1	12-34	N	Dredged Material, New York Harbor
Red Clay	Brick red, plastic clay.	0-12	7-49	40-90	3-8	1.8-3.5	+0.1- -0.9	0.8-1.9	-	5 yr 4/4	Dredged Material, Raritan Formation Newark Bay (D. Suszkowski, personal communication)
Gray Clay <sup>1</sup>	Gray, dense plastic clay; medium grained silt poorly sorted, strongly coarse skewed.	0	4	96	7.9- 7.3	1.7	-0.7	0.8-1.7	7.3-16.2	5 yr 3/2	Natural, Holocene lagoonal sediment (Swift <i>et al.</i> , 1976)
Greensand	Green muddy sand, poorly sorted, fine skewed, very platy-kurtic frequently heavily burrowed and mottled.	0-1	56-91	44-8	4.9- 2.3	2.5-1.0	0.2-0.5	0.6-2.0	1-2.9	5 yr 4/2	Natural, Matawan Group, Upper Cretaceous (Boyer, 1977)
Yellowsand <sup>1</sup>	Brown, yellow iron-coated medium grained sand; poorly sorted, fine to coarse skewed, very leptokurtic.	75	18	3	-1	0.6	-0.5	1	1.1	2.5 yr 4/4	Natural, Regional Coastal Plain Sediment
White Sand	Very coarse gravelly sand; poorly sorted, strongly fine to strongly coarse skewed, very platykurtic.	25-77	21-73	0-3	+0.3- -0.9	1.6-0.9	-0.4- +0.4	1.1-0.7	<1.0	white	Natural, Holocene sediment veneer

<sup>1</sup>For yellowsand and the gray clay, average values are reported because of lack of variation in grain size parameters.

on grain size, texture, color, oxidizable organic matter, and the inferred sediment source.

Figure 8 is a ternary plot showing the relative amounts of gravel, sand and mud in all of the samples analyzed for sedimentological study. In addition, ternary plots, showing the percentages of gravel, sand, and mud for all of the samples in each core, are provided in Fuhrmann, 1980. In addition, a core log for each station is presented. These include a lithological schematic of each core. Also depicted are Munsell color codes, percentages of gravel, sand, mud, oxidizable carbon, and water content (Fuhrmann, 1980).

#### 4.2.1 Black Mud

The principal sediment type in the dredged material dumpsite is black mud which frequently ranges to sandy mud. It occurs in varying frequency within the cores. The ubiquitous nature of this sediment type in the dumped material is clearly illustrated in the core logs (Fuhrmann, 1980). Figure 9 is a color photograph of a portion of core 3 (section 0-300 cm) which was primarily composed of black mud. Table 11 summarizes the characteristics of this material.

Olsen *et al.* (1978), Gross (1972), McCrone (1967) and Panuzio (1965) have described the sediments of the Hudson River and the New York Harbor as black, clayey silts with high water and organic contents with frequent contamination of surficial sediment by metal flakes, coal, cinders, glass, brick and concrete fragments.

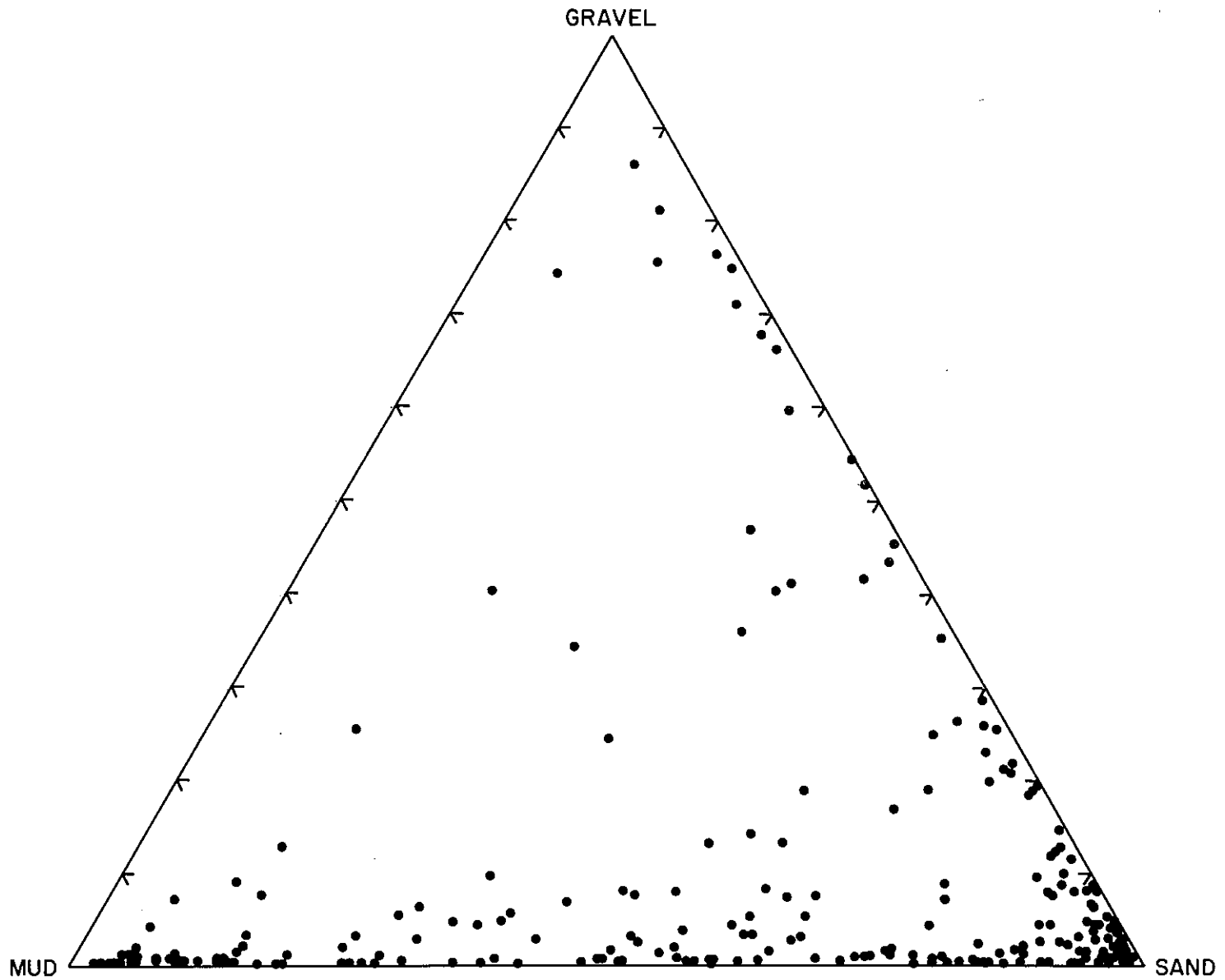


Figure 8. Ternary plot showing the relative percentages of gravel, sand and mud contents of all core samples analyzed.

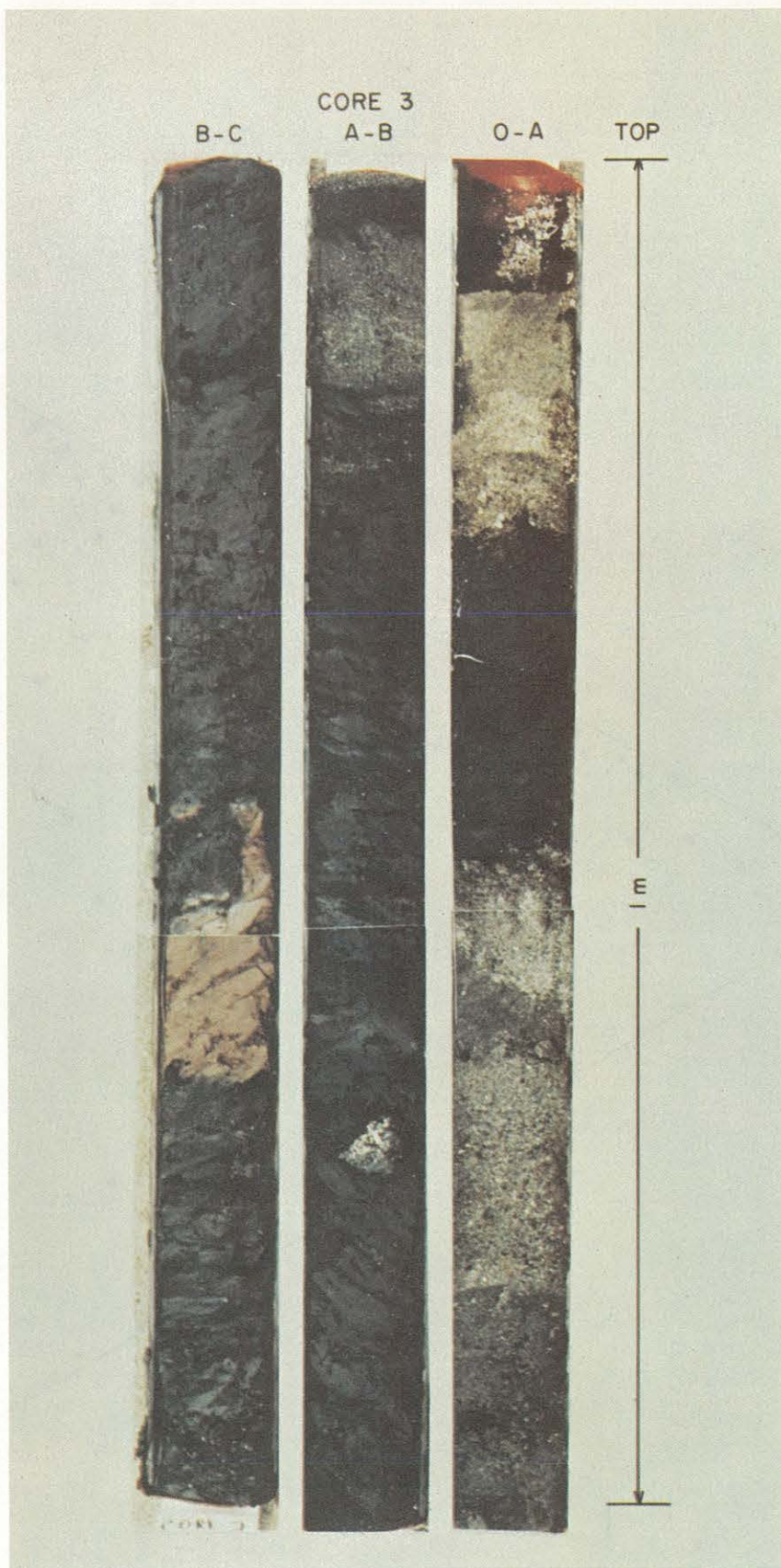


Figure 9. Color photograph showing sections of core 3. Section OA, representing the top 100 cm, is underlain by sections AB and BC. Black mud (top of BC), red clay (middle of BC), and white sand (top of OA) can be seen.

This sediment type is not as variable in its parameters as the other sediment types (Table 11). The distinctive features of this material are, of course, the fine grain size and the black color. Often a strong odor of oil was noted in the mud samples. On the ternary plot (Figure 8), showing the grain size distribution, the cluster of points close to the mud apex represent the black mud sediment type. The continuous range of points, along the length of the mud/sand axis of the plot, reflect sand incorporated within the mud.

The oxidizable organic content of the black muds in the dumpsite is generally high, ranging between 9% and 34%; the mode occurs around 15%. This is much higher than the levels reported for samples of Hudson River muds, upstream of the harbor, where values range between 2% and 5% (McCrone, 1967). Gross (1972) reported that the Lower Hudson River, the East River and Newark Bay sediments contained high total carbon content, frequently due to the presence of sewage in sediment. Much of the organic detritus of the dumpsite muds was present in the form of short fibers of plant matter, the coarsest of which, when dried, resembled peat.

In all samples any coarse fraction that was present in the muds consisted, with few exceptions, of small bivalve shells, shell fragments and artifact material. The sand fraction was found to be a very fine grained micaceous sand which often contained fly ash spherules.

Figure 10 shows the gravel composition of individual samples of black mud or muddy sand from cores 6, 7, and 9. The variety of materials is evident from the three photographs. Figure 10a from core 6 is

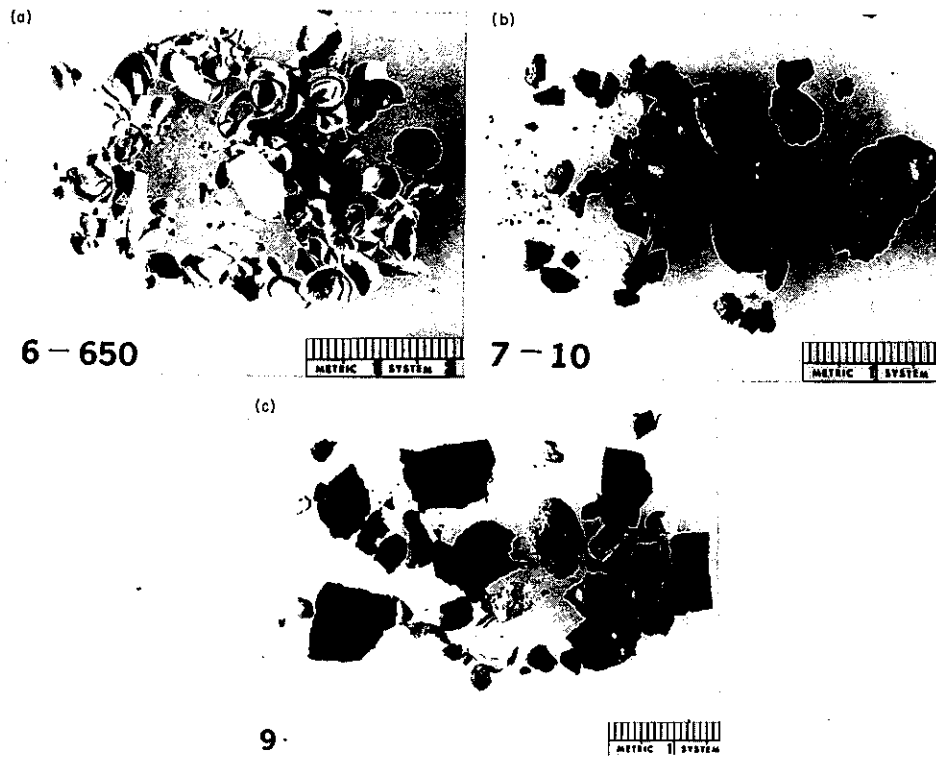


Figure 10. Gravel fraction of black mud in dredged material sediments: (a) shell fragments in core 6 at 650 cm depth; (b) coal in core 7 at 10 cm depth; and (c) iron flakes in core 9 at 15 cm depth.

relatively artifact free, being primarily composed of shells of the pelecypod *Nucula Proxima*. Figure 10b shows the gravel content of a muddy sand sample. Some rounded quartz was present but the principal constituents were angular coal fragments. Figure 10c (core 9), in turn, contained numerous rust scale fragments.

Nearly all of the mud in the Bight apex has been deposited by dumping. Meade (1972) found that little of the fine fraction of the river borne sediments has accumulated on the continental shelf, instead it is either trapped in estuaries and lagoons or is carried offshore. In either case, Gross (1972) concluded that there is little naturally occurring fine grained sediment on the continental shelf. Other than in the area of the various dumpsites, there are relatively few locations in the immediate proximity of the dumpsites where very fine grained sediments may be found. Freeland *et al.* (1979) report that only two major areas in the Bight contain sediment with over 50% mud content; they are the dredged material dumpsite and a small, central portion of the Christiaensen Basin.

#### 4.2.2 Clay Types

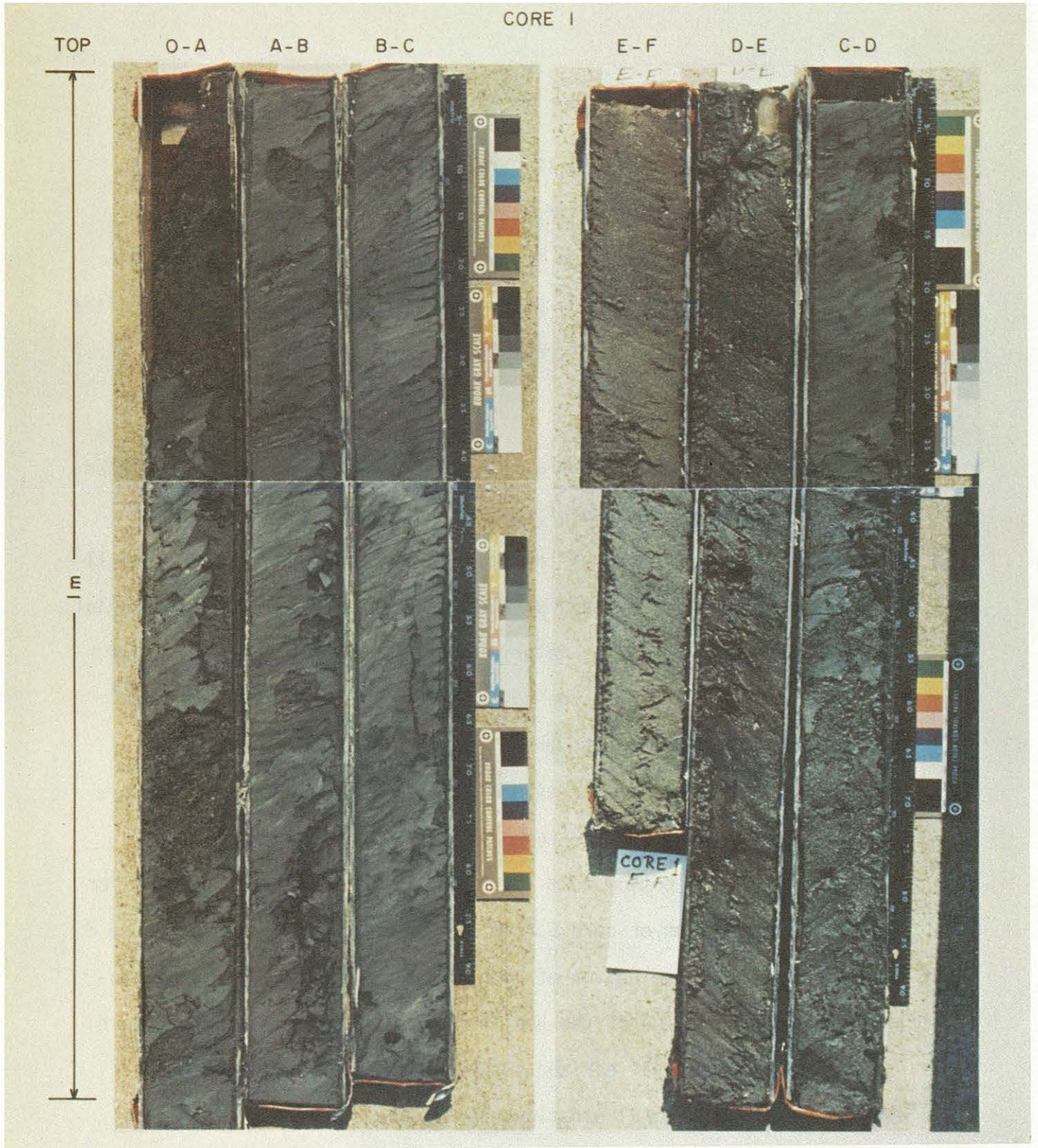
The two principal clays, found at the dredged material dumpsite, are both plastic clays. One variety is characterized by its brick red color and was found only in the dumped material itself. It occurred as laminations, galls of contorted clay and as beds of up to 25 cm thickness. The red clay was used extensively as a horizon tracer in the deposit stratigraphy to be discussed later. The second clay type is a gray clay that only occurs as a naturally deposited bed in core 1. Table 11 contains the sediment parameters for these clay types.

Red Clay. This material was found throughout the dumpsite deposit (see Fuhrmann, 1980). Figure 9 displays a bed of this clay type that was found in core 3 at 260 cm depth. This sediment type varied widely in gravel, sand and mud content. Based on its grain size distribution, much of it cannot properly be classified as clay. The distinct brick red color and the plastic texture are the principal identifying characteristics of the material.

The gravel content of the red clay is almost exclusively composed of fragments of red shale. This agrees with the observation by Ries *et al.* (1904) who showed that this component is an erosion product of the Triassic red shale which is frequently seen as the lowermost member of the Raritan Formation. The original depositional environment of the red clays may have been lacustrine. A bed of red clay, exposed by dredging, has been observed in Newark Bay (Dennis Suszkowski, personal communication). Consequently, it has been assumed that this material, seen in the dumpsite, has been dredged from Newark Bay.

Gray Clay. The second variety of clay found at the site is a gray plastic clay observed only as natural sediment in core 1, outside of the dumpsite, in a bed of three meters thickness (Figure 11).

The gray clay was remarkably consistent throughout the bed in its various sediment parameters. A ternary plot of the gravel, sand and mud fractions of gray clay in core 1 shows that the cluster around the mud apex represents this gray clay (Fuhrmann, 1980).



Occasional sand balls (Figure 12) and twigs, up to one centimeter in diameter, were found within this bed.

The gray clay is believed to be one of a series of deposits described by Swift *et al.* (1976) as lagoonal sediments that were deposited and then covered over as the transgression of sea level proceeded.

#### 4.2.3 Greensand

The greensand sediment is a muddy sand which is primarily composed of angular quartz grains and of the various forms of glauconite. In appearance it was heavily mottled and of a light green color. Table 11 provides a synopsis of certain parameters used to describe this material. It should be noted that this material was highly variable in terms of the grain size statistics. The most indicative characteristics were color, mineralogy and, in the thick underlying beds, the burrowed texture (Figure 13). The position of the beds may be seen in the core logs (Fuhrmann, 1980) and are found between 335 and 441 cm in core 1, (Figure 11), as the bottom most layer of core 2, between 560 and 711 cm in core 4, the bottom of core 5 from 282 cm depth to the base of core 8 and from 261 cm to the bottom of core 10. Figure 14 is a color photograph showing a section of the bed in core 4. The greensand beds were used as the transitional horizon between anthropogenic and natural sediments in the textural stratigraphy discussed later.

The thick beds of greensand are apparently naturally deposited sediments that were associated with the Marshalltown formation which appears as part of the Cretaceous outcrops extending as a band across

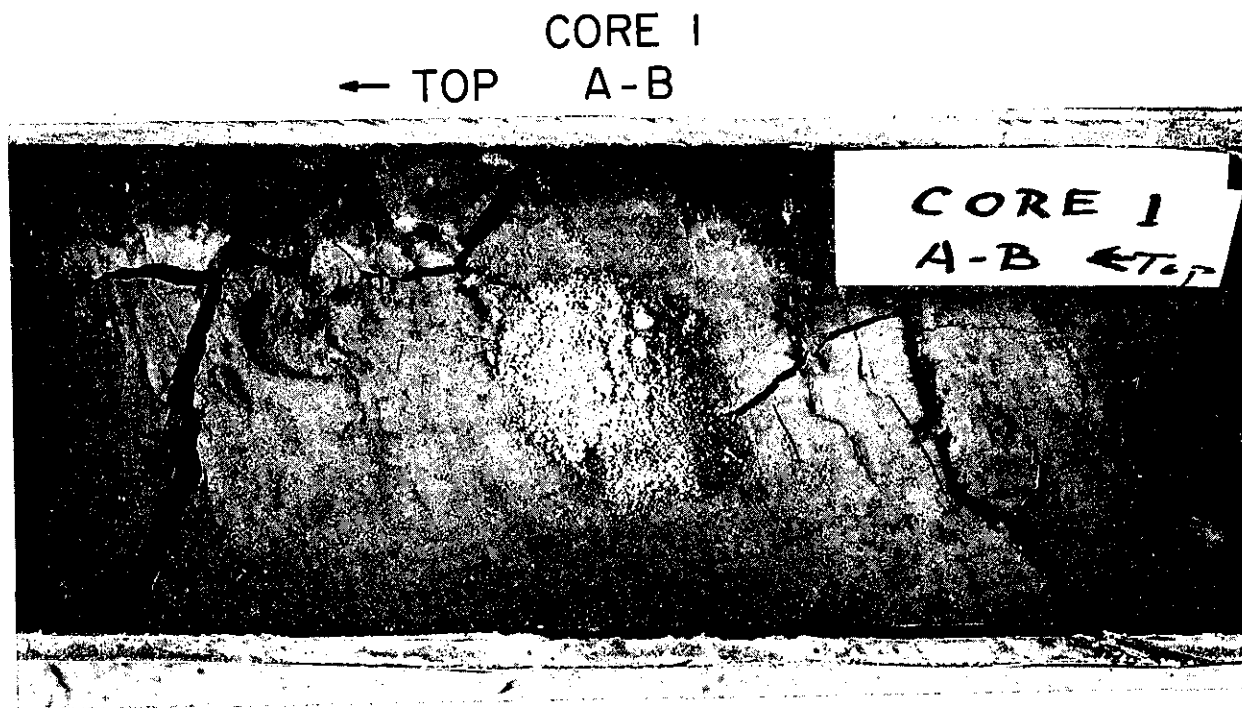
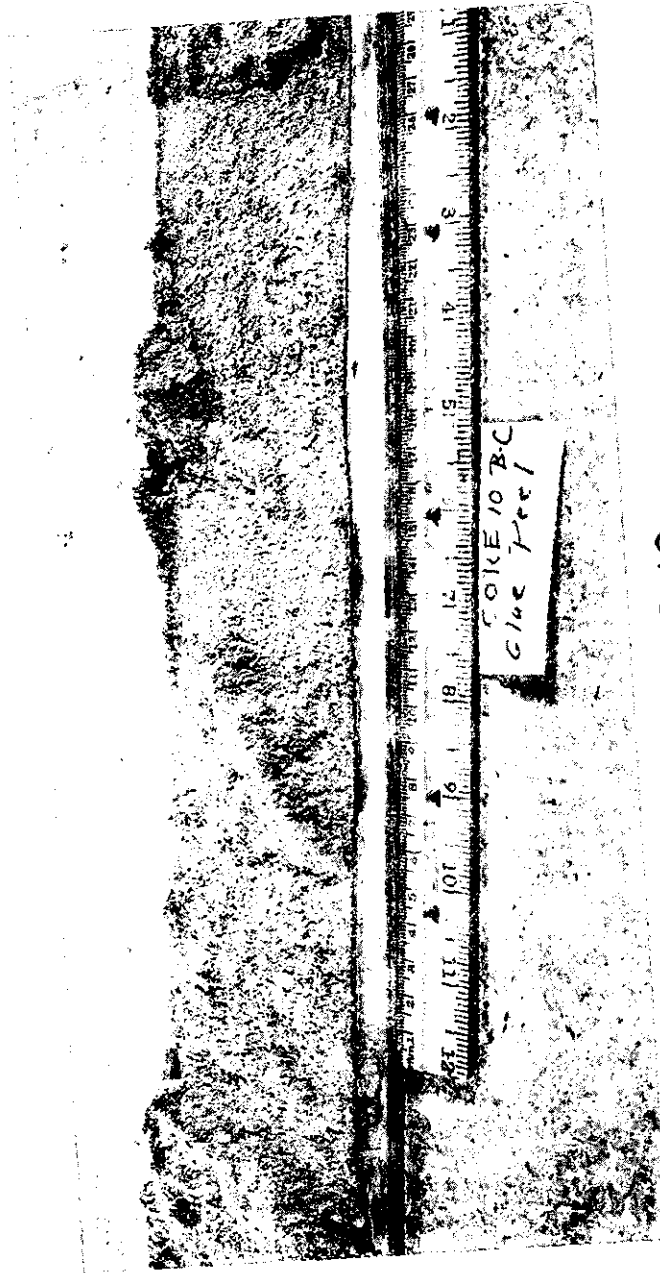


Figure 12. A section of the gray clay bed in core 1, containing a sand ball. The core length shown is  $\approx$  25 cm.



← TOP CORE 10  
B-C  
GLUE PEEL

Figure 13. A peel section of core 10 showing the burrowed texture observed in the greensand bed.

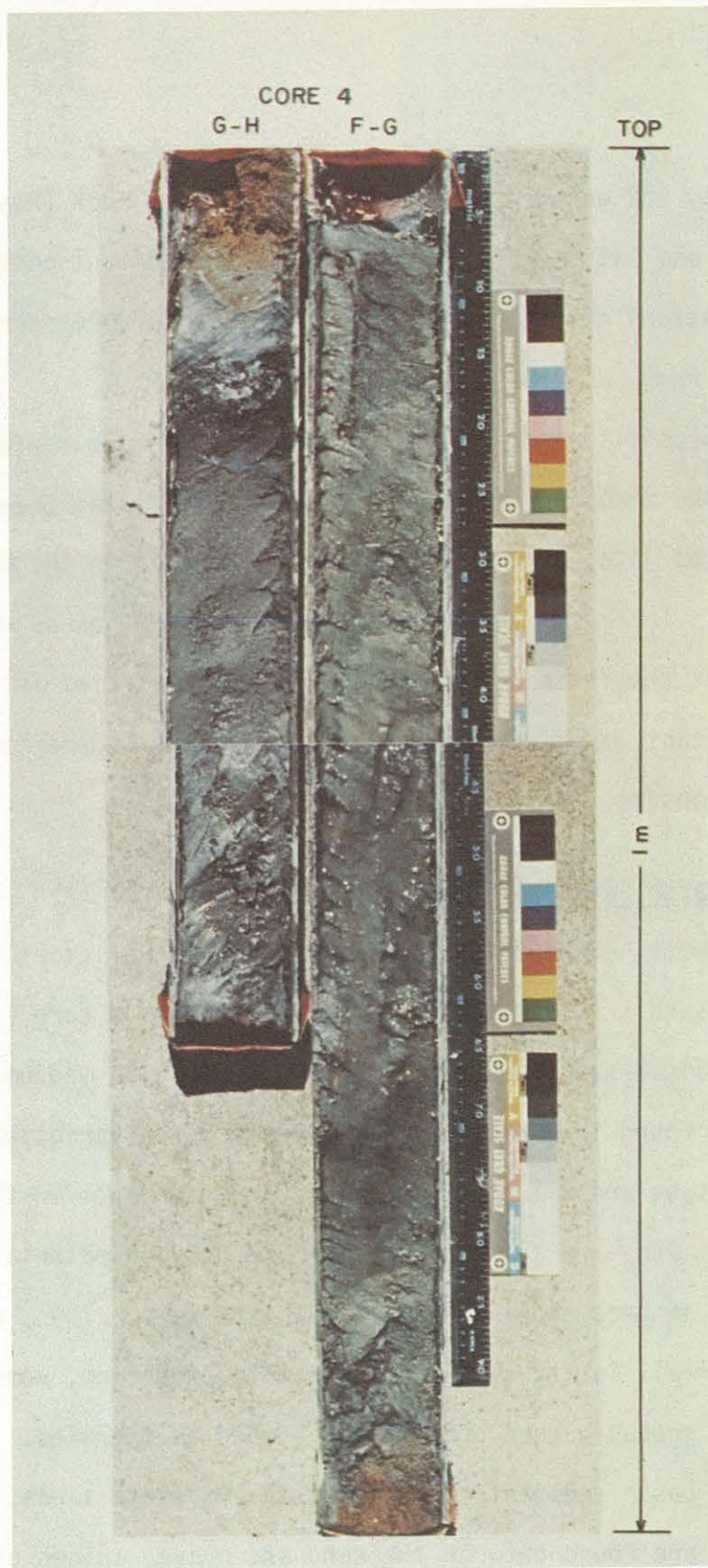


Figure 14. Color photograph showing a greensand bed in section FG of core 4. Section GH represents the basal unit of core 4 and is located at a depth of 600-665 cm.

New Jersey and entering the ocean around Sandy Hook (Boyer *et al.*, 1977). Freeland and Swift (1978) report a lobe of sediment containing elevated concentrations of glauconite (characteristic of greensand) extending offshore from Sandy Hook, New Jersey.

Glauconitic sand, which is exposed at erosion surfaces in the vicinity of the dumpsite (Freeland and Swift, 1978) has been episodically transported onto the mud dumpsite. It occurred in the dredged material deposit as irregular, frequently laminated sand lenses which are common throughout the cores. The presence of this material in the deposit has important implications with respect to the sedimentary processes at the dumpsite.

#### 4.2.4 Coarse Sands

A fourth sediment type consists of three varieties of sand and gravelly sand: (1) white, gravelly sand found in core 7; (2) yellow, coarse grained sand observed in core 4; and (3) a medium grained white/gray sand found in cores 4 and 10. These three varieties of a single sediment type are all naturally occurring sediments in the area of the dumpsite. They are also seen within the dredged material deposit, generally in beds showing no internal structure. Thus, while most of this material, in the cores, is naturally occurring, some similar sediment has probably been dredged and dumped at the site. Table 11 provides the basic sediment characteristics of these sands. All of these materials are found between the sand and gravel apices of Figure 8. Core logs depicting these materials are presented in Fuhrmann, 1980.

White Sand. Gravelly white sand, seen in core 7 (Figure 15), was originally natural surficial sediment. It is presumably derived from the Holocene veneer of sediment that covers the inshore continental shelf (Freeland and Swift, 1978). Similar material was reported, on sediment distribution maps of the area (Jones *et al.*, 1979), to cover an elongated area extending to within 1 km of the New Jersey coast, offshore from Sandy Hook. The ternary plot and the core log show the high gravel content of this material (Fuhrmann, 1980). Figure 16 shows the gravel fraction, primarily well rounded quartz, of a sample from core 7. The sand fraction showed little iron oxide staining but the gravel fraction showed that as many as 50% of the grains were stained. Iron oxide coating occurs frequently in pits and grooves on the grains. Similar material was found in sand lenses near the bottom of cores 2 and 3.

Fine Grained White Sand. Finer grained, white sand was observed underlying the dredged material in cores 4 and 10. This material was surficial sand that had been buried by dumping. It is similar in composition to the gravelly white sand but contains relatively less gravel (Figure 17; Table 11). A major difference between the two sediment varieties was the extremely intense burrowing that was evident in the fine grained sand.

Yellow-brown Coarse Sand. A yellow-brown gravelly sand (Figure 18) was found immediately above the greensand bed of core 4. Table 11 summarizes its characteristics. A ternary plot showing the relative gravel, sand, and mud contents of this material is given in Fuhrmann (1980).

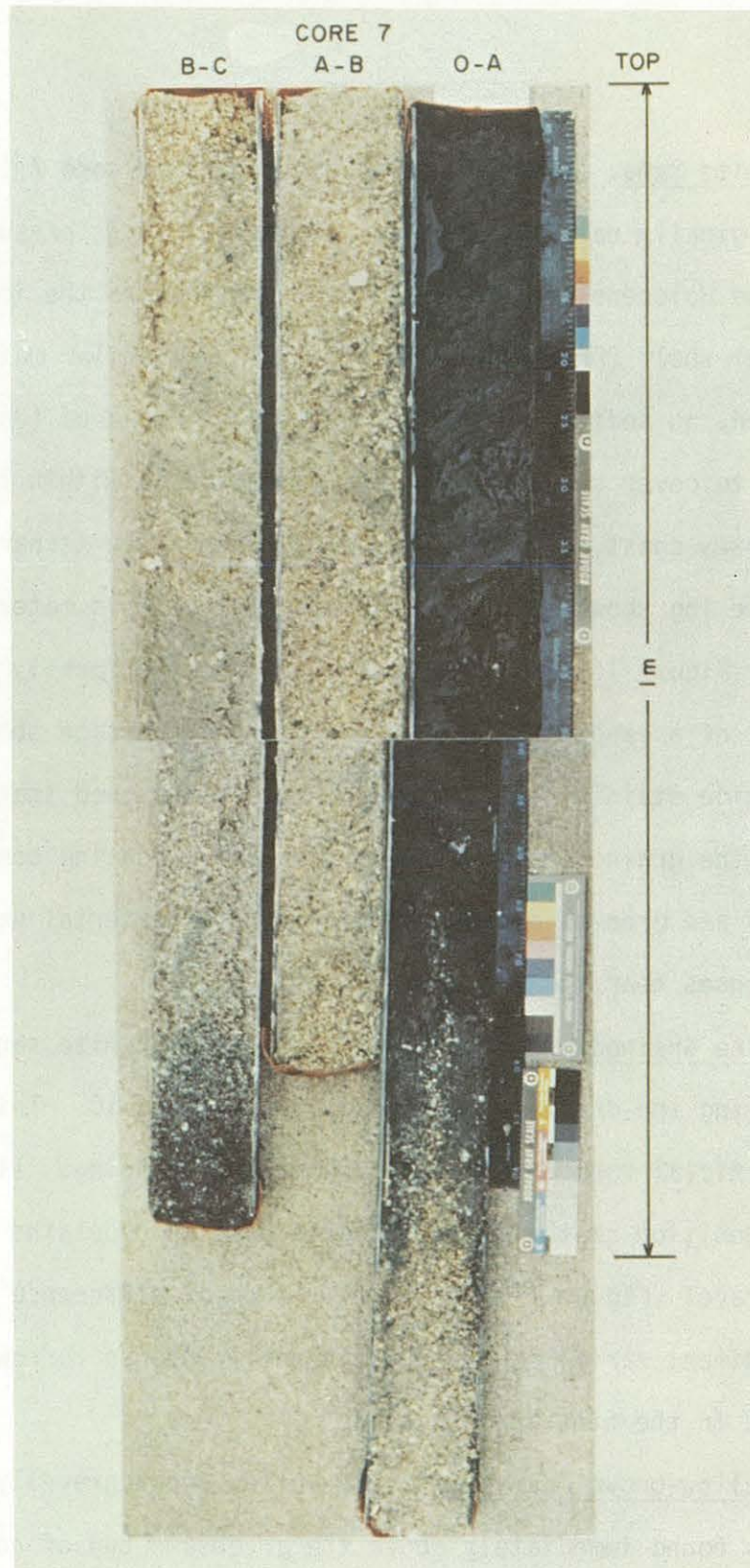


Figure 15. Color photograph showing black mud at the surface overlying white, gravelly sand in core 7. Section OA represents the core top.

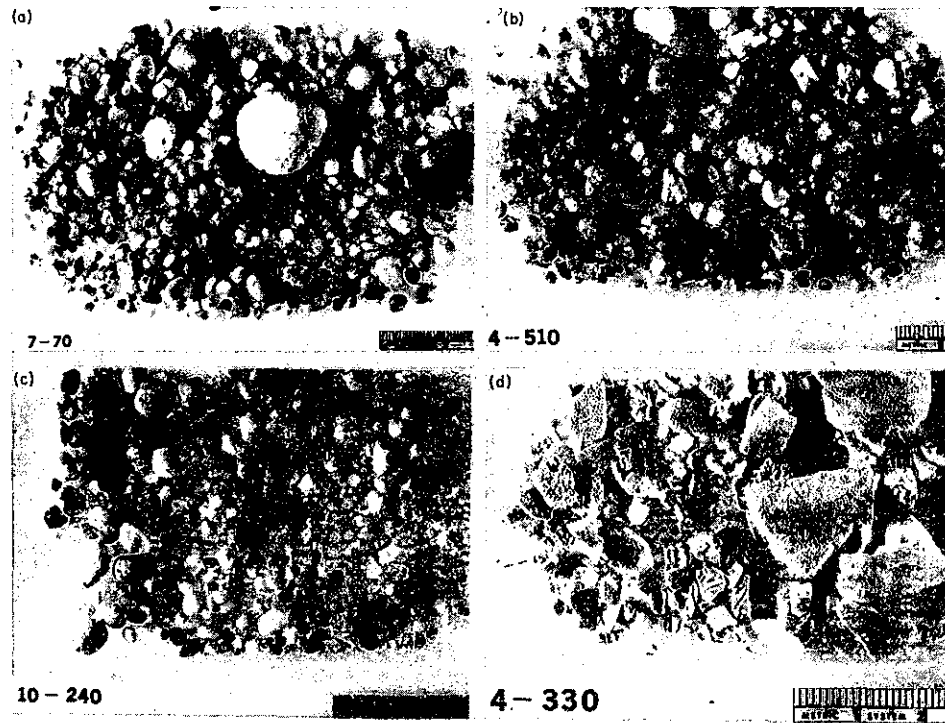


Figure 16. Gravel fraction of four sandy sediment types from cores 4, 7 and 10: (a) core 7 at 70 cm depth; (b) core 4 at 510 cm depth; (c) core 10 at 240 cm depth; and (d) echinoderm assemblage observed in the white sand present in core 4 at 330 cm depth.

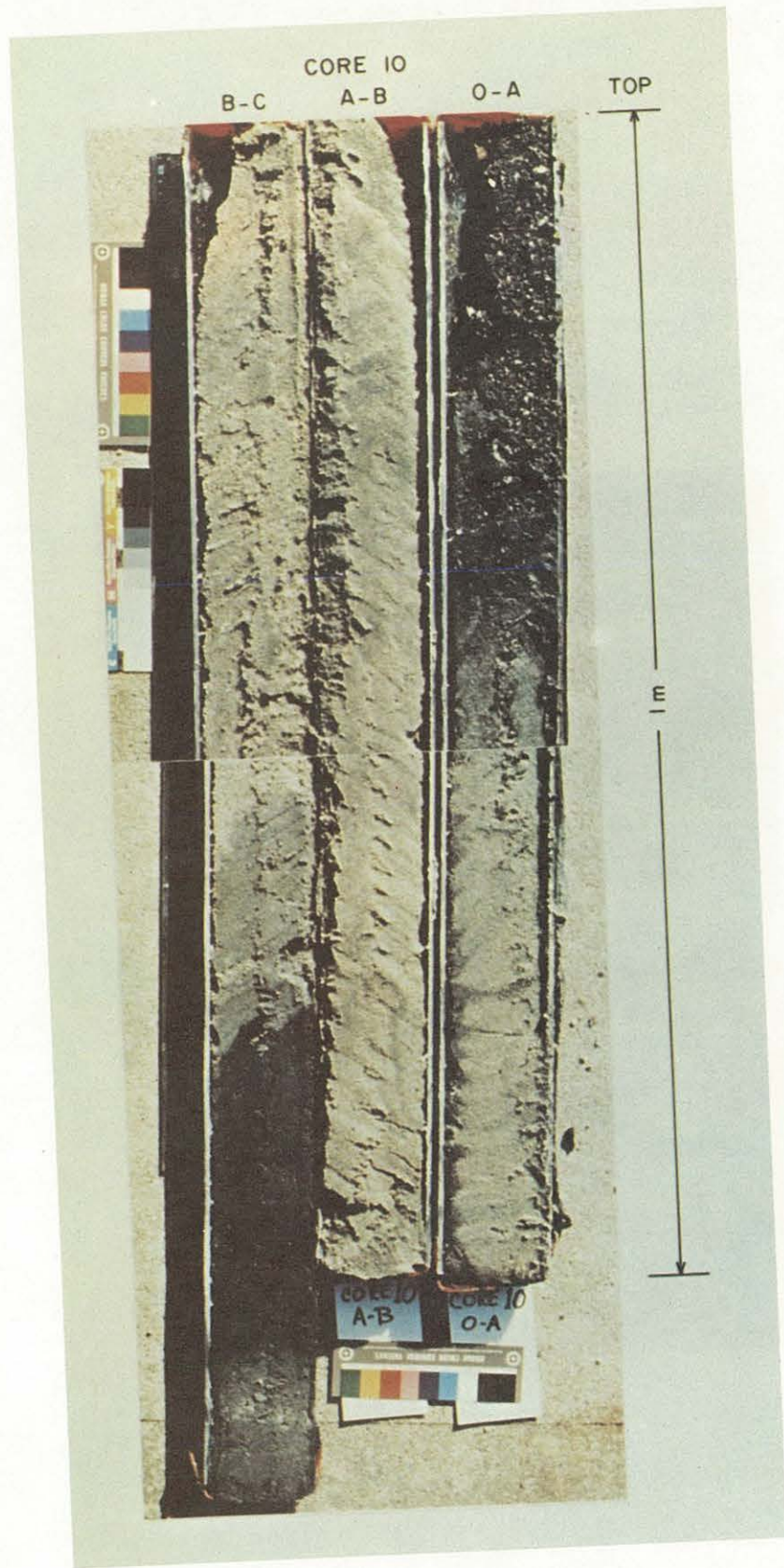


Figure 17. Color photograph showing dredged material at top of section OA of core 10 underlain by fine grained, white sand. The bottom of section BC, representing the basal unit of core 10, consists of black sand.

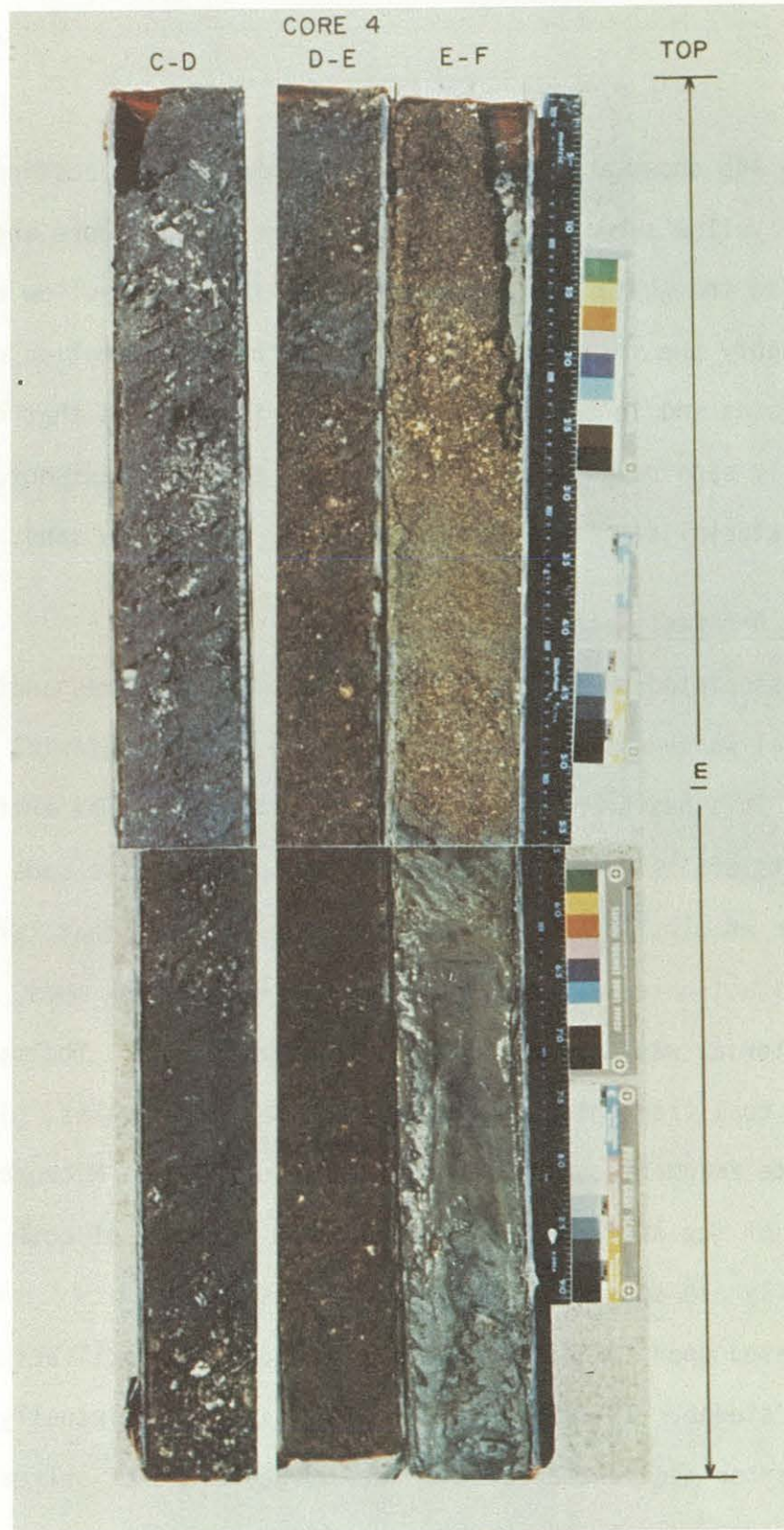


Figure 18. Color photograph showing sections CD, DE and EF represent 3 meters of natural sandy sediment observed below the dredged material/natural sediment boundary in core 4. Section EF represents the basal unit of the core.

Figure 16b shows a light photograph of the gravel fraction of a sample of the yellow sand. The sand grains were notably more angular than those in the white sand shown in Figure 16a. The yellow color was presumably the result of iron oxide which was present as coatings on the grains and in the mud fraction. It is believed that the white, gravelly sand represents a more mature, reworked sediment, derived from material similar to that comprising the yellow sand.

#### 4.2.5 Artifact Material

Associated predominantly with the black muds was another type of material which was characteristic of the dredged material at the study site. This has been termed "artifact material". The artifact material consists of: sludge, broken concrete, spent caustic soda and ash (Conner *et al.*, 1979). In our study, we observed that large amounts of artifact material were intermixed with the black muds, implying that the material was derived from the New York Harbor. The material included coal fragments, wood cinders, metal/rust flakes, glass shards, concrete fragments, a nail and a swatch of cloth. Microscopic examination of the sand fraction revealed the presence of both metallic and glass fly ash spherules in the dredged material.

Based upon COE data, the major component of artifact material was sewage sludge. This material, however, is often virtually indiscernible from harbor sediment because of the large volume of untreated sewage that is dumped into the harbor area (Gross, 1970).

Olsen *et al.* (1978) reported that in many parts of the Hudson River Estuary metal slag, fly ash, and coal were found in the top 10 cm

of the sediment. In the harbor area itself this material was found to depths of 250 cm.

Coal and the combustion products of coal (fly ash and cinders), as mentioned previously, are common in the dredged material and tend to be associated with the black muds and sandy muds. In some cases, small but distinct beds of pea-sized coal were observed such as in core 3 at 440 cm depth. Coal ash has been dumped at the site continuously. Gross (1976) reported that between 1960 and 1968 an average annual mass of  $0.1 \times 10^{12}$  g coal ash was dumped at the mud dumpsite. In 1970 a similar amount was disposed of (Conner *et al.*, 1979). By 1975, apparently due to reductions in the use of coal as a fuel by power plants, and the increased use of the ash elsewhere, there was no coal ash disposed of at the site. It is thought that the coal horizons shown later in the textural stratigraphy may correspond to the year of peak input of coal ash in 1963.

No grain size or precise description is given for the artifact material as there is no classification scheme available. To best illustrate the variety of artifact material found, light photographs of this material are shown in Figures 19-21. Gravel, cinders, shells, wood fragments, coal, metal flakes and glass are all present. Figure 23a displays the fossilized remains of a crab observed in core 5.

#### 4.3 Gravel/Sand/Mud Depth Profiles

Figures 22 and 23 represent the depth distributions of the gravel, sand, and mud fractions in cores 1-10. Water content, bulk density,

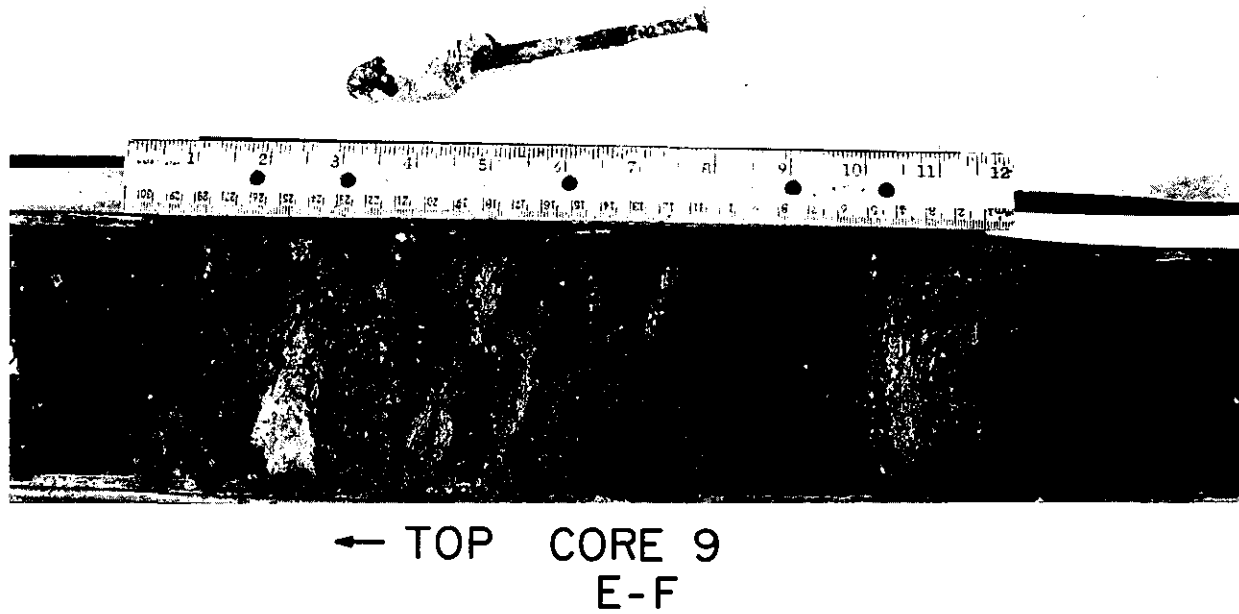


Figure 19. Artifact material observed in core 9. The nail, found at a depth of 4.9 m, was 13 cm long.

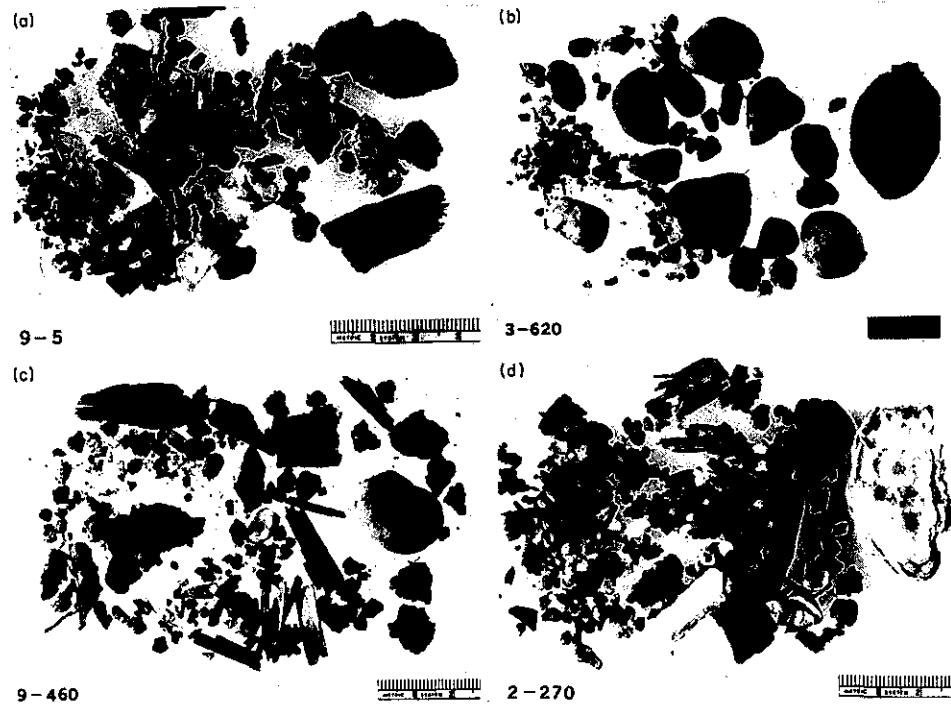


Figure 20. Artifact material found in the dredged spoils at the dumpsite: (a) in core 9 at 5 cm depth; (b) in core 3 at 620 cm depth; (c) in core 9 at 460 cm depth; and (d) in core 2 at 270 cm depth.



Figure 21. Artifact material observed in the dredged spoil sediment:  
(a) the fragmented, fossilized remains of a crab;  
(b) industrially shaped mica flakes.

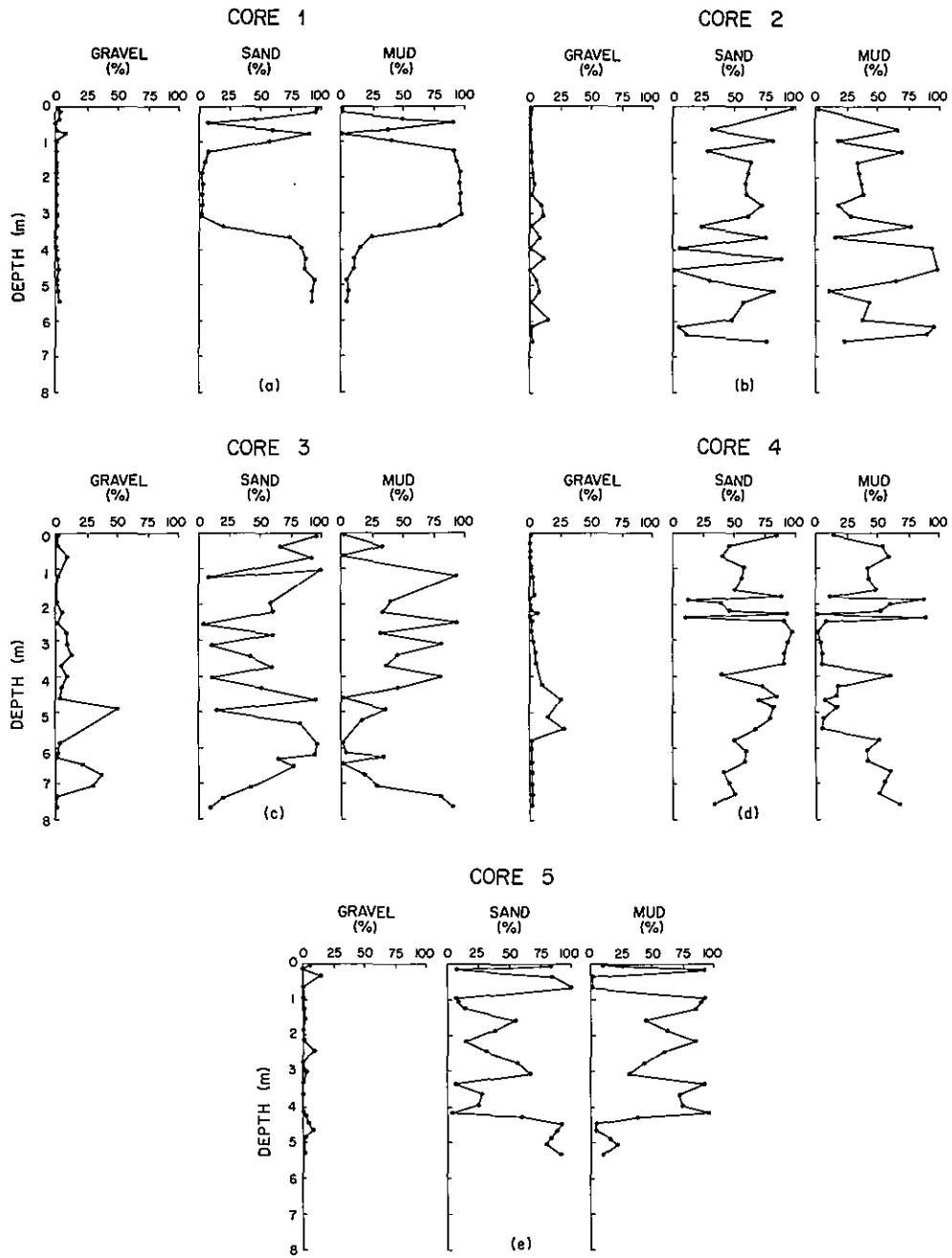


Figure 22. Depth distribution profiles of gravel, sand, and mud in cores 1, 2, 3, 4, and 5.

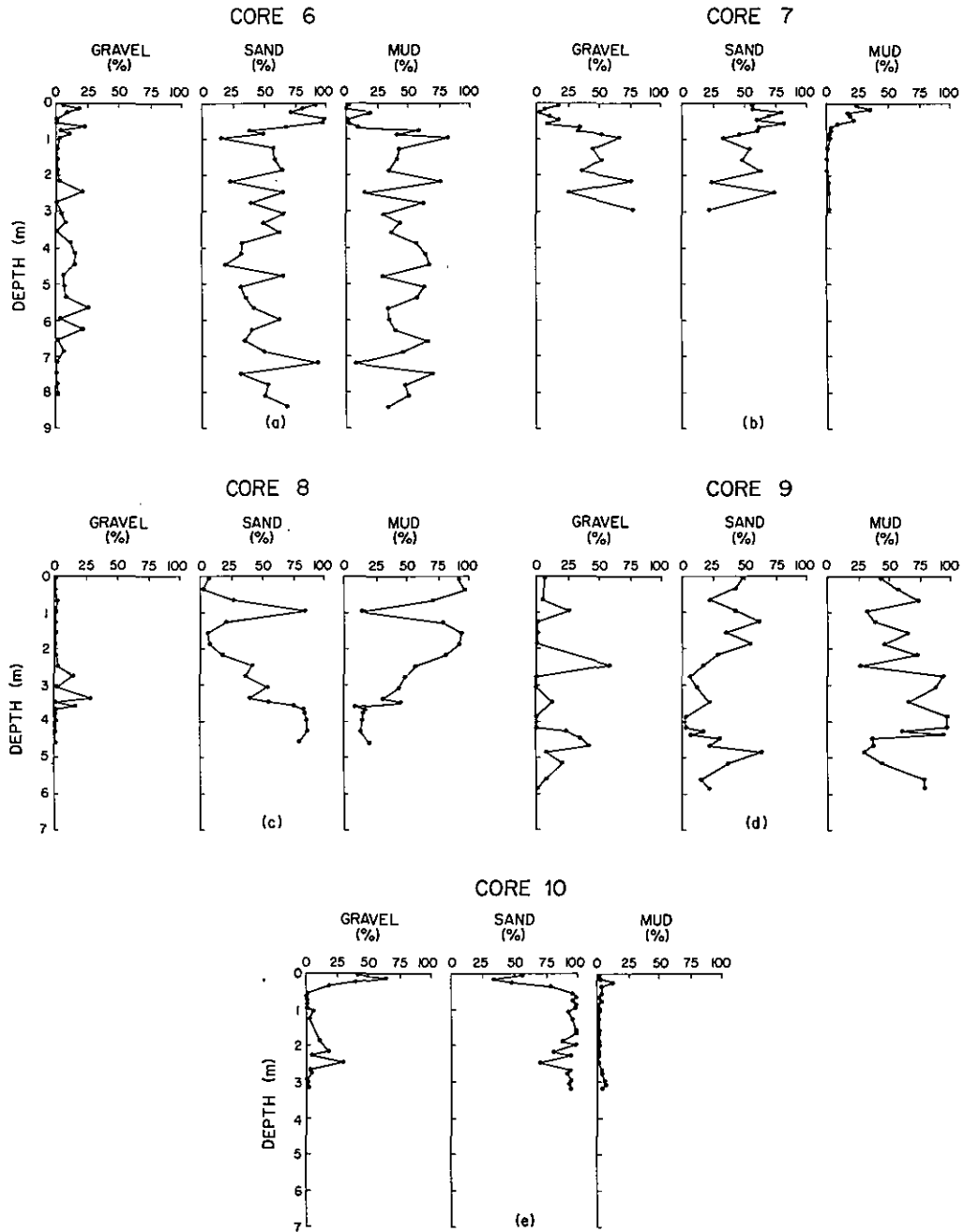


Figure 23. Depth distribution profiles of gravel, sand, and mud in cores 6, 7, 8, 9, and 10.

and porosity were also determined on the same samples and their depth distributions are presented in Appendix A.

The data, presented in Figures 22 and 23, depict the textural changes observed in the cores. The dredged materials are generally very erratic in texture. The depth profiles are characterized by a sawtooth form of distribution. Natural sediment is typically less varied and often shows a relatively smooth profile. The sawtooth form of distribution observed in a number of cores reflects the varied textural character of dredged material derived from various sources.

The top meter of core 1 is comprised of natural sand mixed with clay, with the sand content ranging from about 5% to 97%. Beneath this depth is a bed of gray clay which, except for a few sand balls, oyster shells and wood fragments, is very homogeneous, containing as much as 97% mud. Below a narrow zone of mixing there is a bed of greensand containing ≈90% sand and small amounts of mud and gravel (Figure 22a).

Core 2 contains dredged material in all but the bottom 4 cm of its length (Figure 22b). It is composed of black, soft mud intermixed with bands of clean sand and gravelly sand. This core, like most of those containing primarily dredged material, has relatively little gravel, and exhibits a typical sawtooth form of distribution. The sand content, however, is highly variable ranging from 2% to 98%; while the depth distribution of mud is a mirror image of the sand distribution. At 250 cm depth there is a 10 cm long fragment of concrete. The segment of the core between about 1.5 and 2.5 m depth contains a thick bed of greensand.

Core 3 is entirely composed of dredged material which was, characteristically, black mud and sand with much interlayering of the two (Figure 22c). The gravel content in this core approached a high of  $\approx 50\%$  at 5 m depth. The sand and mud profiles are typically highly erratic, exhibiting a sawtooth form of distribution.

Core 4 is particularly interesting because it penetrated the natural sediment to the greatest depth beneath the dredged material deposit (Figure 22d). In doing so it cored three beds of underlying natural sediment. The top 2.6 meters are dredged material, with the sand and mud contents being highly variable with depth. Beneath the dredged material is a 1.2 m thick bed of gray-green, medium grained sand bearing sand dollar shells. This material contains only 5% mud and about the same percentage of gravel. An 11 cm thick bed of gravel follows and this, in turn, is followed by a 1.5 m thick bed of coarse grained, iron-stained gravelly sand typical of some coastal plain outcrops nearby. Underlying this is a bed of fine grained glauconite sand which contains approximately 60% sand and 40% mud.

The top  $\approx 5$  m of core 5 are dredged material consisting of the characteristic alternating sand and mud interlayers (Figure 22e). The bottommost sediment in the core, a natural bed of glauconite sand, contains between 79% and 91% sand.

Core 6 consists of entirely dredged material but contains less mud than is observed in other cores. The mud and sand contents are highly variable as a function of depth (Figure 23a). Each profile exhibits the erratic sawtooth pattern. Gravel is present throughout the core ranging from 0 to 26%.

Core 7 was taken outside of the perimeter of the dumpsite (Figure 23b). However, the top 0.8 m are composed of black muddy sand which is clearly dredged material. The mud content was 18-36%. Underlying the dredged material was clean, quartzose, gravelly sand.

The topmost 3.7 m of core 8 are comprised of dredged material (Figure 23c). In this particular core the distributions do not show the typical sawtooth form, instead there is a grading from almost 100% mud at the top to 20% mud at 3.6 m depth. This core contains the highest average mud content (65%) of the ten cores. It is located at the base of the northwest slope of the deposit where we believe fine grained materials are preferentially deposited. From 3.7 m depth to the base of the core is a bed of glauconite sand.

Core 9 is, with the exception of the lowermost 4 cm, comprised entirely of mud and muddy sand with lenses of gravelly mud (Figure 23d). The mud layers are frequently cut by sand lenses. The gravel content of the dredged material was highest in this core than in any of the others; ranging from 0 to 58%. Sand and mud contents are highly variable with depth.

Core 10 was intended as background core but contained dredged material at the top (Figure 25e). There is little mud present at all, with a maximum content of 12%. The dredged material at the core top is identifiable by the presence of gravel size, anthropogenic material. Clean, quartzose heavily bioturbated sand is present below the dredged material. Much of the gravel at the top of the core is composed of cinders, rust flakes and coal; the fine grained material apparently removed by the stronger currents and wave action in this area.

The mean grain size, standard deviation, coefficient of variation and ranges for gravel, sand and mud for each core are discussed later in terms of sediment differentiation processes.

#### 4.4 Overall Stratigraphy

Based on the spatial distributions of sediment types observed, an overall stratigraphy of the deposit has been established, defining the boundary between the dredged materials and the underlying sediment basement. A schematic cross-section, along the northwest-southeast transect, showing the lithology of the deposit is given in Figure 24. Also shown in Figure 24 are the core station locations.

The quartzose sand observed in cores 7 and 10 and, to the southeast in Core 1, are materials typical of the inner continental shelf. The gravelly sand, in these cores, is part of a lobe of sediment that extends outward from the New Jersey coast immediately south of Sandy Hook (Freeland and Swift, 1978).

The greensand stratum has been characterized previously. The bed apparently underlies the entire dumpsite deposit. Shallow seismic reflection profiling has indicated that this bed may extend as far inshore as core 10. The dumpsite itself rests directly upon the once exposed greensand bed. The dashed lines at the base of the greensand shown in Figure 24 indicate uncertainty of the thickness of the bed. Core 4 penetrated through both the dredged material and the

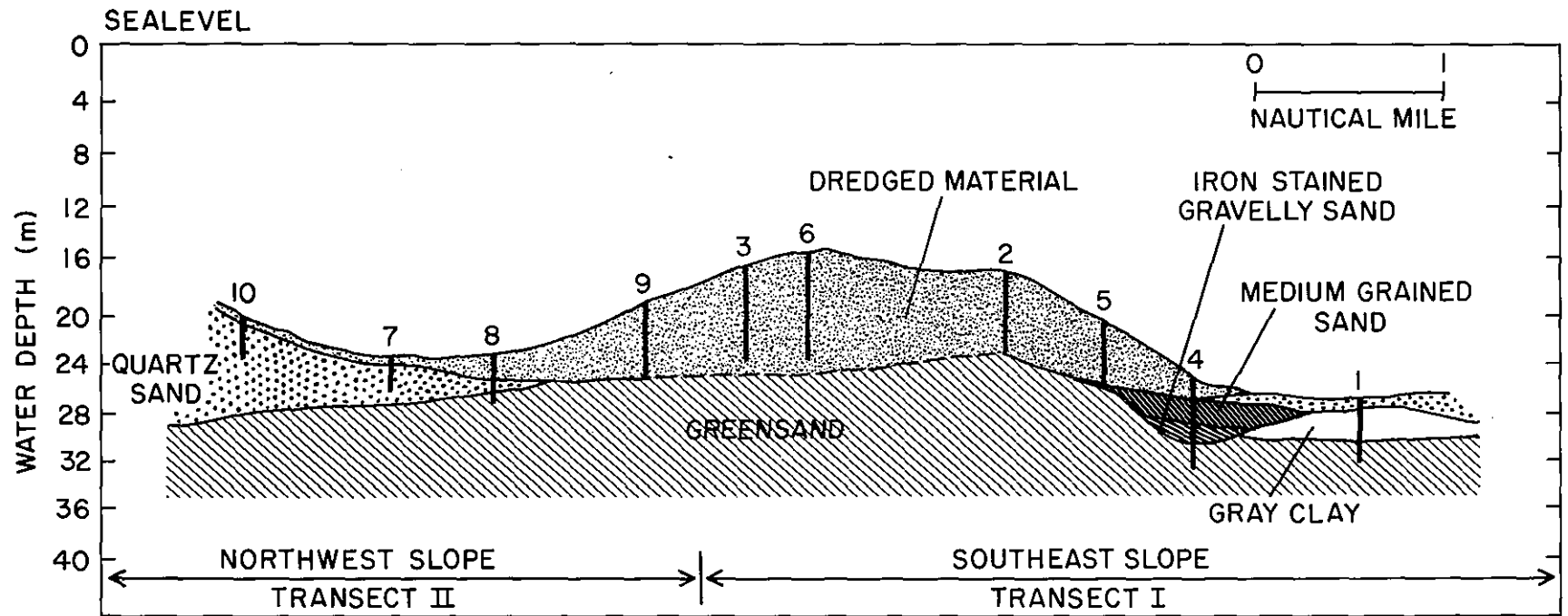


Figure 24. Cross-sectional profile of the study area along the two transects I and II, illustrating the lithology of the deposit. Vertical lines represent the actual lengths of the cores collected. Broken line indicates the uncertainty in the exact position of the dredged material/natural sediment boundary.

underlying natural sediment. This station provided the greatest penetration of the natural sediment of any of the 10 cores. Core 4 revealed the presence of a trough in the greensand that was later filled with two other sediment types. The lowermost stratum is a yellow, gravelly sand overlain by a bed of medium grained sand that contained significant amounts of echinoid (Sand Dollar) shells. This same material was also observed, overlying the greensand, in an adjacent core at station 5. A bed of gray clay, believed to be part of a back bay deposit, was observed in core 1, located downslope southeast of core 4.

#### 4.5 Sedimentary Processes

A factor of principal concern in this study is the movement of sediment at the dumpsite. Here, we have used the sediment distribution, on the deposit itself, to determine sediment movement and large scale sorting. Comparison of the mud fraction from the dredged material, in each of the cores, has yielded significant differences among cores. This differential movement of sediment from one portion of the deposit to another and the associated bed forms appear to be the direct result of movement of suspended and resuspended material away from the center of deposition. Other bed forms indicate that natural continental shelf sands, which are typical of the nearby sediment, are brought onto the deposit probably through storm events.

#### 4.5.1 Large-Scale Sediment Differentiation

Table 12 gives the mean, standard deviation, coefficient of variation and the range of the percentages of mud, sand and gravel for the samples taken from each of the cores. These were calculated separately for natural sediment and for dredged material. Cores 1 and 10 which were taken outside the perimeter of the deposit are also included in Table 12. The mud content (Table 12) is higher in three downslope cores (5, 8 and 9) than in the cores from the crest. Both cores 5 and 8 contain natural sediment at their bases which is clearly distinguishable from the dredged material. For instance, in core 8 the mean mud content of the dumped material is 65% while that of the natural sediment is 15%. The sand content of most of the cores is higher in the natural sediment than in the dredged material but we found that sand is a less sensitive indicator than mud and therefore sand content was not used in this analysis. Gravel content is, in most cases, rather low. Clearly there are differences in the characteristics of the dredged material from one core to another. The analysis of variance discussed below lends further statistical support to the above statement by providing the 95% confidence intervals for the means of these parameters.

In order to determine if there is any movement of the discharged material during or after dumping, an analysis of variance was performed on data for percentages of mud and gravel derived from the cores taken at the dumpsite. Only the dredged material component of each core was statistically analyzed. The results of the analysis of variance

Table 12. Mean composition, standard deviation, coefficient of variation, and the compositional range for the sediment cores collected in the New York Bight.

Core No.	Sediment Type	Parameter	Sediment Texture		
			Mud (%)	Sand (%)	Gravel (%)
1	Natural Sediment	Mean <sup>1</sup>	48	51	1
		SD <sup>2</sup>	41	40	2
		CV <sup>3</sup>	85	78	200
		Range <sup>4</sup>	1-97	2-97	0-8
2	Dredged Material	Mean	45	51	4
		SD	31	29	5
		CV	69	57	120
		Range	0.5-98	2-98	0-15
3	Dredged Material	Mean	37	54	9
		SD	32	33	13
		CV	86	61	144
		Range	0.3-95	5-99	0.3-50
4	Dredged Material	Mean	47	52	5
		SD	27	26	9
		CV	57	50	180
		Range	1-89	11-88	0-7
	Natural Sediment	Mean	27	68	3
		SD	24	21	2
		CV	89	31	67
		Range	1-67	33-97	0-28
5	Dredged Material	Mean	60	38	2
		SD	33	31	4
		CV	55	82	50
		Range	1-96	4-99	0-15
	Natural Sediment	Mean	11	86	3
		SD	7	5	3
		CV	64	6	100
		Range	4-21	79-91	0-8
6	Dredged Material	Mean	40	53	7
		SD	23	22	8
		CV	58	42	114
		Range	1-82	15-92	0.2-26
7	Dredged Material	Mean	24	64	11
		SD	7	10	7
		CV	29	16	64
		Range	18-36	56-79	3-18
	Natural Sediment	Mean	3	51	46
		SD	3	19	21
		CV	100	37	46
		Range	0-9	21-81	9-77
8	Dredged Material	Mean	65	31	4
		SD	26	23	8
		CV	40	74	200
		Range	20-97	3-81	0-29
	Natural Sediment	Mean	15	82	3
		SD	4	4	6
		CV	27	5	200
		Range	9-20	75-86	0-16
9	Dredged Material	Mean	61	28	11
		SD	24	18	16
		CV	39	64	145
		Range	26-97	3-63	0-58
10	Dredged Material	Mean	5	54	41
		SD	5	19	19
		CV	100	35	46
		Range	2-12	33-78	19-64
	Natural Sediment	Mean	2	93	5
		SD	2	7	8
		CV	100	8	160
		Range	1-7	70-99	0-29

<sup>1</sup>Mean Composition

<sup>2</sup>Standard Deviation

<sup>3</sup>Coefficient of variation

<sup>4</sup>Compositional range

are shown in a graphic form in Figure 25. Core 1 was omitted because it contained no dredged material. The results indicated that some cores contained significantly different amounts of gravel and mud.

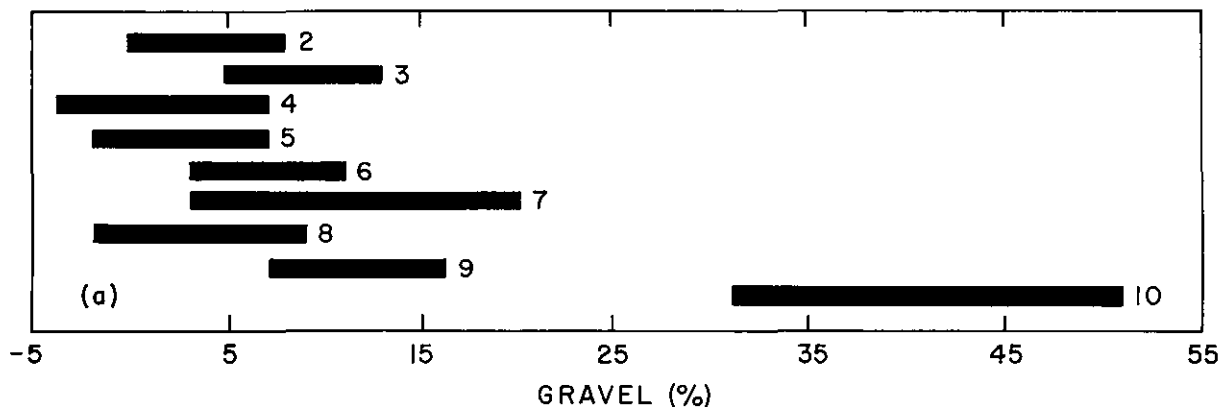
Dredged material from core 10 clearly was not related to the other cores based on gravel content. The differences in other cores were generally minor to each other in this respect. The high gravel content, representative of dredged material, in core 10 is surprising in view of the distance ( $\approx 3$  km) of this station from the designated disposal site. It is extremely unlikely that material in this size class could be transported to such an extent by any natural process. The probable cause of this anomaly is so-called "short dumping" outside the legally designated site and then winnowing of the fine fraction by currents.

The analysis of variance of the percentages of the mud fraction of these samples (Figure 25b) clearly shows differences among the cores and the grouping is different than that of gravel content. Cores 5, 8, and 9 contain significantly more mud than do cores 2, 3, 6, 7, and 10. Core 4 falls between the two groups.

The analysis of variance demonstrates that there is significantly more mud in cores taken at the base of the deposit (5, 8, and 9) than in those from the crest. All of the stations containing higher mud content are below 22 meters depth. Stubblefield *et al.* (1977) have observed, through surface grabs and side-scan sonar, that a high percentage of mud is present in surficial sediments around the perimeter of the site. They also observed that mud deposits elsewhere in the bight generally occurred at depths greater than 24 m. The evidence,

A. ANOVA TABLE

	DF	SS	MS=SS/DF	F-Ratio
Treatments	8	6494	812	8.00
Error	128	12980	101	
TOTAL	136	19473		



B. ANOVA Table

	DF	SS	MS=SS/DF	F-Ratio
Treatments	8	29370	3671	4.77
Error	112	86169	769	
Total	120	115539		

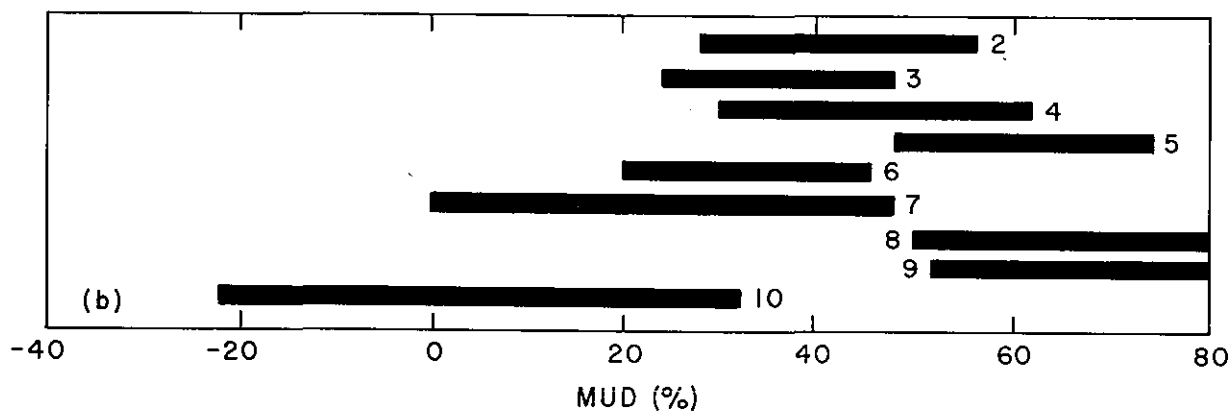


Figure 25. Statistical variations about the mean value of gravel and mud fractions in each core, based on 95% confidence intervals. The core numbers are given. Core 1 is not included because it apparently contained no dredged material.

therefore, indicates that fine grained sediments are effectively transported to and deposited on the slopes of the deposit, particularly the northwest slope.

Recent work by Proni *et al.* (1980) wherein acoustic profiling was employed to trace individual dump events has demonstrated that there is an outward pulse, along the bottom, away from the site of the dump event. This pulse has been observed to reach velocities of 50-60 cm/sec, sufficient to transport unconsolidated sediment and to erode fine grained sands. Thus the shock wave generated by the dumping event provides a mechanism to move finer grained sediment away from the center of dumping.

Bed Thickness. In the cores of the dredged material dumpsite the form and thickness of individual beds of sediment are important indicators of the individual dumping events. Color and sediment type were the obvious characteristics by which various distinct dump events could be recognized. For example, a color photograph of core 6 shows these features distinctly (Figure 26). In this section, seven discrete beds of clearly differentiated sediment can be seen. This observation is also evident in the x-radiographs of the same core section shown in Figure 27. The radiographs also reveal the internal structure of the sediment that may otherwise not be seen. This is illustrated by the mud layer found in the basal unit of section OA in core 6 (Figure 27). The top part of the mud unit exhibits laminar structure while the lower portion of the unit has a mottled internal structure and may therefore be a separate dumping event.

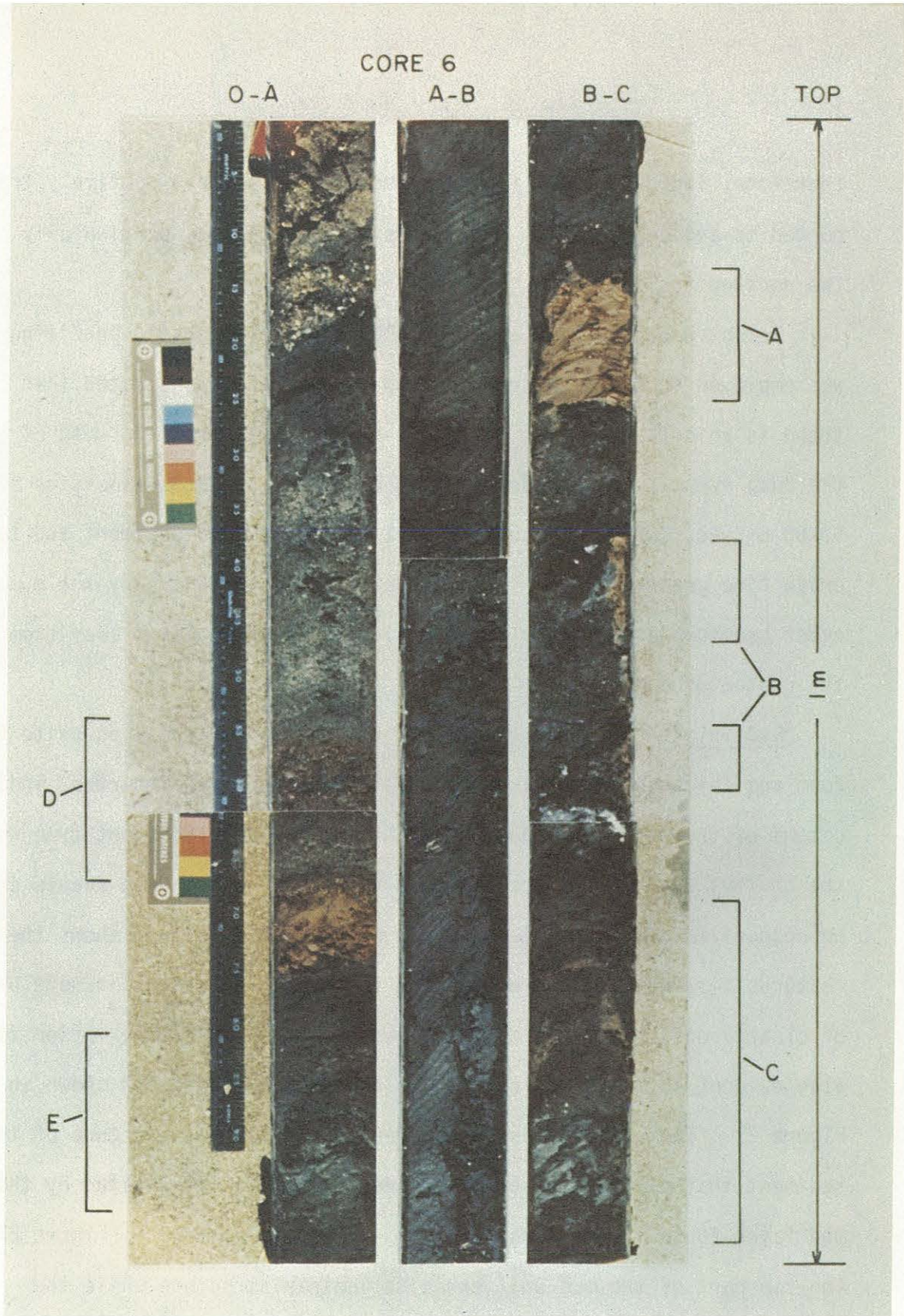


Figure 26. Color photograph showing distinct textural features in sections OA, AB, and BC of core 6: (A) varved red clay; (B) clay galls; (C) massive bedding; (D) graded bedding; and (E) laminated bedding.

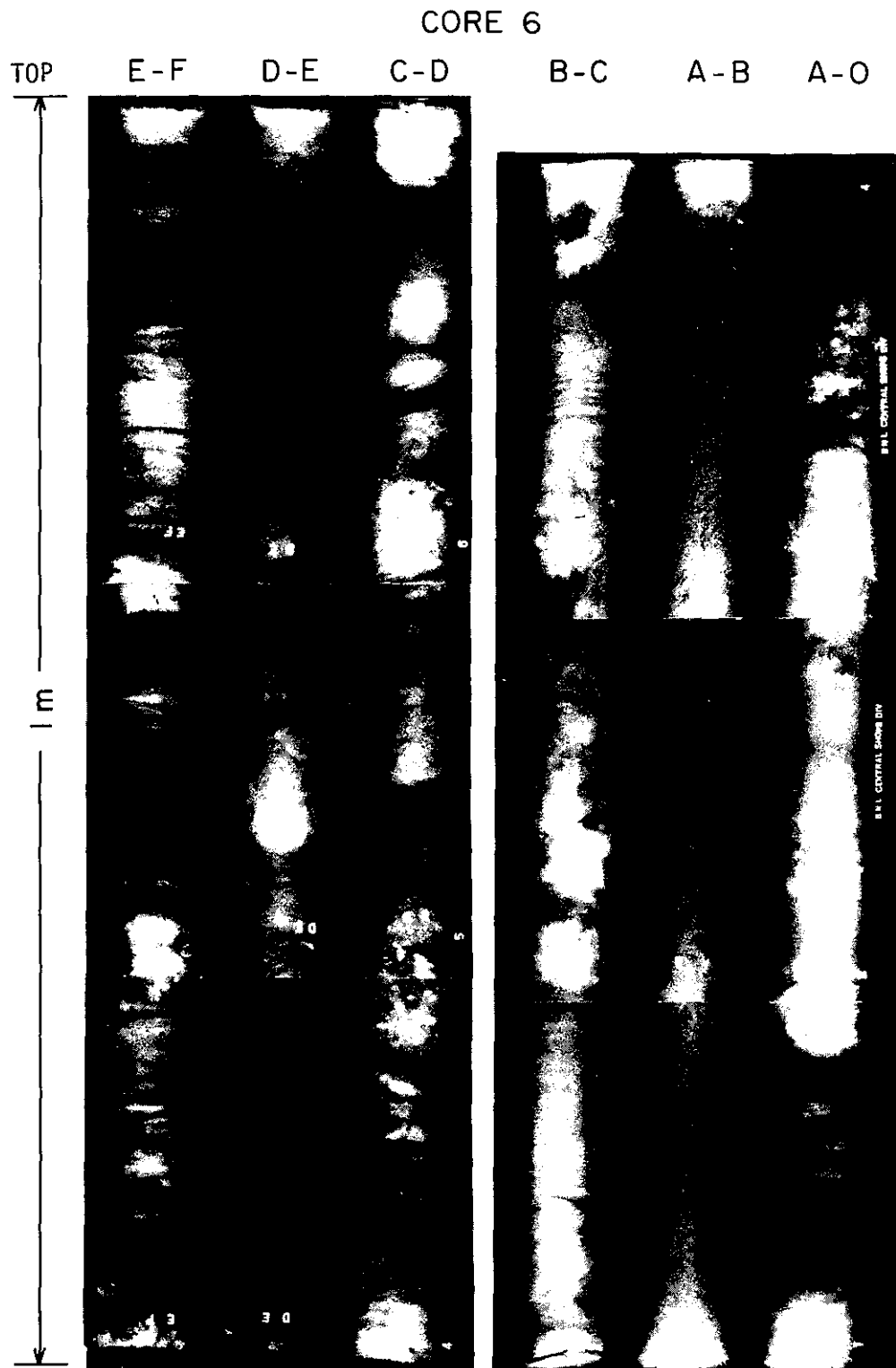


Figure 27. Contact prints of x-radiographs of the top six meters of core 6. Sections OA and EF represent the core top and the basal unit, respectively.

Very thick massive bedding ( $\approx 1$  m thick) is illustrated in section AB of core 6 shown in Figure 26. The material is relatively homogeneous, in this case a sandy mud containing small shell fragments. The x-radiographs (Figure 27) show it to have an undifferentiated mottled texture. Massive bedding also occurs in thinner layers and, again, is characterized by a lack of differentiation within the bed. This form of bedding is also seen in the natural sediment at the bottom of core 4.

Although one would expect to see frequent examples of graded bedding occurring in the cores, there were actually very few observed. In these cases, the grading involved large gravel sized clasts which had sufficient mass to sink through the cloud of dumped material rapidly enough to settle first. Figure 26 (section OA) shows a coarsely graded unit. In most cases, the settling time appears to be too short to allow noticeable differentiation of sizes.

In order to better define the thicknesses of the beds resulting from the discharge of sediment at the site, three cores 2, 3, and 6 from the apex of the pile were examined for bedding thickness. Only clearly defined, discrete beds were counted. In many cases there were thick beds present which showed no clear boundaries. These were not counted as it appears that they are the product of a series of dump events which deposited similar sediment. The cores taken at the edge of the pile show relatively few instances of discrete, identifiable beds. This would be expected if most of the sediment on the periphery of the deposit were transported material. This is borne out by the

statistical evidence mentioned previously and by the stratigraphy discussed later. The stratigraphic correlations are much better for the cores taken at the apex of the deposit than for those at the downslope stations.

Figure 28 is a histogram showing the thickness of the observed beds in the dredged material deposit. Figure 28a illustrates a broad range of bed thicknesses; the most frequently occurring beds being 0-5, 5-10, 10-15 cm in thickness. A further breakdown of these three bed thicknesses is presented in Figure 28b, showing the overall average thickness to be approximately 10 cm, with about 50% of the sampled layers being 7 cm or less in thickness. Beds greater than 10 cm in thickness are relatively less common.

Sediment Sorting and Mixing. An analysis of the data collected on mean grain size and standard deviation provides further information on the sediment differentiation processes within the deposit. A plot of standard deviation versus mean grain size shows the relationship of these two parameters for all samples analyzed. Standard deviation is the measure of spread within a sample; in this context, it has been taken to denote the degree of sorting of a sample. A low value of standard deviation means that the sediment is well sorted. According to Folk (1974), a sample with a standard deviation greater than  $2\phi$  is considered to be very poorly sorted. Folk and Ward (1957) observed that minima in sorting values (good sorting) correspond to modes in the sediments' grain size. Maxima in sorting values occur between two modes where mixing of the two sediment types take place. Thus a

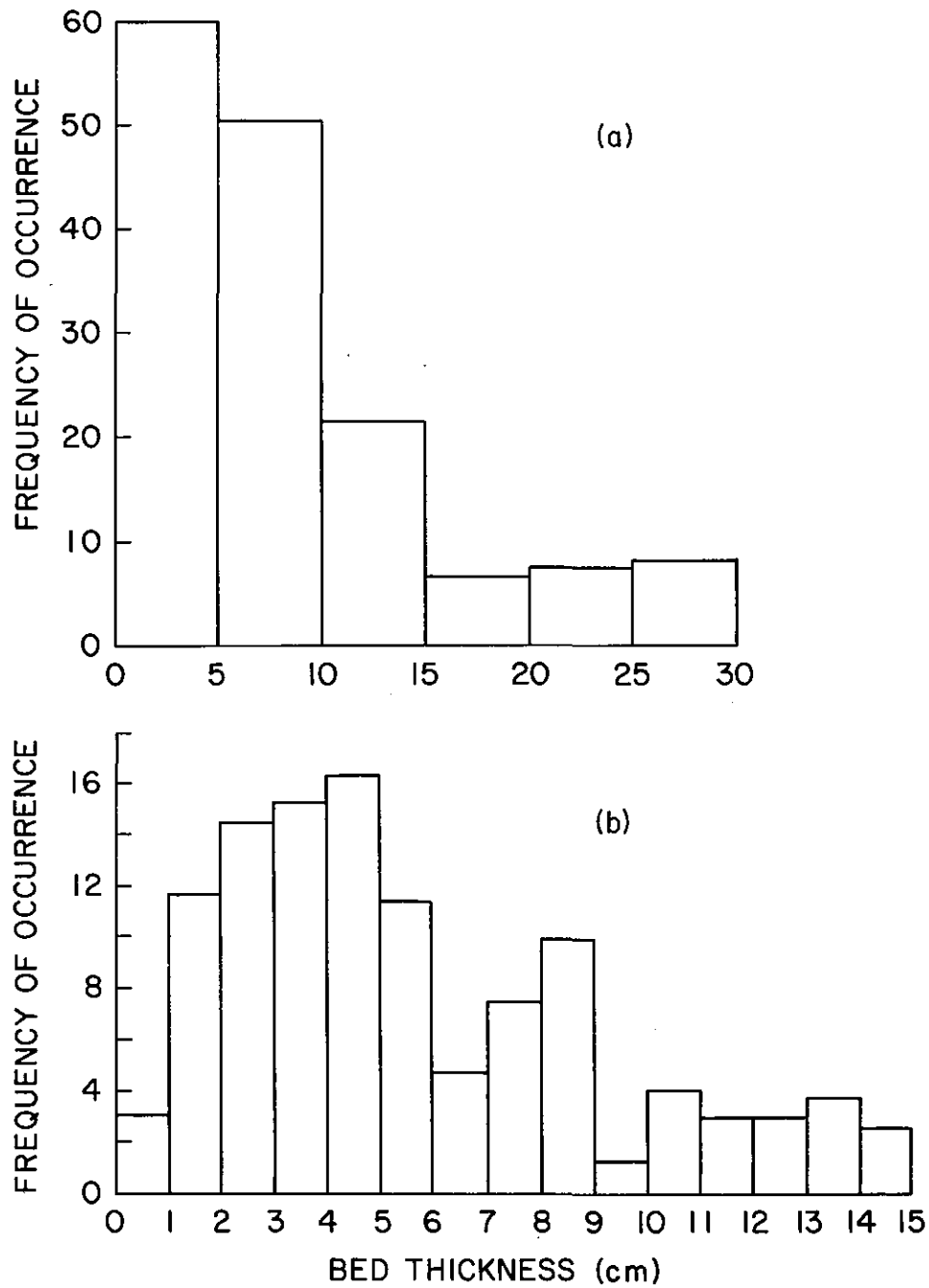


Figure 28. Histograms showing the frequency of occurrence of beds of various thicknesses in cores 2, 3, and 6 within the dredged material deposit: (a) frequency of occurrence of beds varying in thickness from 0-5 to 25-30 cm; and (b) a breakdown of the first three intervals given in (a) into bed thicknesses varying from 0-1 to 14-15 cm.

plot of mean grain size versus standard deviation can be used to identify major groups of sediment within a deposit.

Figure 29a depicts the mixing and modality of the study area samples, showing the presence of three distinct clusters. One is located between  $0\phi$  and  $2.5\phi$  on the grain size axis (group A) which is relatively well sorted. A second minor cluster (group B), around  $3.5\phi$  on the grain size axis, is more diffuse and represents poorly sorted material. The third cluster (group C) represents fine grained ( $5\phi$ - $8\phi$ ), very poorly sorted material. In general, the dredged material muds are represented by group C and the natural sediments of the area are found in group A. The less distinct cluster, group B, may illustrate the mixing that occurs between the two and, in some cases, sediment types such as the greensand facies. This division is more clearly illustrated in Figure 29b-d which show mean grain size plotted against standard deviation for individual cores. Figure 29b represents core 10 containing, primarily, natural shelf sediment. The observed distribution closely resembles that of natural sediments shown as group A in Figure 29a. Figure 29c shows core 6 that contains only dredged material. As expected, this distribution exhibits a wide scatter in terms of sorting and mean grain size. Comparison of this plot with Figure 29a shows an overlap with clusters B and C, representing dredged material and mixed sediments. Figure 29d illustrates core 4 that consisted of both dredged material and natural sediment. This is reflected by two distinct clusters, within the sampling, the relatively well sorted, coarse grained material representing natural sediment and the very poorly

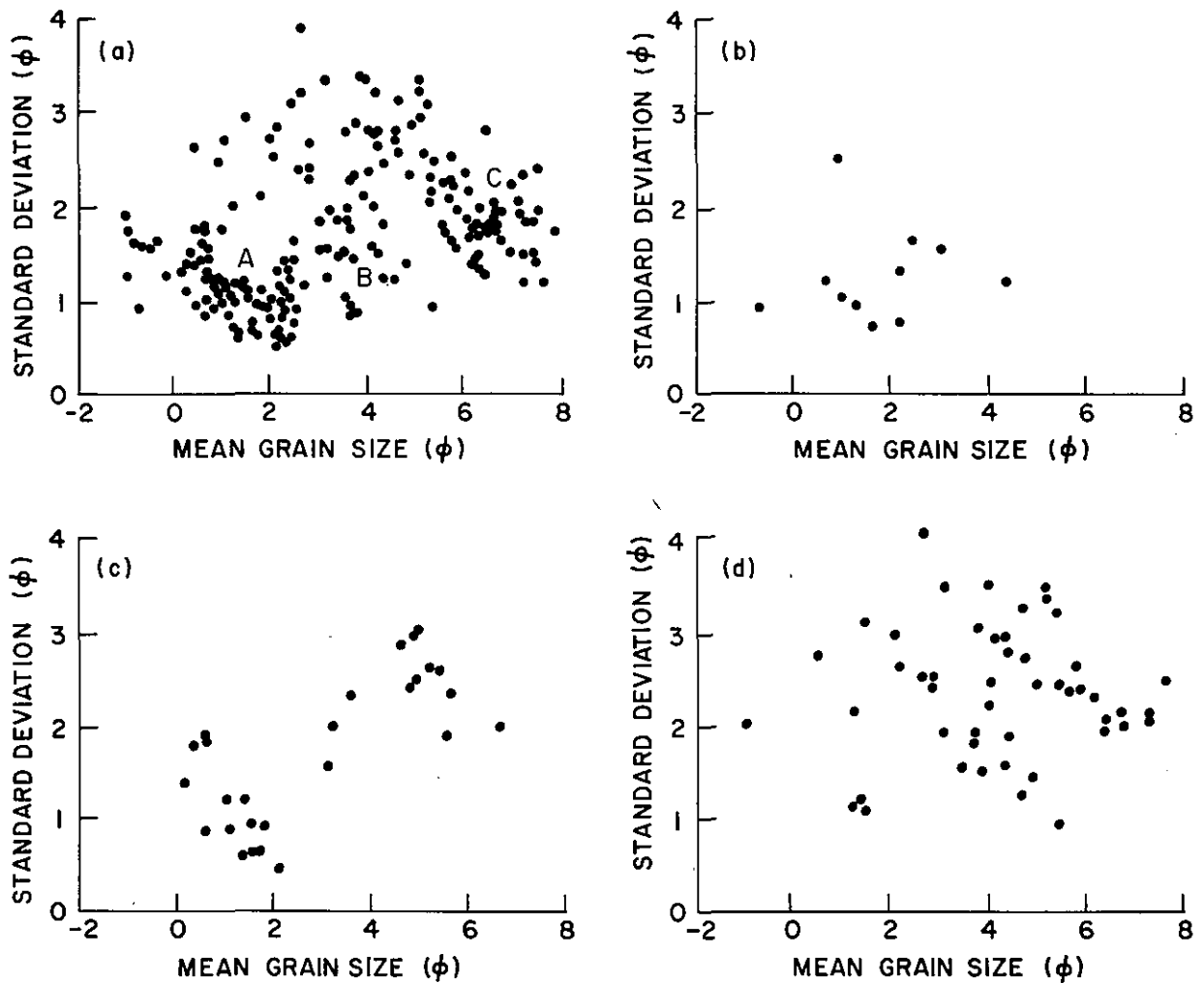


Figure 29. Plots of mean grain size versus standard deviation for dredged material deposit sediments: (a) for all samples analyzed. Note the clustering into three groups - natural sediments (A), dredged material (C) and a mixture of the two (B); (b) for samples from core 10. Most of this material is natural sediment; (c) for samples from core 4. Approximately one-half of the length of this core was composed of dredged material and one-half was natural sediment underlying the deposit; and (d) for samples from core 6. Most of this material falls into the dredged material and mixed sediment groups shown in (a).

sorted, fine grained sediment of the dredged material. This grouping corresponds to clusters A and C in Figure 29a.

Sediment Lamination. Certain sedimentary structures which are illustrative of the processes that are associated with dumping were observed in the dredged material cores. For example, both laminated and coarsely interlayered sediments were frequently observed. Only one set of ripples and relatively few instances of graded bedding were noticed. Neither load deformation structures nor water escape structures were found.

A major feature of many of the sediments found at the site was the presence of laminated beds 2-15 cm in thickness. This bed form was, generally, found to be comprised of sand and sandy muds and was seen throughout the cores. Individual laminae were observed to be about 1 mm or less in thickness and often each was composed of sediment that was clearly of a different nature than that of the adjacent laminae. The sediment structure being discussed here is not the interlayered, flaser-like bedding of clean sand in thick beds of mud, rather, the horizontal beds of laminations of different sediment types. Frequently some of this material was clearly artifact in nature.

Figure 30 depicts two typical beds of laminated sediment observed in sections of core 6. X-radiographs of cores 4 and 6, showing similar sedimentary structure, are given in Figures 31, 32 and 33. It is estimated from these two cores that laminated sediments comprise a significant proportion of the material in the deposit. For example, the x-radiographs of the two cores show that in core 6, taken at the pile apex,

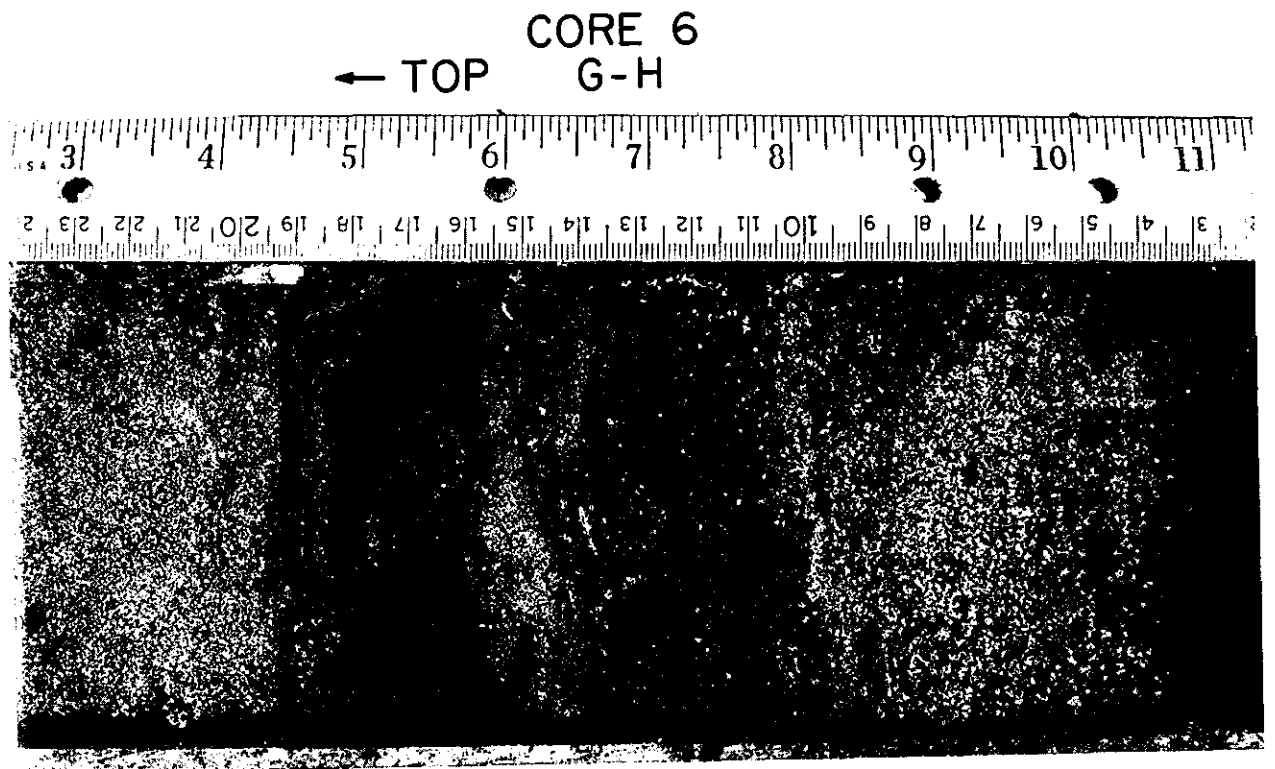
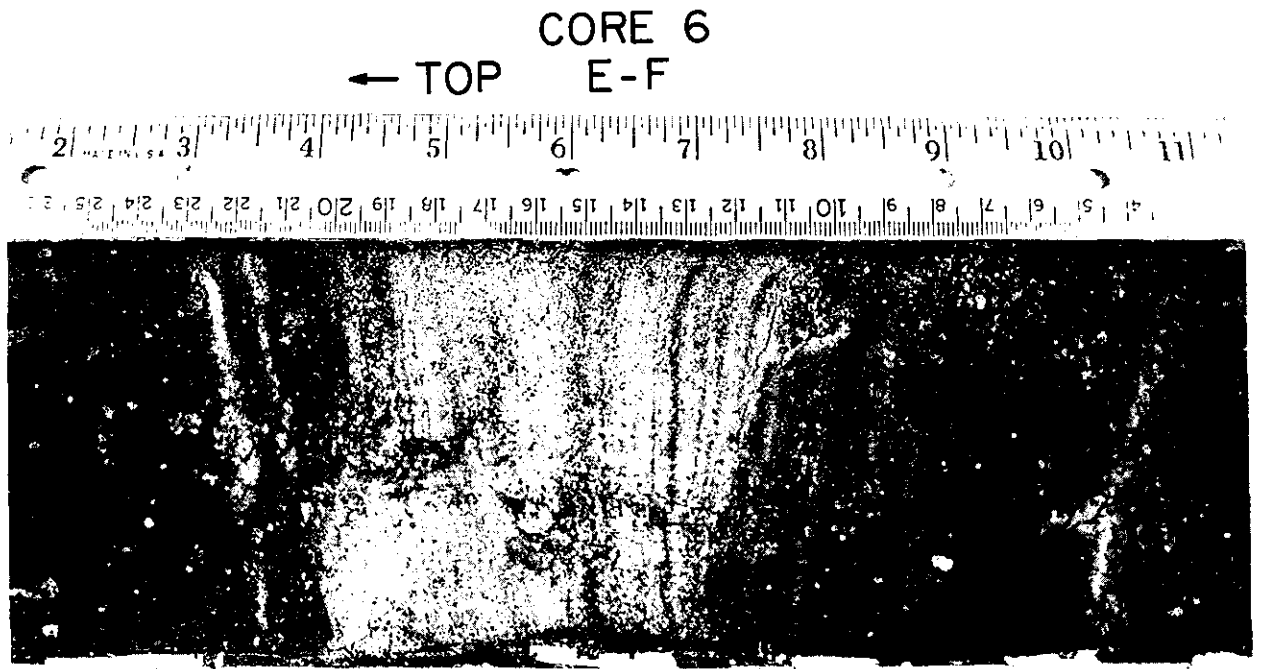


*Figure 30. Two sections of core 6, showing the laminated sediment structure.*

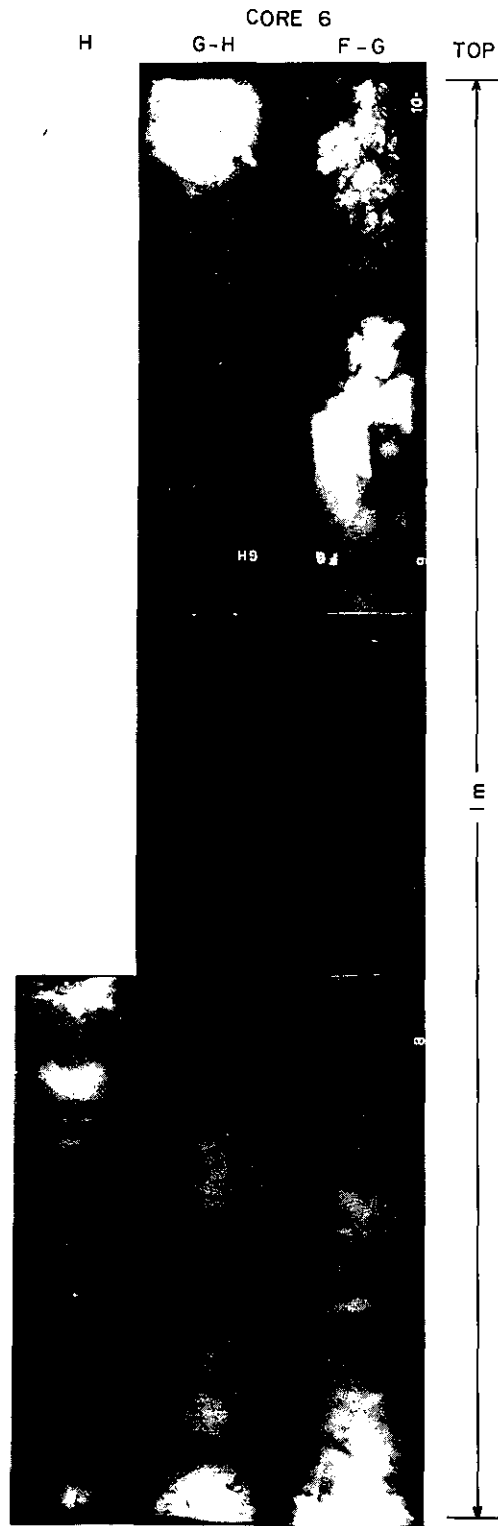


Figure 31. Prints of x-radiographs of the lower sections of core 6.

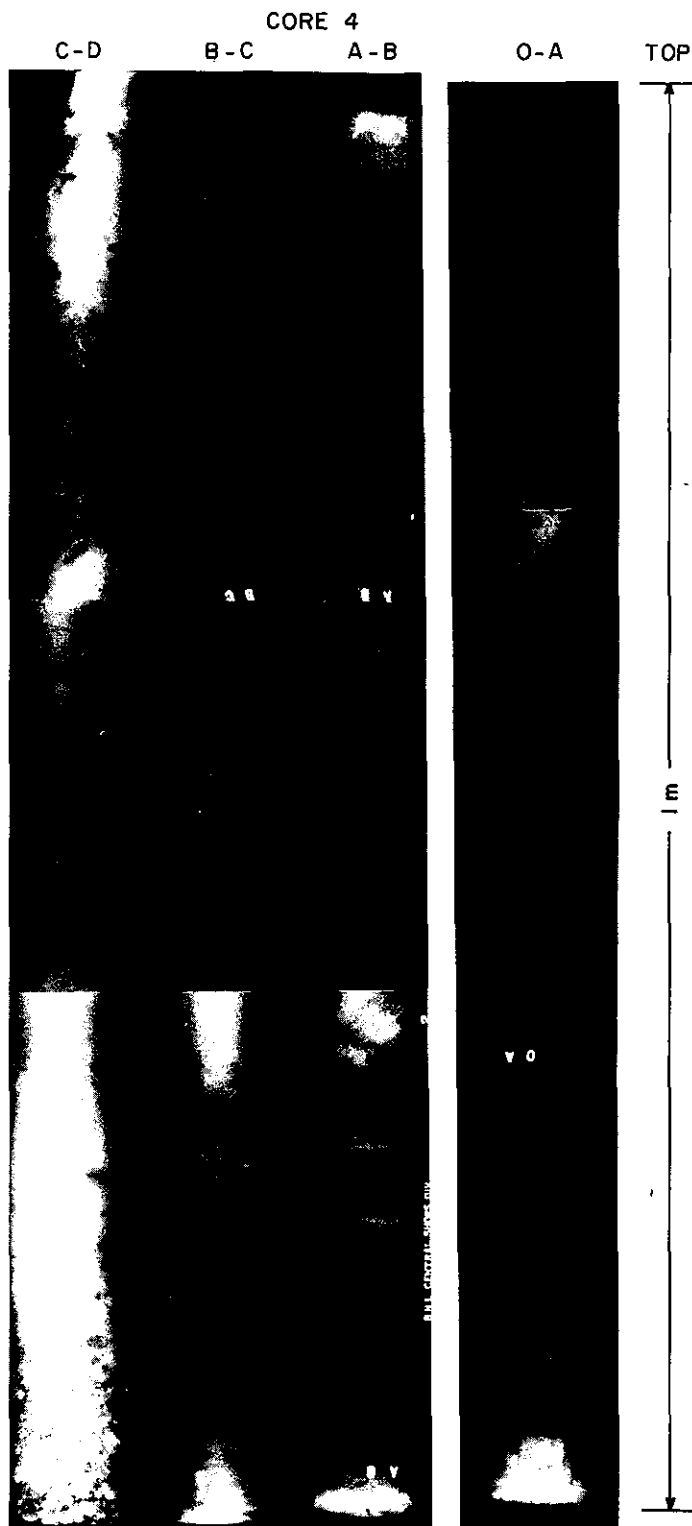


Figure 32. Prints of x-radiographs of the upper sections of core 4. Note the foreset and bottomset bedding in section AB. Section OA represents the core top, underlain by AB, BC, and CD.

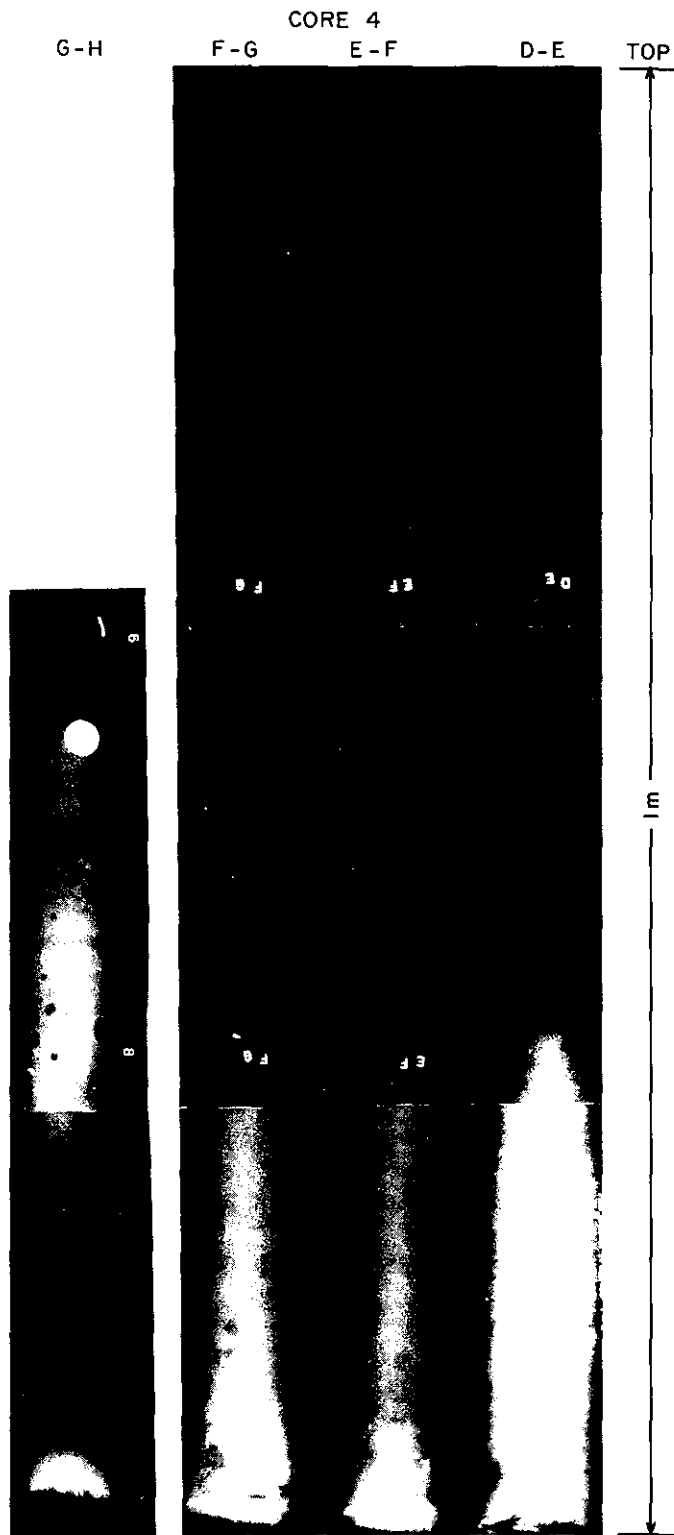


Figure 33. Prints of x-radiographs of the lower sections of core 4. Section GH represents the basal unit of the core.

22% of the dredged material was laminated. In core 4, which is located on the southeastern flank of the pile, only 6% of the dredged material was laminated. The horizontally laminated sediments are directly related to dredged material dumping while in the 5 m of natural sediment x-radiographed there is not one instance of laminated sediment. The laminated sediments are confined to the primary area of dumping (center of the deposit) and are present throughout the length of the cores. In contrast, very little horizontal lamination was observed in the dredged material sampled on the fringes of the deposit in core 4.

Another related sedimentary structure observed in core 4 was a series of very thin cross-laminae of sand embedded in mud. The angle of these laminae varied from 15° at the top of the bed to almost 45° near the bottom of the 2 meter thick bed. At the core base horizontal bedding reappeared. X-radiographs of core 4 faintly show the cross-bedding. Station 4 is located on one of the steepest slopes of the deposit, therefore, cross-bedding observed in the dredged material section of this core may be foreset bedding, the result of a post-dumping flow of material down the slope which eventually (as shown by the changing angle of the bedding with depth) was deposited in the downslope area; the horizontal bedding being bottom-set bedding.

#### 4.5.2 Sand Incursion

Sand lenses and thin laminae were commonly found throughout the beds of mud on the dumpsite. Figures 34 and 35 show these sedimentary

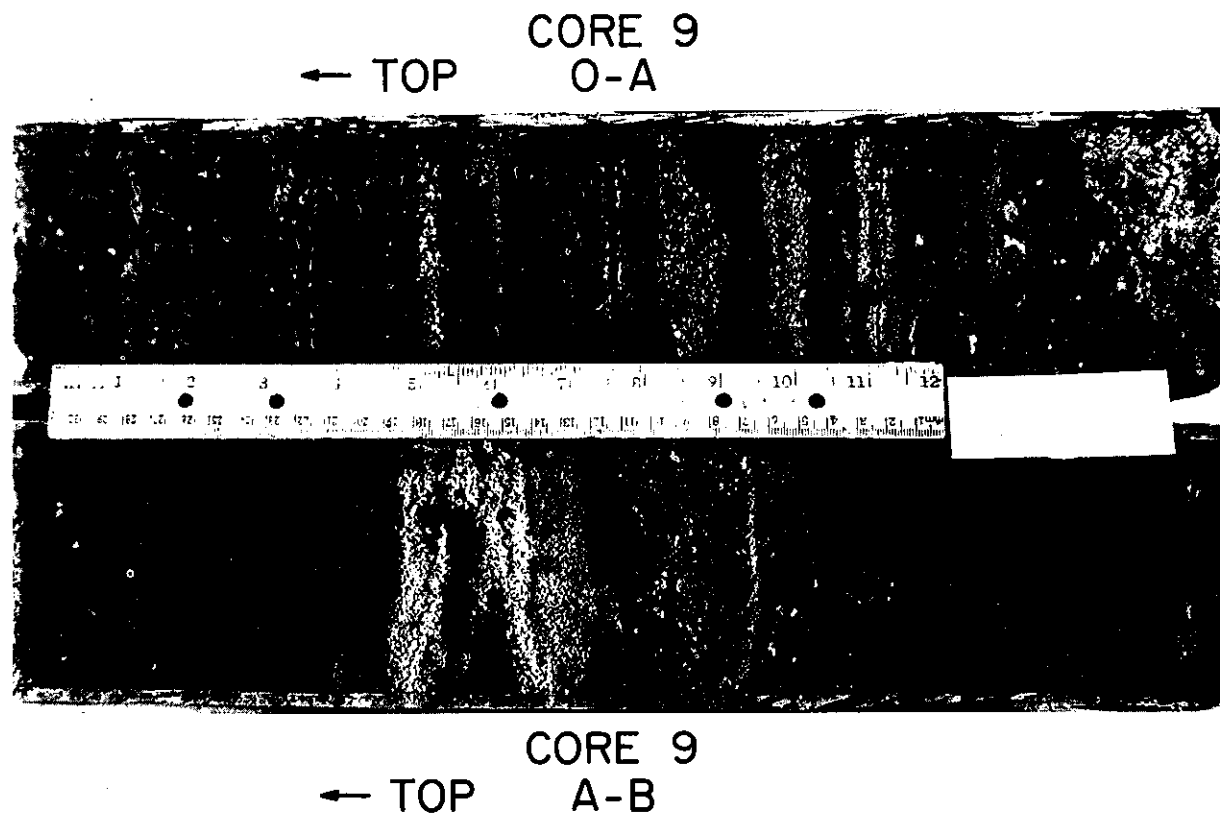


Figure 34. Typical interlayered sand and mud texture observed in dredged material in core 9.

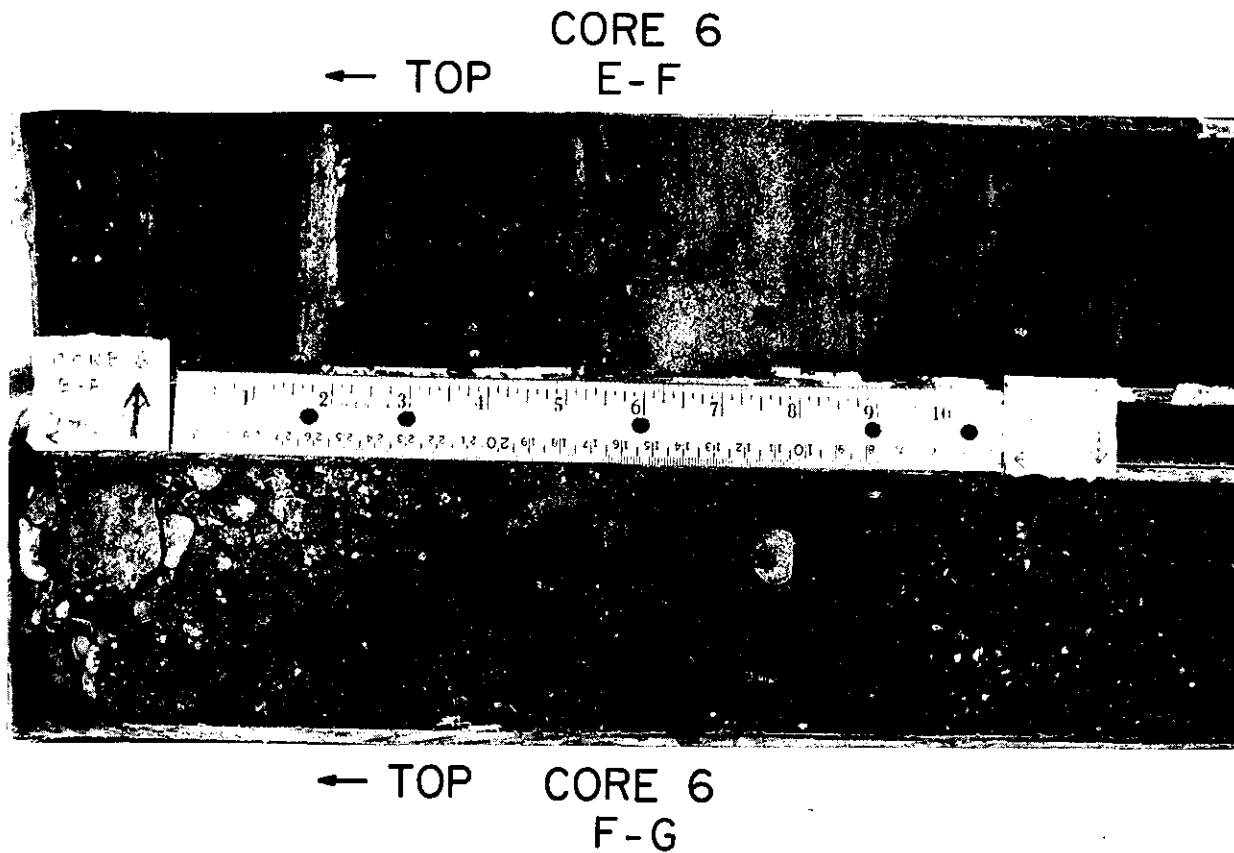


Figure 35. Sections EF and FG of core 6. Section EF shows interlayered sand and mud as well as a bed of laminated sand. Section FG shows massively bedded sandy mud containing fragments of the bivalve *Nucula*. Note the presence of gravel intermixed with mud at the top of section FG.

features in cores 9 and 6. The sand lenses are generally composed of medium to fine grained glauconite sand. This is similar to the greensand found beneath the dredged material deposit and at the natural sediment surface in many small erosional windows in proximity to the site. It is thought, therefore, that the sand forming the lenses originated from the surrounding areas and was carried onto the dumpsite as traction load by storm currents and/or waves. Conner *et al.* (1979) observed that bottom currents in the New York Bight, due to storms, can reach velocities of 30 to 70 cm/sec which are sufficient to erode and transport fine sands. Similar sedimentary forms, within thick beds of mud, have been attributed to storms and unusually strong tidal action (Reineck and Singh, 1973). These structures have also been found in the Hudson estuary (Olsen *et al.*, 1978) and in a Georgia tidal inlet (Oertel, 1973) and are reported to be the result of similar processes.

In order to estimate the amount of material brought onto the dredged material deposit from surrounding areas, as a result of strong currents, the thickness of the flaser-like greensand structures were measured in cores 5, 6, and 9. It was found that these beds comprised an average of 8% of the thickness of the dredged material found in the cores. If this is representative of the entire dumpsite it is a significant input to the accumulation, with a corresponding dilution effect on pollutants within the pile. Conner *et al.* (1979) believe that as much as 10% of the annual amount of dredged material dumped

on the site may be carried away by currents. Strong currents may, therefore, carry away as much material from the site as they bring to it. It is important to note that most of the material lost would be finer grained contaminated mud while the sediment replacing it would be clean sand.

Evidence presented previously shows that within samples of mud taken from the dredged material there are sometimes modes in the 4-5 $\phi$  size class. This sediment appears to be greensand. Therefore, this material is not only brought to the deposit in discrete lenses but also mixed with the dumped mud. The estimate of 8% addition to the volume of the deposit must therefore be regarded as a conservative estimate.

#### 4.6 Geochemical Depositional Record

##### 4.6.1 Depth Distributions of Metals and Organic Matter

The metal concentration versus depth profiles are displayed in Figures 36-40. Results show that the concentrations of metals present in the dredged material sediments are highly variable and considerably elevated, in some cases more than three orders of magnitude, over concentrations observed in sediment outside the deposit and in natural sediment underlying the deposit. Table 13 shows the range of values observed for each metal and organic matter within individual cores and from one core to another. Depth distribution of metals varies widely for individual metals and from one station to another. In most cases, Pb and Cu profiles show close correspondence. Ag, Cd, and Hg and Fe and Mn also co-vary strongly with depth.

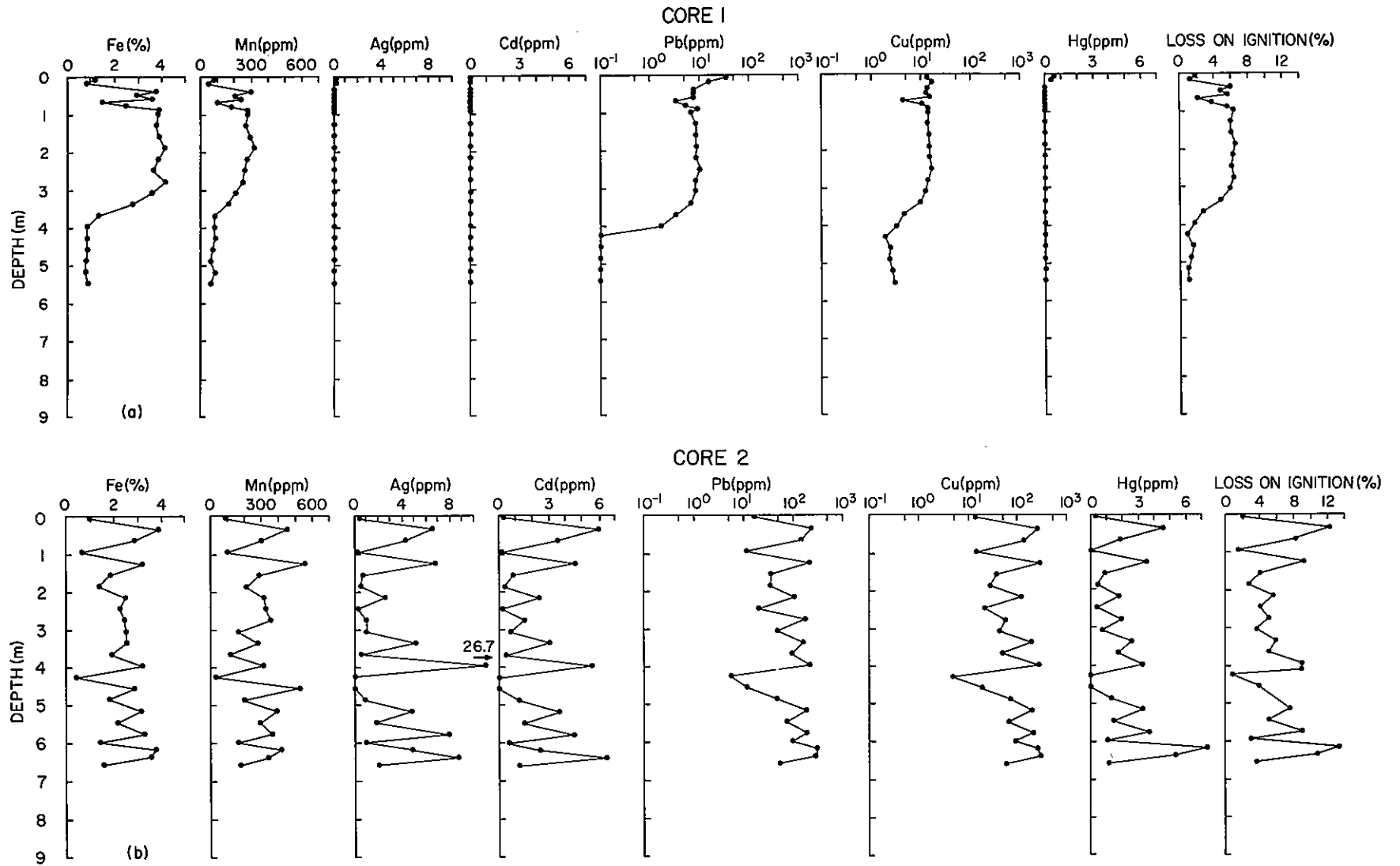


Figure 36. Depth distribution profiles of metals and organic matter: (a) core 1; (b) core 2.

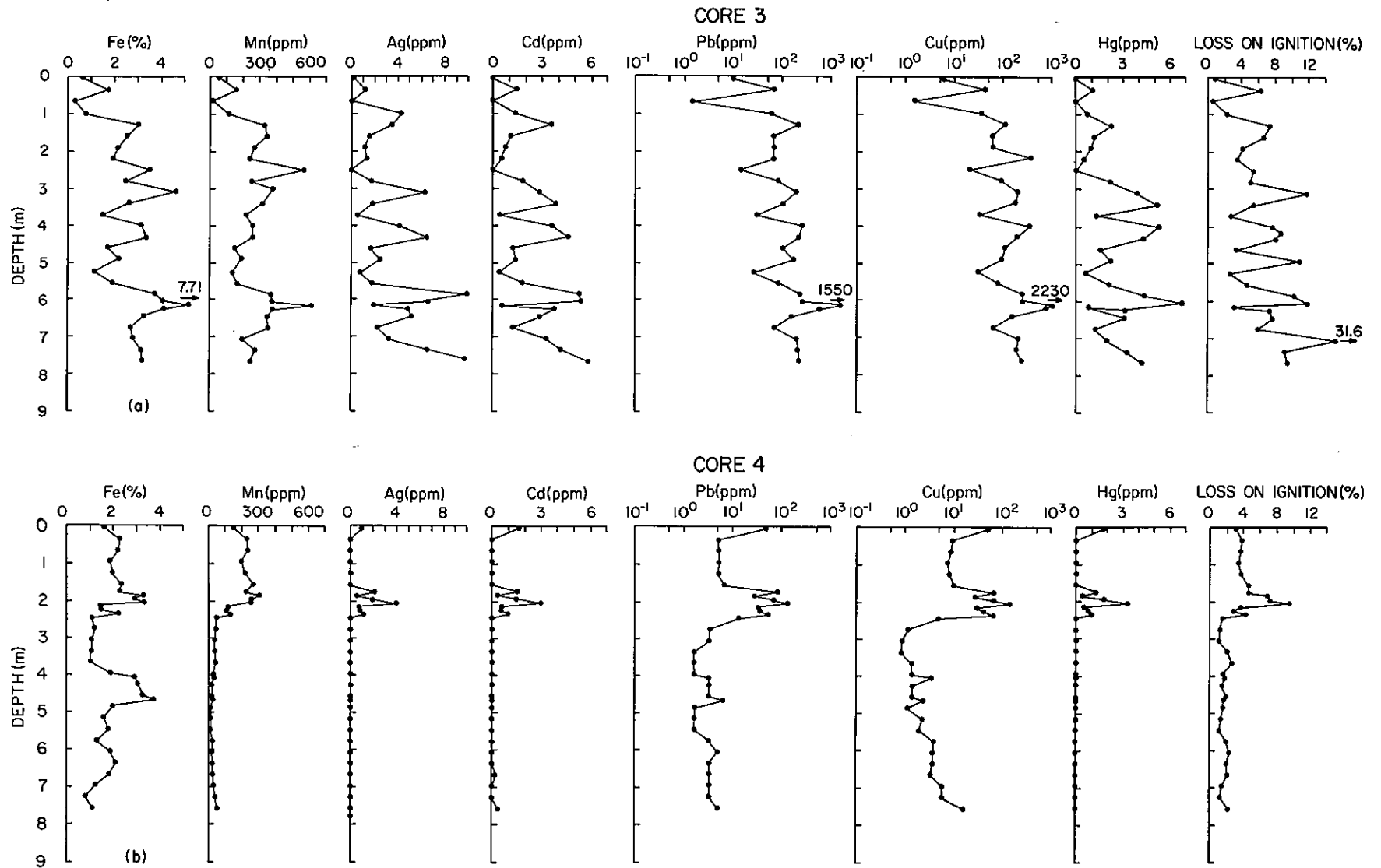


Figure 37. Depth distribution profiles of metals and organic matter: (a) core 3; (b) core 4.

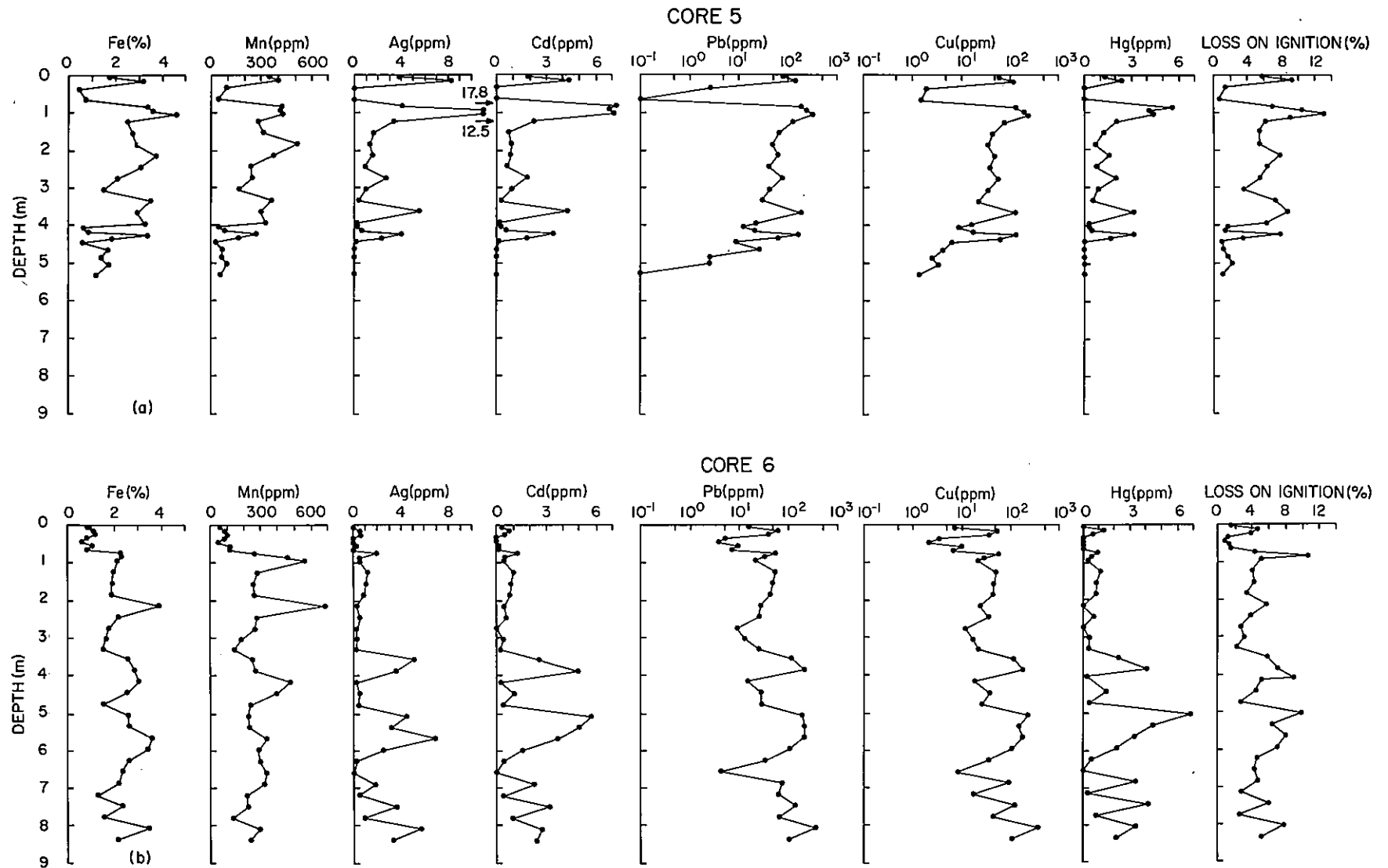


Figure 38. Depth distribution profiles of metals and organic matter: (a) core 5; (b) core 6.

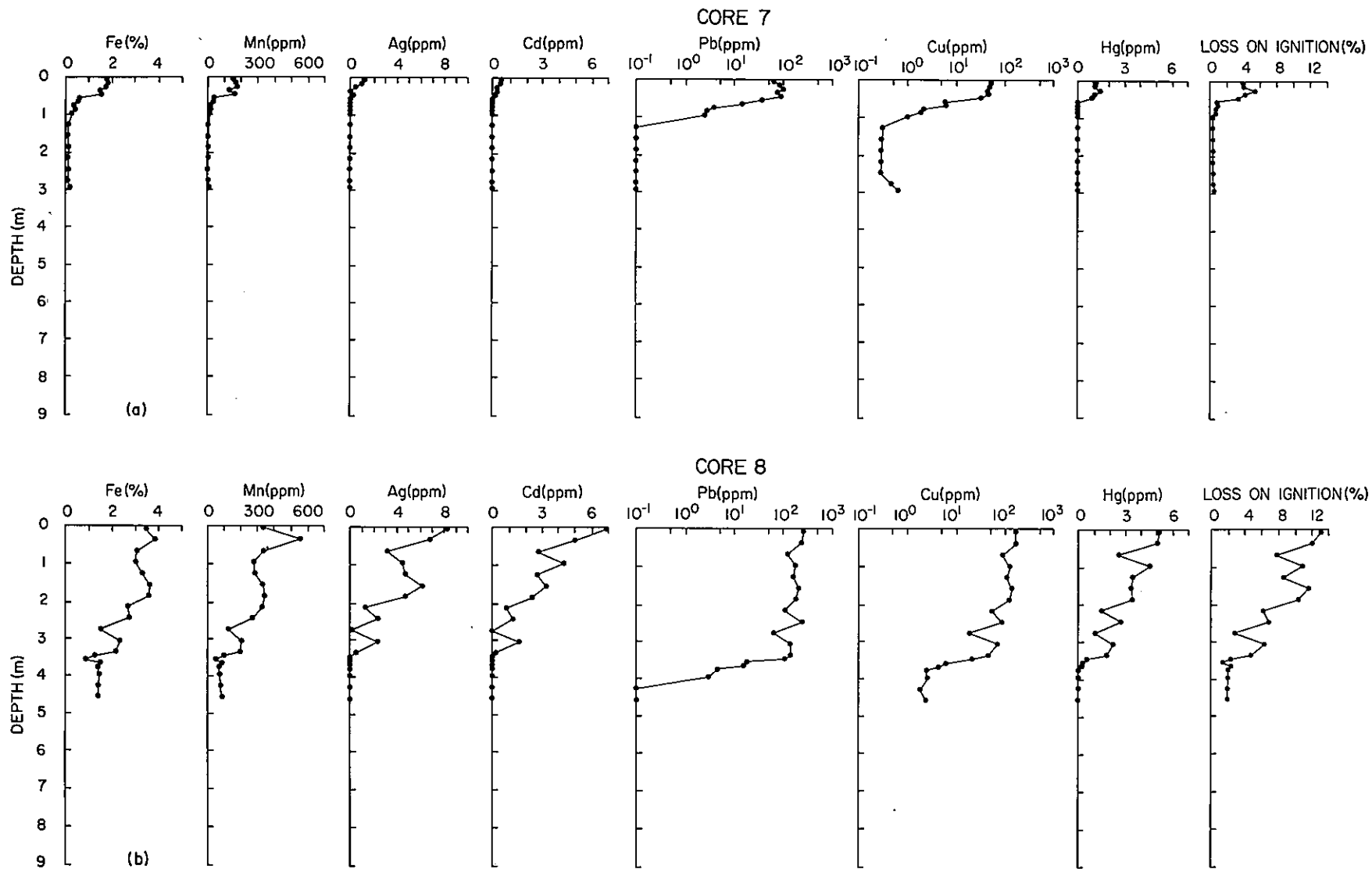


Figure 39. Depth distribution profiles of metals and organic matter: (a) core 7; (b) core 8.

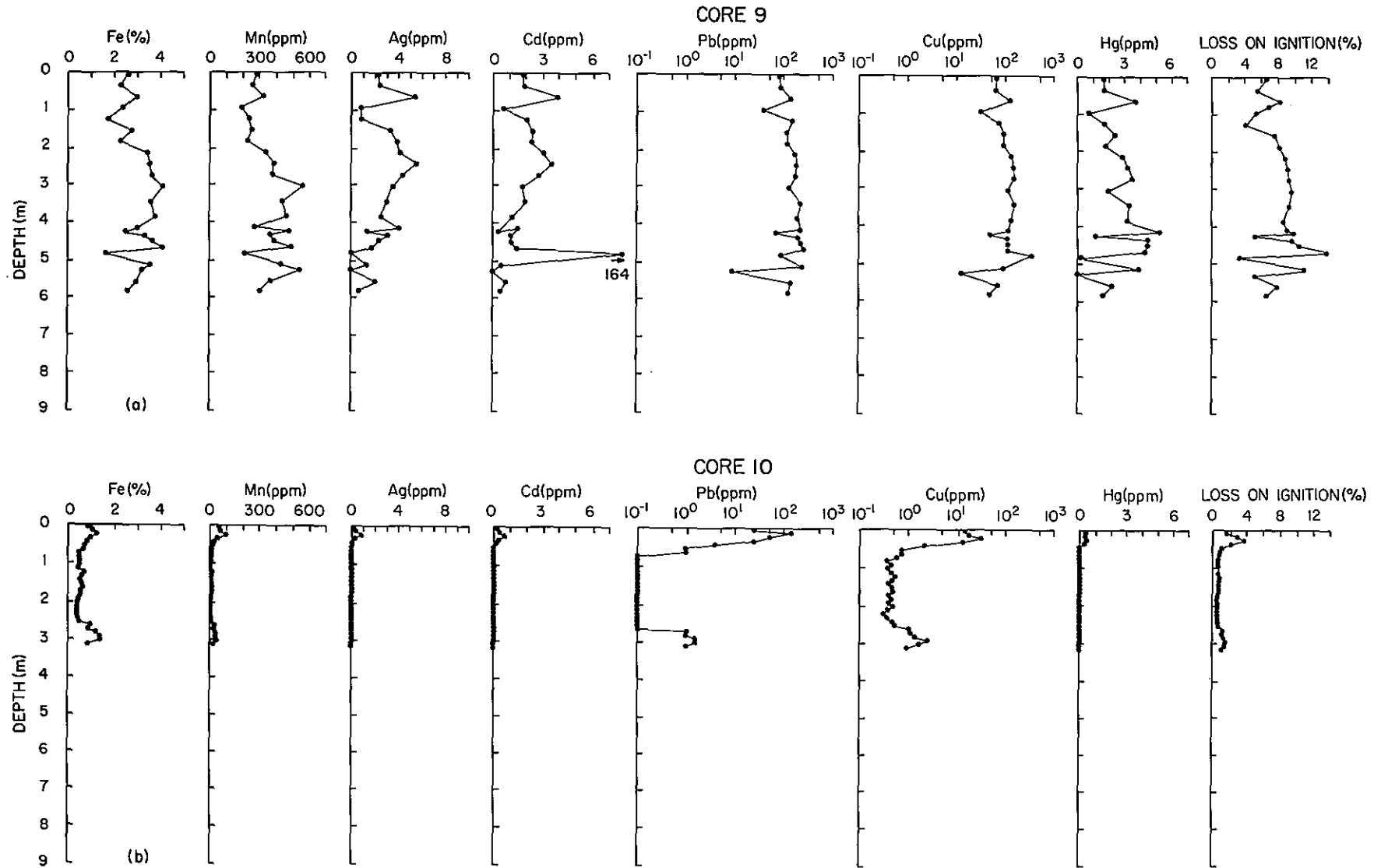


Figure 40. Depth distribution profiles of metals and organic matter: (a) core 9; core 10.

Table 13. Range of metal concentrations and organic matter in sediment cores from the dredged material deposit.

Core No.	Fe (%)	Micrograms per Gram						Organic Matter (%) <sup>1</sup>
		Mn	Cu	Pb	Cd	Ag	Hg	
1	0.83-4.19	46.7-318	2.0- 17.3	b.d.- 33.6	b.d. <sup>2</sup>	b.d.- 0.3	b.d.-0.45	0.89- 6.6
2	0.43-3.92	26.9-556	4.9- 302	5.7- 308	b.d.- 6.5	b.d.-26.7	b.d.-7.43	0.84-13.5
3	0.31-7.71	21.0-614	1.6-2230	1.5-1550	b.d.- 5.8	b.d.-10.0	b.d.-6.80	0.58-31.6
4	0.80-3.72	11.4-306	1.1- 143	0.8- 139	b.d.- 1.7	b.d.- 4.0	b.d.-3.32	1.14- 9.5
5	0.47-4.61	31.0-512	1.9- 330	3.9- 328	b.d.- 7.3	b.d.-17.8	b.d.-5.58	0.75-13.1
6	0.62-3.90	51.8-683	2.2- 363	4.0- 365	b.d.- 5.8	b.d.- 6.9	b.d.-6.90	0.82-10.7
7	1.82-0.09	2.8-176	0.3- 50.7	b.d.- 101	b.d.- 0.5	b.d.- 1.2	b.d.-1.44	0.37- 5.5
8	0.88-3.86	48.6-554	2.6- 238	b.d.- 240	b.d.- 7.1	b.d.- 8.3	b.d.-5.16	1.50-13.1
9	1.65-4.11	192 -559	16.6- 457	9.1- 262	b.d.-164	b.d.- 5.6	b.d.-4.28	3.34-11.1
10	0.39-1.37	9.2- 99.3	0.3- 31.8	b.d.- 139	b.d.- 0.7	b.d.- 0.8	b.d.-0.41	0.50- 3.7

<sup>1</sup>Weight loss on ignition at 550°C.<sup>2</sup>Below detection limit.

The core collected at station 3 exhibited the maximum intra-core variation; the range of concentrations observed for Cu and Pb being greater than three orders of magnitude. Cores 4, 5, 7, 8, and 10 appear to contain both dredged material and natural sediment while cores 2, 3, 6, and 9 are comprised entirely of dredged material. Based on the metal-depth distribution profiles, shown in Figures 36-40, the natural sediment transition occurs at depths which probably reflect the time of initial dumping of dredged material. Cores 2, 3, 6, and 9 did not penetrate the underlying natural sediment, while core 1 was taken well outside the perimeter of the deposit.

In addition to the metal analyses, the sediment samples were also analyzed for their organic content. The weight loss on ignition (L.O.I.) at 550°C was used as a measure of the amount of organic matter in sediment, Figures 36-40 also show depth distributions of L.O.I. in sediment cores 1-10. In a number of cores, the values range within an order of magnitude. Cores 2, 3, 5, 6, and 7, however, exhibit variations greater than an order of magnitude; core 3 showing the maximum intracore variation. The depth distribution profiles of L.O.I. correspond closely to the metal profiles. The dredged material exhibits greatly enhanced concentrations of L.O.I. as compared with underlying natural sediment.

Enrichment factors (EF) for metals and organic matter were calculated from the relationship:

$$EF = \frac{C_a}{C_b} \quad (2)$$

where  $C_a$  is the average concentration of metal or organic matter in dredged material present in a core and  $C_b$  is the concentration in the underlying natural sediment. For sediment samples having undetectably low metal concentrations, the analytical detection limit for a given element was used as its concentration value for estimating enrichment factors. Since cores 2, 3, 6, and 9 did not penetrate the underlying natural sediment, average natural sediment concentrations of metals and organic matter from the other cores, collected within the pile, were used for  $C_b$  in equation (1). For Cd, Hg, and Ag, however, their analytical detection limit of 0.2 ppm was used for  $C_b$  in all cores. The calculated enrichment factors are included in Table 14.

Core 1. This core was collected at the edge of the Hudson Shelf Valley, outside the dredged material pile on transect AB (Figure 24). With the exception of Fe, and Mn, metal concentrations in this core were low relative to those observed in cores within the pile. Depth distributions of the metals in this core exhibited two sets of characteristics (Figure 36a): Concentrations of Fe, Mn, Cu, and Pb were somewhat elevated from about 0.3 m down to 3.4 m depth; beyond this depth, an abrupt drop in concentrations of these metals to lower and less variable values was observed. These metal concentrations are within the range of concentrations exhibited by naturally occurring sediments in the region (Carmody *et al.*, 1973; Gross, 1970). The sharp drop in metal concentrations at a depth of 3.4 m reflects a transition to a different sediment type.

Table 14. Average concentrations of metals and organic matter and their enrichments in dredged material deposit.

Core No.	Sediment Type <sup>2</sup>	Average Concentrations (mg/Kg) and Enrichment Factors (EF) <sup>1</sup>															
		Fe × 10 <sup>4</sup>	Mn	Cu	Pb	Cd <sup>4</sup>	Ag <sup>4</sup>	Hg <sup>4</sup>	Organic Matter × 10 <sup>4</sup>								
2	Dredged Material	2.32	274.2	117.5	114.7	2.14	3.73	2.07	5.78	(2.1)	(6.3)	(33.9)	(21.9)	(10.7)	(18.7)	(10.3)	(4.3)
	Natural Sediment <sup>3</sup>	1.08	43.5	3.46	5.25	0.20	0.20	0.20	1.36								
3	Dredged Material	2.42	243.8	197.3	160.6	1.96	2.88	1.94	6.01	(2.2)	(5.6)	(57.0)	(30.6)	(9.8)	(14.4)	(9.7)	(4.4)
	Natural Sediment <sup>3</sup>	1.08	43.5	3.46	5.25	0.20	0.20	0.20	1.36								
4	Dredged Material	2.09	215.8	18.9	17.3	0.46	0.43	0.46	4.05	(1.3)	(6.6)	(4.6)	(4.7)	(2.3)	(2.1)	(2.3)	(2.2)
	Natural Sediment	1.58	32.6	4.10	3.70	0.20	0.20	0.20	1.82								
5	Dredged Material	2.51	279.8	81.5	79.1	1.69	2.97	1.46	5.83	(1.9)	(4.5)	(17.3)	(9.9)	(8.5)	(14.8)	(7.3)	(4.2)
	Natural Sediment	1.29	62.7	4.70	8.0	0.20	0.20	0.20	1.38								
6	Dredged Material	2.04	254.4	66.5	71.9	1.40	1.57	1.46	4.29	(1.9)	(5.9)	(19.2)	(13.7)	(7.0)	(7.9)	(7.3)	(3.2)
	Natural Sediment <sup>3</sup>	1.08	43.5	3.46	5.25	0.20	0.20	0.20	1.36								
7	Dredged Material	1.37	118.0	40.9	60.2	0.35	0.60	0.95	3.53	(13.7)	(23.6)	(63.9)	(24.1)	(1.8)	(3.0)	(4.8)	(12.6)
	Natural Sediment	0.10	5.00	0.64	2.50	0.20	0.20	0.20	0.28								
8	Dredged Material	2.75	275.9	129.7	152.7	2.42	3.46	2.82	7.86	(2.1)	(3.8)	(29.5)	(22.5)	(12.2)	(17.3)	(13.4)	(3.9)
	Natural Sediment	1.33	73.6	4.40	6.80	0.20	0.20	0.20	1.98								
9	Dredged Material	2.66	299.6	131.9	136.1	9.15	2.44	2.31	6.98	(2.5)	(6.9)	(38.1)	(25.9)	(45.8)	(12.2)	(11.6)	(5.1)
	Natural Sediment <sup>3</sup>	1.08	43.5	3.46	5.25	0.20	0.20	0.20	1.36								
10	Dredged Material	0.59	39.2	11.2	28.3	0.20	0.23	0.19	1.47	(1.1)	(2.9)	(19.6)	(26.7)	(2.0)	(2.3)	(1.9)	(2.1)
	Natural Sediment	0.53	13.4	0.57	1.06	0.10	0.10	0.10	0.69								

<sup>1</sup>Ratio of average concentration in dredged material to that of underlying natural sediment (Enrichment Factor =  $C_{\text{dredged material}}/C_{\text{natural sediment}}$ ).

<sup>2</sup>Sediment sampled at the study area - anthropogenic dredged material underlain by natural sediment.

<sup>3</sup>Since these cores did not penetrate the underlying natural sediment, average concentration of metals and organic matter in natural sediment sampled in cores 4, 5, 7, and 8, collected within the dredged spoil pile, were used for estimating enrichment factors in cores 2, 3, 6, and 9.

<sup>4</sup>Since the natural sediment concentrations of these metals were below detection, their analytical detection limits were used as concentration values for calculating enrichment factors.

Concentrations of Ag, Hg, and Cd were generally near or below the detection limit of less than 0.2 ppm at all depths (Figure 36a). Relative to the underlying sediment, the core top (0-20 cm) showed some enrichment in Cd, Hg, Ag, and Pb while Fe and Mn concentrations were depressed. The profiles show that Pb and Cu and Fe and Mn covary with depth.

The organic matter in core 1 varies from 0.9 to 6.6% by weight, the mean value being 3.6%. The depth distribution profile closely resembles the Fe and Mn distributions.

Core 2. This core was collected on the southeast slope of the pile on transect AB, about 1 km downslope from the apex of the pile. As seen in the cross-sectional profile of the pile (Figure 24), the core did not penetrate the underlying natural sediment. This is also evident from the metal profiles (Figure 36b). Generally, the metal profiles exhibit erratic distributions, showing no systematic trends with depth. Highest concentrations of Ag (26.7 ppm) and Hg (7.4 ppm) were found in this core. The enrichment factors range from 2.1 for Fe to 33.9 for Cu.

The depth distribution of organic matter in core 2 displays elevated concentrations throughout the core, varying by more than an order of magnitude. Two sharp maxima dominate the profile at the top and bottom of the core. Both maxima approach concentrations of 12-13% by weight. A close correspondence exists between the depth distribution of organic matter and that of metal concentrations.

Core 3. This station is located at the apex of the pile where the two sampling transects intersect (Figure 24). All the sediment sampled in this core was comprised of dredged material. Figure 37a shows erratic distributions of metals with depth. Relative to the other cores analyzed, this core exhibited the greatest variations in the concentrations of Fe, Cu, and Pb. Within the core, the concentrations of Cu and Pb varied by more than three orders of magnitude (Table 13). Highest concentrations of Fe (7.71%), Cu (2230 ppm) and Pb (1550 ppm) were observed within the same sub-section at a depth of 6.1-6.2 m. Two distinct minima are present: one in the upper meter of the core at 0.6-0.7 m depth and another at about 2.5 m. The lower subminimum is followed by a sharp maximum at 6.1-6.2 m. The metal enrichments at this station were Fe, 2.2; Mn, 5.6; Pb, 30.6; Cu, 57.0; Cd, 9.8; Ag, 14.4; and Hg, 9.7. The enrichment factors for Cu and Pb were significantly higher than those found in core 2.

Core 3 exhibits the greatest range of organic matter measured in all cores, varying from 0.85% at the core top to 31.6% at 7 m depth. The distribution displays a general trend of increasing concentration with depth interrupted by several maxima and minima recorded at various depths. The organic matter profile is similar to those observed for the metals, except for the presence of a sharp organic matter maximum at 7 m which does not coincide with the maxima observed for metals at a depth of 6 m.

Core 4. This core was taken at the base of the southeast slope, ≈2 km downslope from station 2 and ≈3 km from the apex of the pile.

As seen in the cross-sectional view of the pile (Figure 24) this core consists partly of dredged material underlain by natural sediment. This is particularly evident from the metal profiles shown in Figure 37b where a distinct inflection occurred at 2 m. For most metals, the sharpest drop in concentration was observed between 2 and 3 m. This transition was assumed to be the boundary between the dredged material pile and the underlying natural sediment. Using the boundary, the enrichment factors were calculated to be 1.3 for Fe, 6.6 for Mn, 4.7 for Pb, 4.6 for Cu, 2.3 for Cd, 2.1 for Ag, and 2.3 for Hg.

The organic matter profile of core 4 displays a distinct maximum at a depth of 2 m. Above and below this inflection, the concentrations remain constant with depth. The observed maximum coincides with those recorded in the metal profiles. Relative to the underlying natural sediment, the dredged material was found to be enriched in organic matter by a factor of 2.2.

Core 5. This core was taken  $\frac{1}{2}$  km upslope from station 4 (Figure 24). As a result, most of the sediment sampled at this station was dredged material underlain by some natural sediment. Based on the depth distributions of metals in this core (Figure 38a), the transition to natural sediment appears to occur at a depth of 4.4 m. Above this boundary, the distributions exhibit elevated and highly variable concentrations. The concentrations for most metals co-vary with depth; the general trend being a decrease in concentration with depth. The distributions exhibit distinct minima for all metals at 0.3-0.7 m depth. This sharp inflection is followed by strong maxima for most metals

at 0.9-1.1 m depth. Downcore at depth of 3.3-3.7 m, a submaximum is observed for all metals.

Using average metal concentrations of dredged material and the natural sediment underlying the transition (Table 14), the enrichments in this core were found to be Fe-1.9, Mn-4.5, Pb-9.9, Cu-17.3, Cu-8.5, Ag-14.8, and Hg-7.3.

The depth distribution of organic matter shown in Figure 38a is very similar to those observed for the metals in this core. Like the metal profiles, the profile of organic matter exhibits a sharp maxima at  $\approx$ 1 m depth and several submaxima at other depths. The concentrations of organic matter vary by more than an order of magnitude; the observed maximum approaches a value of 13% by weight. The sharp drop in concentration of organic matter at a depth of 4.4 m reflects the transition of organic-rich dredged material to natural sediment. Using average concentrations of organic matter above and below this boundary, a value of 4.2 was calculated for the enrichment factor of organic matter in this core.

Core 6. This core was taken at the apex of the dredged material pile, near station 3. As can be seen from the cross-sectional profile of the pile (Figure 24), the entire length of this core consisted of dredged material. Depth distributions of metals (Figure 38b) exhibit highly variable and elevated concentrations throughout the core. The erratic distribution of metals observed in this core is similar to that observed in core 3 taken nearby. At a depth of 0.7 m, the sediments exhibit a sharp increase in concentrations of all metals. This

feature is followed by another maximum at a depth of 2.1-2.2 m in the Fe and Mn distributions. At greater depth, the distributions display highly variable but systematic trends in metal concentrations. Comparison of profiles indicate that Ag, Cd and Hg, and Cu and Pb co-vary with depth, particularly between 5.0 and 6.5 m where an extensive stepwise decrease occurs. Relative to background values obtained from other stations (Table 14), the enrichment factors were found to be Fe, 1.9; Mn, 5.9; Pb, 13.7; Cu, 19.2; Cd, 7.0; Ag, 7.9; and Hg, 7.3.

The organic matter profile, displayed in Figure 38b, resembles closely the metal profiles discussed above. An enrichment factor of 3.2 was calculated for organic matter in dredged material in this core.

Core 7. This core was collected at the base of the northwest slope, about 4 km downslope from the apex, (Figure 24) and well outside the designated dredged material disposal area. Depth profiles of metals (Figure 39a), exhibit metal enrichment in the upper meter of the core. These elevated levels decrease systematically until the concentrations approach background levels at a depth of  $\approx 1$  m. Down-core the metal concentrations remain constant with depth. Based on the depth profiles, it appears that the boundary between the anthropogenic dredged material and the natural sediment basement lies at a depth of  $\approx 1$  m. As in other cores, the Pb and Cu profiles exhibit close resemblance as do Fe and Mn, and Ag, Hg, and Cd. The enrichment factors are given in the order of enrichment of metals: Cu (63.9), Pb (24.1), Mn (23.6), Fe (13.7), Hg (4.8), Ag (3.0), and Cd (1.8).

The Cu and Mn values represent the highest enrichment factors found for all the cores studied reflecting the extremely low concentrations found in the underlying natural sediment at this station.

The depth profile of organic matter shows that the top  $\frac{1}{2}$  m of sediment in this core is greatly enriched in organic matter as compared with the underlying sediment. The profile of organic matter is identical to those observed for metals. The dredged material in this core was found to be enriched in organic matter by a factor of 12.6 as compared with natural sediment. This was the highest value found for the enrichment factor of organic matter.

Core 8. This core was collected at a station  $\approx 2$  km from the apex of the pile on the northwest slope. The vertical cross-sectional view of the pile (Figure 24) shows that this core penetrated the natural sediment underlying the pile. This is also evident from the depth distributions of metals (Figure 39b). The sharp drop in all concentrations at 3.3-3.5 m depth reflects the transition to natural sediment. Overlying the natural sediment, the concentrations are variable, but display a systematic increase with decreasing depth toward the core top. The metals Pb, Cu, Fe, and Mn exhibit identical distributions with depth. Ag, Cd, and Hg also co-vary with depth. The calculated enrichment factors given in the order in which the metals are enriched: Cu (29.5), Pb (22.5), Ag (17.3), Hg (13.4), Cd (12.2), Mn (3.8), and Fe (2.1).

The concentrations of organic matter decrease systematically with increasing depth until  $\approx 3$  m where, as with the metals, a sharp drop in

concentration occurs. Beyond 3.5 m depth, the concentration remains constant. Using average concentrations of organic matter above and below this boundary, an enrichment factor of 3.9 was calculated for this core.

Core 9. This core was taken at a station about 1 km upslope from station 8 and a similar distance from the mound apex on the northwest slope (Figure 24). The depth distributions of metals in this core are highly variable, showing no trends with depth. The Pb and Cu distributions again exhibit close resemblance. Fe, Mn, Cd, and Ag concentrations exhibit similar behavior with depth. This core did not penetrate the natural sediment basement. Enrichment factors were calculated to be: Cd (45.8), Cu (38.1), Pb (25.9), Ag (12.2), Hg (11.6), Mn (6.9), and Fe (2.5).

The depth profile of organic matter, displayed in Figure 40a, shows that the concentrations of organic matter in core 9 are highly elevated and variable. In the 1.5-4.0 m depth interval, however, the concentrations remain relatively constant. This part of the profile resembles closely the profiles of Pb and Cu. The bottom part of the core (4-6 m) displays a highly erratic distribution; the concentrations ranging from 3.3 to 11.1%. The enrichment factor was calculated to be 5.1.

Core 10. This core was collected at a station located far outside the dredged material deposit approximately equidistant (~6 km) from the New Jersey coast and the pile apex (Figure 24). The depth distributions of metals (Figure 40b) reveal two minima in concentrations

at depths of  $\approx 0.3$ - $0.7$  m and 3 m; the inflection near the core top being more pronounced, perhaps indicating the presence of anthropogenic dredged materials. As observed in other cores, Pb and Cu covary with depth. It must be noted that the elevated metal concentrations observed in the upper part of the core are considerably lower than maxima reported for other cores. The enrichment factors, given in Table 14, are much lower than for metals in other cores except Pb and Cu having values of 26.7 and 19.6, respectively.

The organic matter profile for core 10 exhibits a distinct maximum at 0.2-0.3 m depth. This sharp inflection is followed by a gradual decrease in concentration down to a depth of  $\approx 0.5$  m. Downcore the concentrations remain constant with depth. The profile closely resembles those for metals in this core. The enrichment factor was found to be 2.1.

#### 4.6.2 Intracore Variability in Metal Concentrations

In order to compare the observed metal concentrations of dredged material and the underlying sediment in each core, their mean and standard deviation values were calculated. These values, including the range of concentrations observed in each core, are given in Table 15. Cores 1 and 10, located outside the perimeter of the dredged material deposit, are not included in Table 15.

Overall the mean dredged material metal concentrations are significantly higher than the corresponding concentrations in the underlying sediment. Using standard deviation as a measure of the variability

Table 15. Mean, standard deviation and range of concentrations (calculated on a gravel free basis) for dredged material and natural sediment in the cores collected at the dumpsite, New York Bight.

Core No.	Sediment Type	Parameter	Metal Concentrations (mg/Kg)							Organic Matter <sup>1</sup>
			Fe <sup>1</sup>	Mn	Pb	Cu	Cd	Ag	Hg	
1	Natural Sediment	Mean <sup>2</sup>	2.4	170	8.0	10	d.l. <sup>5</sup>	d.l.	d.l.	3.6
		SD <sup>3</sup>	1.4	100	7.0	6.0	-	-	-	2.5
		Range <sup>4</sup>	4.2-0.8	318-45	33-2	17-2	-	-	-	7-1
2	Dredged Material	Mean	2.3	274	115	118	2.1	3.7	2.1	5.8
		SD	1.0	140	95	105	2.1	5.6	1.9	3.7
		Range	4.3-0.4	547-24	286-5	302-4	7-d.l.	27-d.l.	7-d.l.	14-2
3	Dredged Material	Mean	2.4	244	161	197	1.9	2.9	1.9	6.0
		SD	1.5	134	288	419	1.6	2.7	1.5	4.3
		Range	3.6-0.3	605-54	1527-2	2197-2	6-d.l.	10-d.l.	5-d.l.	22-0.5
4	Dredged Material	Mean	2.1	216	17	19	0.5	0.4	0.5	4.1
		SD	0.6	60	17	16	0.5	0.3	0.5	1.2
		Range	3.3-1.4	305-119	5-48	51-7.3	1.7-d.l.	0.8-d.l.	1.7-d.l.	4.6-3.0
5	Natural Sediment	Mean	1.6	29	3.4	2.5	d.l.	d.l.	d.l.	1.7
		SD	0.6	13	2.8	1.7	-	-	-	0.5
		Range	3.0-0.8	47-8	13.1	6-1	-	-	-	2.5-1.0
5	Dredged Material	Mean	2.5	280	79	82	1.7	2.9	1.5	5.8
		SD	1.0	120	70	74	1.9	2.4	1.2	2.6
		Range	3.7-0.4	511-5	245-2	268-2	7-d.l.	18-d.l.	4-d.l.	11-0.8
6	Natural Sediment	Mean	1.3	63	8.0	4.7	d.l.	d.l.	d.l.	1.4
		SD	0.5	24	10	2.4	-	-	-	0.6
		Range	1.8-1.2	96-30	25-2	8-2	-	-	-	2.2-0.9
6	Dredged Material	Mean	2.1	255	73	68	1.4	1.6	1.5	4.3
		SD	0.7	123	81	78	1.5	1.8	1.6	1.9
		Range	3.8-0.6	545-57	359-4	357-4	35-d.l.	6-d.l.	4-d.l.	8-1.2
7	Dredged Material	Mean	1.5	130	66	42	0.4	0.7	0.9	3.6
		SD	0.2	21	12	2.2	0.1	0.4	0.0	0.3
		Range	1.7-1.3	154-113	77-53	44-40	0.5-0.3	1.0-d.l.	1.0-0.9	3.8-3.3
8	Natural Sediment	Mean	0.1	5.0	2.5	0.6	d.l.	d.l.	d.l.	0.3
		SD	0.1	6.7	2.7	1.3	-	-	-	0.2
		Range	9-0.3	23-0.7	10-d.l.	4-0.1	-	-	-	0.7-0.1
8	Dredged Material	Mean	2.8	276	153	130	2.4	3.6	2.8	7.9
		SD	0.9	121	59	74	2.1	2.5	1.5	3.7
		Range	4-1.3	554-100	240-96	283-23	7-d.l.	8-d.l.	5-0.6	13-2.4
9	Natural Sediment	Mean	1.3	74	6.8	4.4	d.l.	d.l.	0.21	1.9
		SD	0.3	18	6.4	1.9	-	-	0.1	0.4
		Range	1.5-0.7	90-41	15-d.l.	7.3	-	-	0.2-d.l.	2.4-1.3
9	Dredged Material	Mean	2.7	300	136	132	9.0	2.4	2.3	7.0
		SD	0.7	98	50	81	34	1.4	1.1	2.0
		Range	4-1.5	557-143	225-29	421-30	151-d.l.	5-0.7	5-0.7	10-4
10	Dredged Material	Mean	0.6	39	28	11	0.2	0.2	0.2	1.5
		SD	0.2	15	16	6.0	0.1	0.2	0.1	0.6
		Range	0.8-0.4	60-23	50-14	19-6	0.4-d.l.	0.5-d.l.	0.3-d.l.	2.2-0.9
10	Natural Sediment	Mean	0.5	13	1.1	0.6	d.l.	d.l.	d.l.	0.7
		SD	0.1	5.0	0.7	0.4	-	-	-	0.2
		Range	0.9-0.3	31-8	4-d.l.	2.4-0.3	-	-	-	1.2-0.4

<sup>1</sup> ×10<sup>4</sup> mg/Kg.

<sup>2</sup>Mean metal concentration.

<sup>3</sup>Standard Deviation.

<sup>4</sup>Range of observed metal concentrations.

<sup>5</sup>Below detection limit.

in concentration about the mean value, Table 15 shows that the standard deviation values for all metal concentrations in dredged material are invariably greater than the corresponding standard deviation values for natural sediment. This can be attributed to the multiplicity of sources of dredged material as compared with the underlying naturally accumulated sediment. Also upslope cores 3 and 6 exhibit the maximum variability in metal concentrations. This indicates that the apex of the pile receives primary undifferentiated dredged material whereas the downslope areas of the deposit receive somewhat sorted secondary finer grained material.

Comparison of the mean metal concentrations in dredged materials of cores 2, 3, 4, 5, 6, 7, 8, 9, and 10 reveals that the apex and upslope cores 2 and 3 exhibit higher average concentrations of toxic metals than the downslope cores 4, 5, 7, 8, 9, and 10. Core 6, located upslope on southeast transect, however, has lower average metal concentrations than cores 2 and 3 and some of the downslope cores. This can be attributed to a high sand content of sediment at this station, presumably resulting from either the removal of fine grained material in the water column during descent of the dredged material or to post-depositional erosional processes. Elevated mean metal concentrations in cores 8 and 9 can be explained on the basis of their high mud and organic matter contents (Table 15) as compared with other stations located on the slopes of the pile.

Cores 4, 5, 7, 8, and 9 are enriched in Fe and Mn as compared with the underlying natural sediment. This indicates that dumping of

dredged material does contribute to anthropogenic input of Fe and Mn. Enrichment of both metals in the dredged material in the slope cores 8 and 9 can be attributed to the high organic matter concentrations and mud contents at these stations.

#### 4.6.3 Metal Enrichments in Coastal Deposits

Comparison of metal enrichments calculated for the dredged material deposit (Table 16) with other coastal deposits provides insight into the relative magnitude of metals deposited, via dredged material dumping, in the New York Bight. Table 16 gives enrichments of metals in naturally deposited sediments from several coastal areas. These areas are known to be heavily impacted by industrialization. Range of enrichment factors for the dredged material deposit are also included in Table 16. The enrichment factors at the lower end of the range of values for the dredged material deposit are comparable to those reported for other naturally sedimented coastal deposits. The low values correspond to the enrichments calculated for the downslope stations. The high values, representing enrichments in the apex or the upslope cores, are significantly greater than the enrichments reported for other areas. Even Fe and Mn, elements that normally show no significant enrichment in coastal deposits, are considerably enriched in the dredged material deposit. Table 16 shows that the metal inputs to the New York Bight, due to dredged material disposal, are significantly higher than the anthropogenic metal inputs resulting from natural sedimentary processes in coastal areas not impacted by dredged material dumping.

Table 16. Metal enrichments in coastal sediment deposits.

Element	California Basin <sup>1</sup>	Kieler Bucht, Baltic Sea <sup>2</sup>	Narragansett Bay <sup>3</sup>	Deutsche Bucht, North Sea <sup>6</sup>	New York Bight Dredged Spoil Deposit <sup>4</sup>	Long Island Sound <sup>5</sup>
Pb	4.2	4.1	4.0	10	4.7 - 30.6	6.8
Cd	1.5	6.9	-	7	2.0 - 45.8	-
Cu	1.8	1.9	6.7	2	4.6 - 63.9	9.6
Mn	1.0	1.0	1.0	4	2.9 - 23.6	1.3
Fe	1.0	1.0	1.0	1.5	1.1 - 13.7	1.1
Zn	1.4	2.9	3.3	4	-	-
Ag	3.0	-	1.0	-	2.1 - 18.7	-
Hg	-	-	-	8	1.9 - 13.4	8.1

<sup>1</sup>Bruland *et al.* (1974)

<sup>2</sup>ErIenkeuser *et al.* (1974)

<sup>3</sup>Goldberg *et al.* (1977)

<sup>4</sup>This study

<sup>5</sup>Average values of 12 cores taken at Eaton's Neck, western Long Island Sound (MSRC, 1978)

<sup>6</sup>Foerstner and Reineck (1974)

It must be pointed out, though, that the enrichment factors calculated for the dredged material deposit represent metal enrichments in dredged material relative to the underlying coarse grained sediment. Because of the difference in grain size of the two materials, the calculated enrichment factors could very well reflect liberal estimates.

#### 4.6.4 Geochemical Correlations

The three important factors that determine the distribution of trace metals in sediments are: (1) adsorption onto, or coprecipitation with, iron and manganese hydrous oxides; (2) formation of metal-organic complexes or adsorption on organic material; (3) association with clays by processes such as adsorption or ion exchange. In order to determine the relative importance of each of these processes, covariance correlations between metal concentrations and selected sediment parameters were used. A least squares linear correlation was performed for each pair of relevant geochemical parameters for all cores collected within the dredged material deposit. For this purpose cores 2, 3, 4, 5, 6, 8, and 9 were selected. Cores 1, 7, and 10 were not included in the geochemical correlations because they were comprised predominantly of natural sediments.

Table 17 gives interelement correlation coefficients between Fe, Mn, Cu, Pb, Cd, Hg, and Ag in the sediment core sections. The correlation coefficients between metals and organic matter and mud content are listed in Table 18. All correlation plots are displayed in

Table 17. Interelement correlation coefficients in dredged material deposit sediments.

	Fe	Mn	Cu	Pb	Cd	Hg	Ag
Fe	1.00						
Mn	0.76	1.00					
Cu	0.68	0.53	1.00				
Pb	0.70	0.53	0.90	1.00			
Cd	0.56	0.27	0.80	0.74	1.00		
Hg	0.68	0.38	0.80	0.86	0.81	1.00	
Ag	0.62	0.33	0.80	0.77	0.89	0.74	1.00

Table 18. Correlation coefficients between metals and organic matter and mud content in dredged material deposit sediments.

	Fe	Mn	Cu	Pb	Cd	Hg	Ag
Organic Matter <sup>1</sup>	0.84	0.72	0.80	0.86	0.65	0.78	0.72
Mud Content <sup>2</sup>	0.66	0.61	0.49	0.49	0.31	0.41	0.32

<sup>1</sup>Measured as weight loss on sample ignition at 550°C.

<sup>2</sup>Correlation coefficient between mud content and organic matter was found to be 0.65.

Figures 41-46. The number of points on the correlation plots varied with the parameters plotted. Since concentration values below the detection limit for Hg, Cd, and Ag could not be included, correlation plots of these metals contain fewer points. In addition, a few extremely high values were not considered since these concentrations lie out of the range of the selected scale on the axes. Concentrations of all geochemical parameters used in the correlation analysis are considered on a gravel-free basis. The number of points plotted ranged from 187 for mud-organic matter plots to 132 for Cd - Ag plots.

Interelement Correlation. The Fe-metal plots (Figure 41) indicate that Fe concentrations are strongly related to Mn but only moderately to the other metals determined in this study (Table 17). Characteristic of the plots of Fe against the trace metals (Cu, Pb, Hg, Ag, and Cd) is scatter along the ordinate, i.e., a wide range of Fe concentrations at low metal levels. This scatter decreases in most of these plots at higher concentrations. Another interesting feature in these plots is a fairly large presence of Fe (1-2%) where other metals are nearly absent. This can be attributed to the presence of relatively uncontaminated sediment such as the natural sediment underlying the deposit.

Since a strong interrelationship is observed between Fe and Mn, the Mn versus trace metal correlation plots (Figure 42) are similar to those observed for Fe. Cu and Pb show a stronger relationship with Mn than Cd, Ag and Hg.

Figures 43 and 44 present the trace metals plotted against each other. The correlations among these metals are strong, particularly

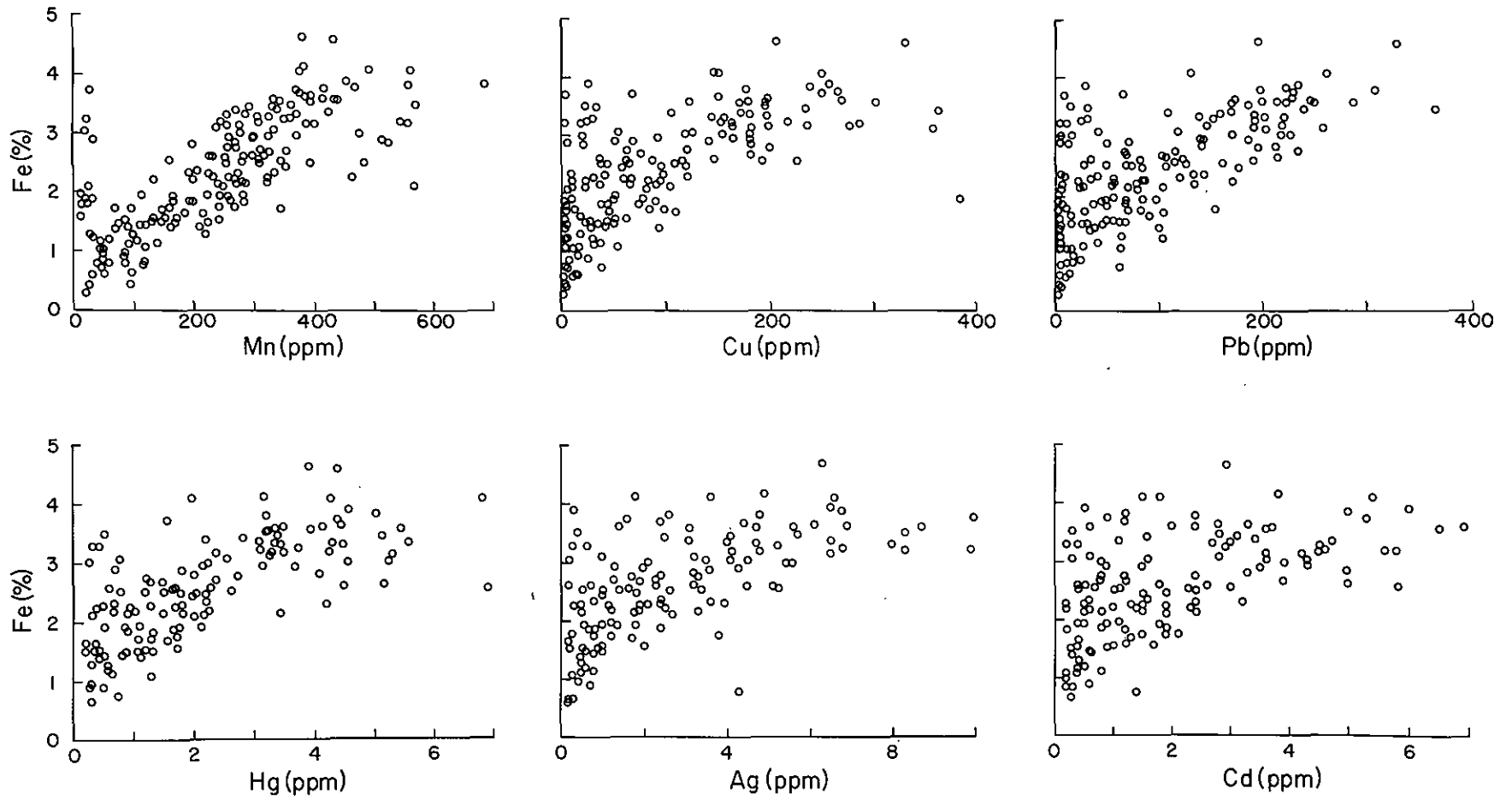


Figure 41. Total iron-trace metals correlation plots.

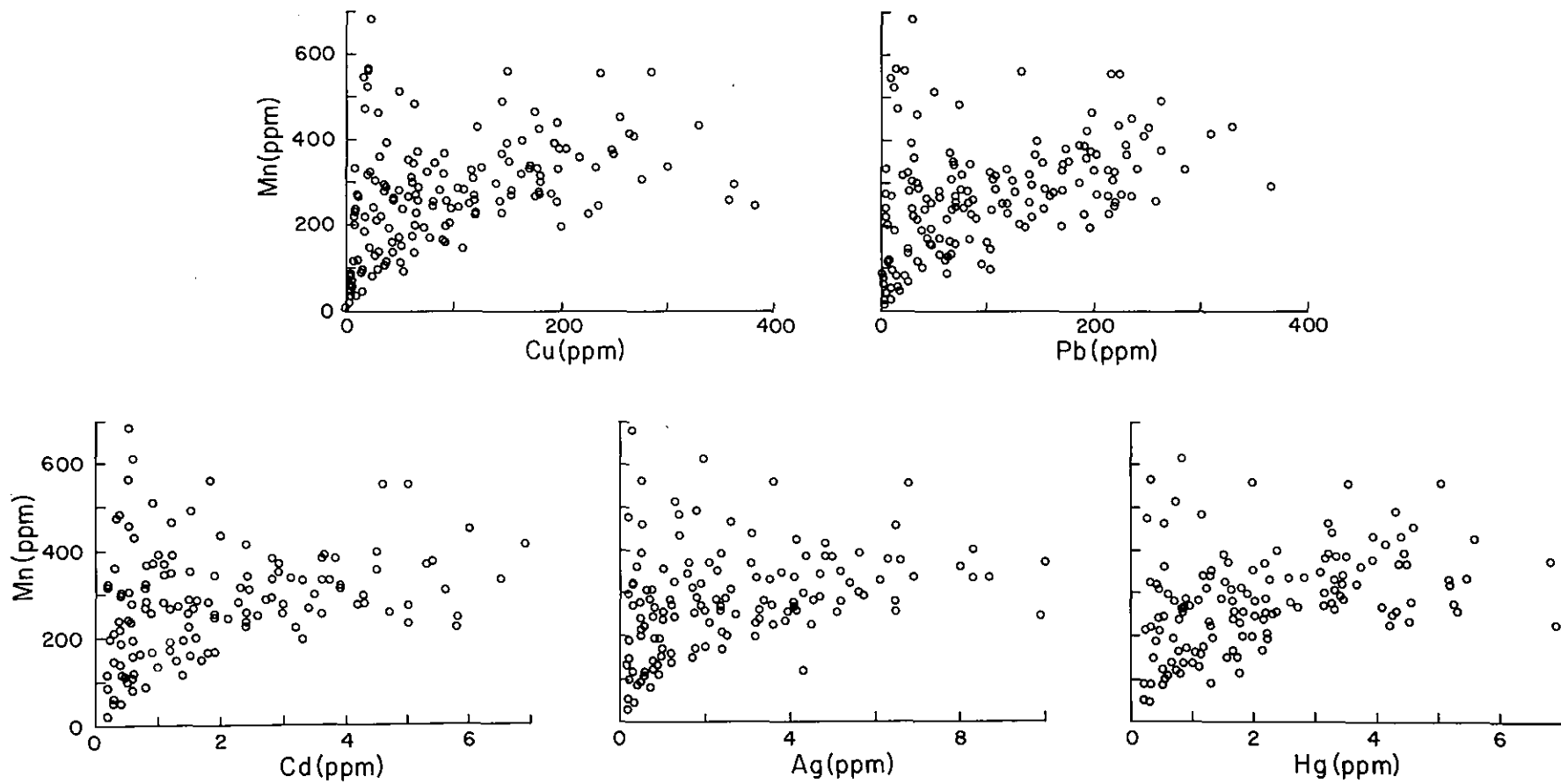


Figure 42. Total manganese-trace metals correlation plots.

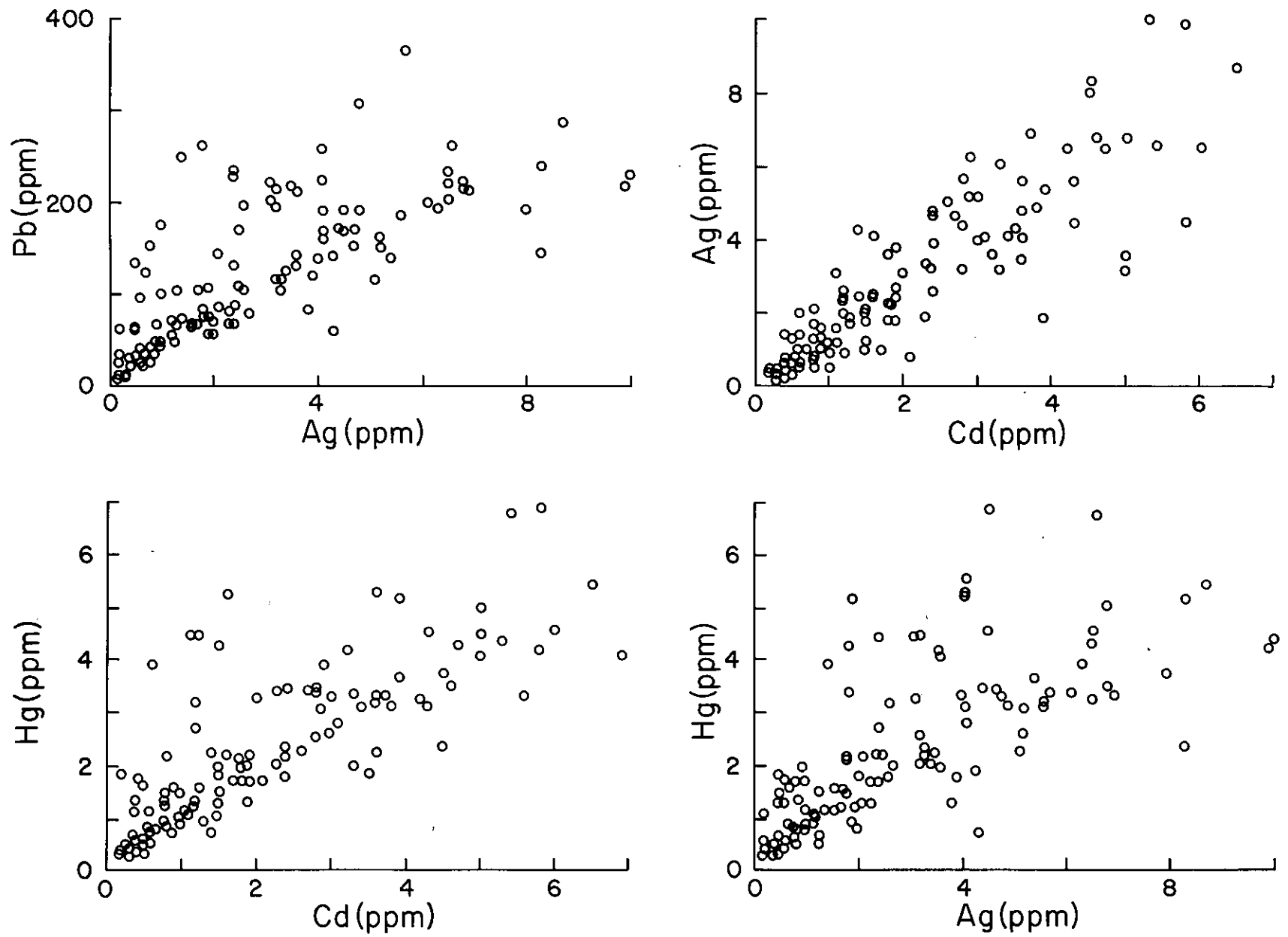


Figure 43. Interelement correlation plots.

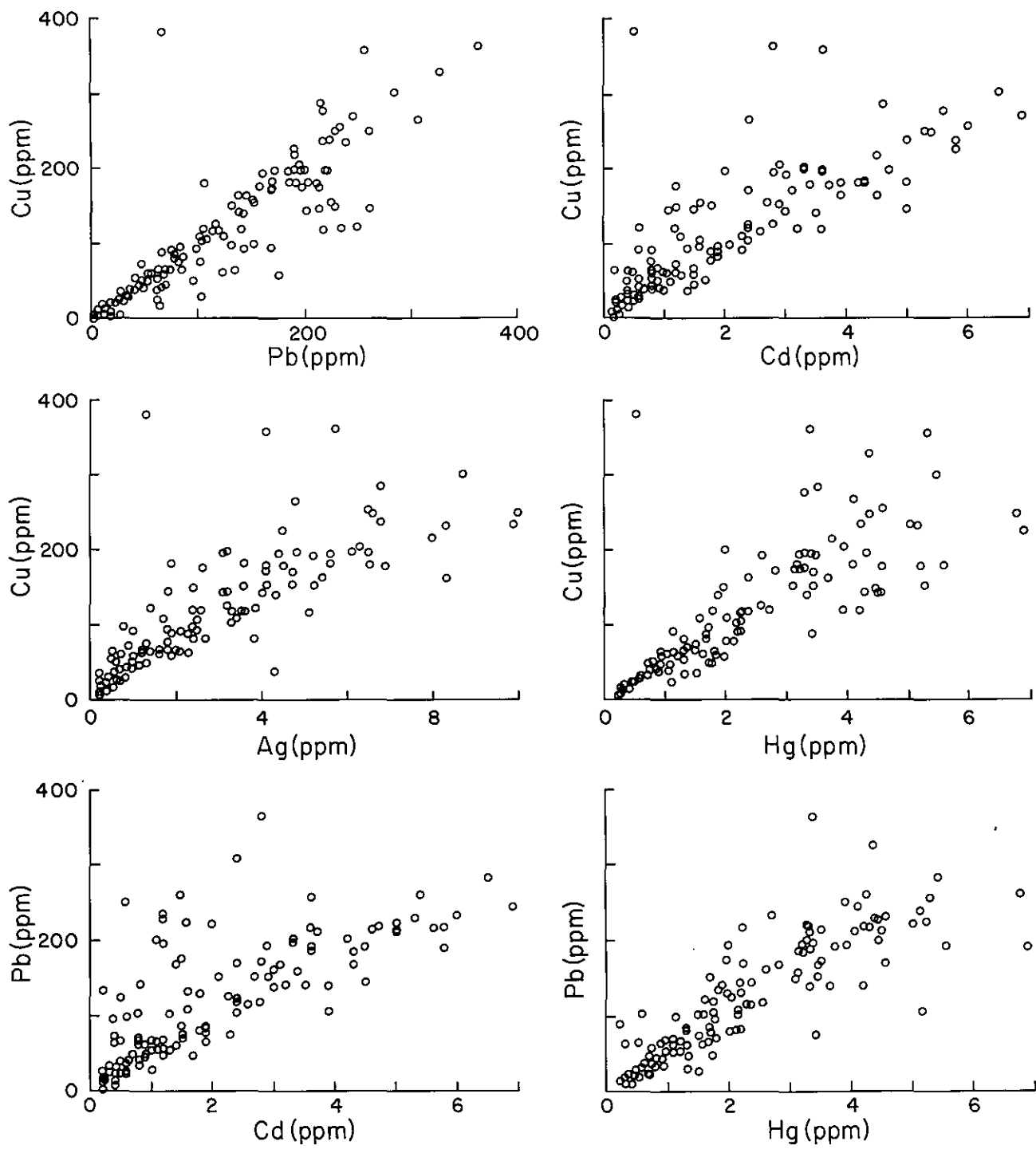


Figure 44. Interelement correlation plots.

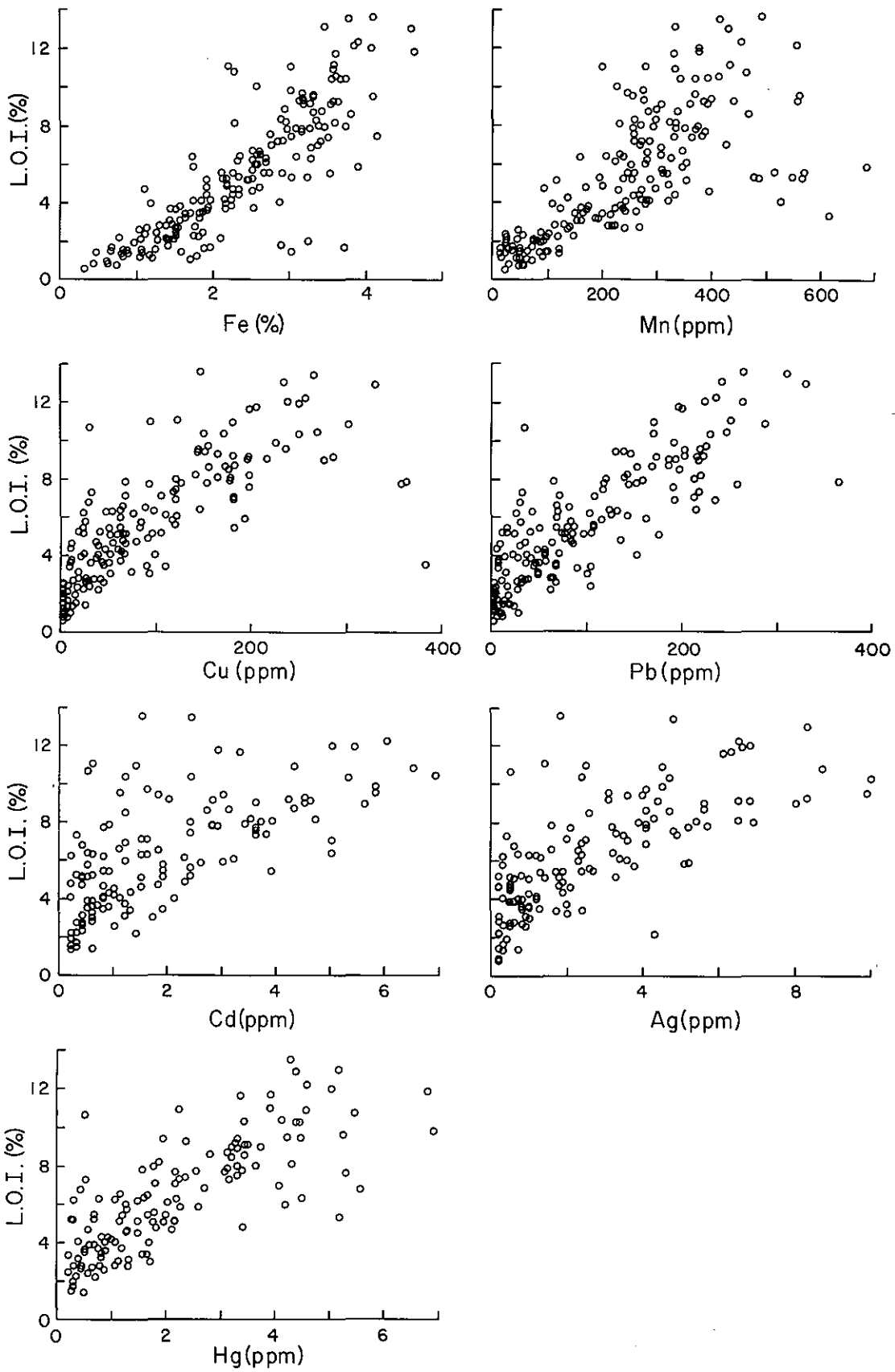


Figure 45. Organic matter (LOI) - metals correlation plots.

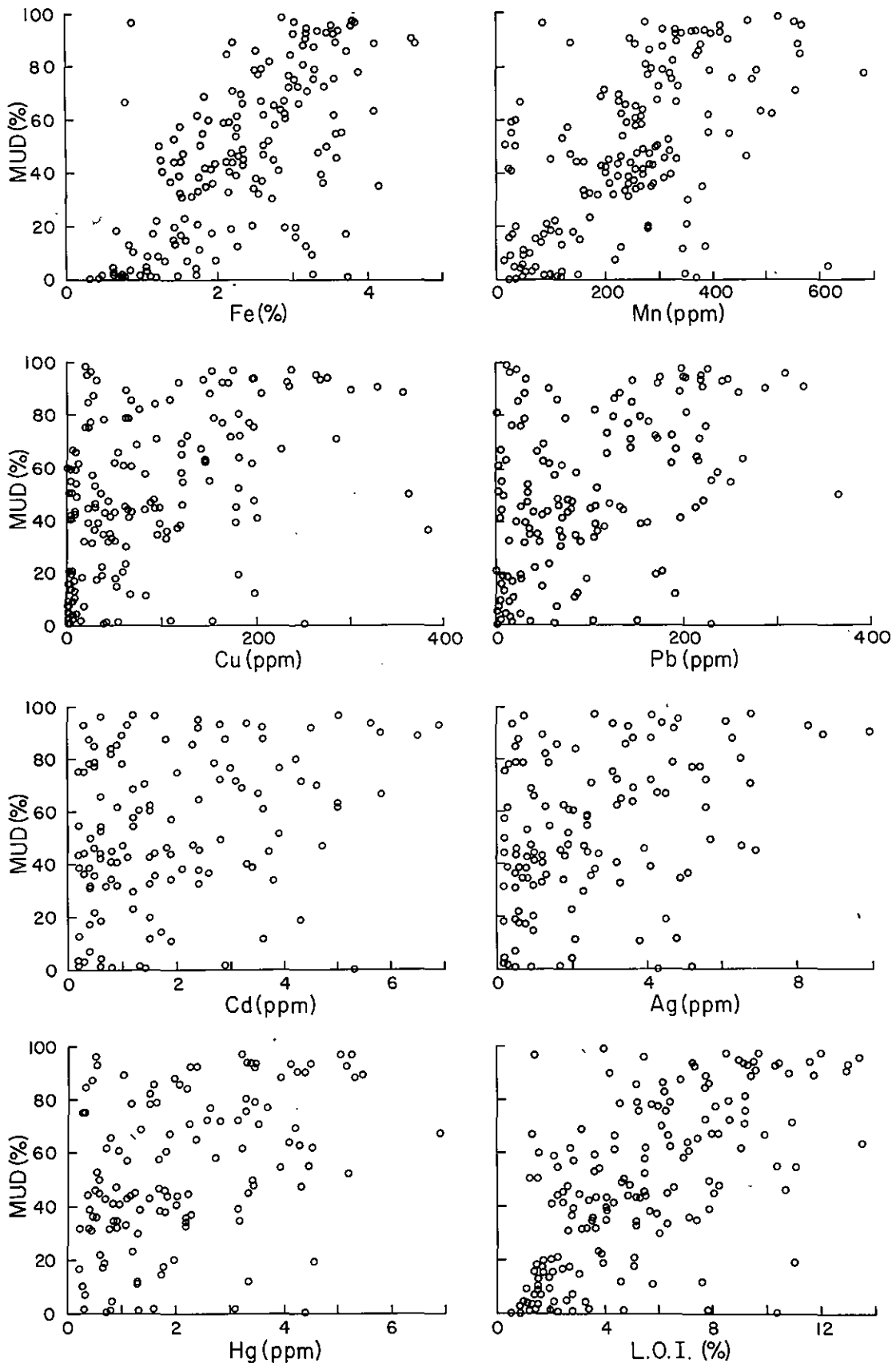


Figure 46. Mud-metals correlation plots.

for Cu versus Pb. Unlike the Fe and Mn versus trace metal plots, the scatter along the lower ends of axes is minimal but increases at higher concentrations.

As expected from their similar chemistries and the predominantly natural sources of these metals, Fe and Mn are strongly correlated in the dredged material deposit. The wide spread in Fe and Mn concentrations at low trace metal levels (Figures 41 and 42) indicates that the dredged materials originate in widely varied environments in terms of anthropogenic metal inputs and that the natural sediment underlying the deposit contains natural concentrations of Fe and Mn but is depleted in trace metals. Overall the metals exhibit strong correlation with Fe and Mn. It appears that iron hydrous oxides and to a lesser extent, manganese hydrous oxides play a significant role in the adsorption of Cu, Pb, Cd, Hg, and Ag. Correlations of Fe and Mn versus Cd and Hg have been observed at other dredged material disposal sites (MSRC, 1978; Heaton, 1978).

The strong interrelationships among some of the metals indicate that they behave similarly geochemically and probably are associated with the same minerals in dredged material sediments.

Metal-Organic Matter Correlation. Correlation between metals and organic matter (Table 18) indicate strong association of Cd, Hg, and Ag with organic matter in dredged material sediments. Correlation plots of Fe and Mn versus organic matter (Figure 45) exhibit a similar relationship but the Mn covariance is weaker. The organic matter versus toxic metal plots (Figure 45) are fairly similar, all showing

scatter at low metal concentrations, but the variation in the relationships differs. The Pb and Cu plots are strongly linear while those for Ag, Cd and Hg are slightly more scattered.

The variation in organic matter content at low metal concentrations implies that plant debris from relatively pristine environments is intermixed with other waste such as sewage derived organic matter. As previously mentioned, the dredged material is taken from areas which are exposed to widely varied degrees of pollutant loading. Mn and Cd appear to be less associated with the organic fraction than the other metals studied.

On the basis of the correlation plots, the degree of covariance for the metals with organic matter in the dredged material sediments follows the sequence: Pb>Fe>Cu>Hg>Ag>Mn>Cd. The strong relationships of organic matter with the metals indicate that the organic matter may have a significant control over Fe, Mn, Pb, Cu, Hg, Ag, and Cd in dredged material sediments. This agrees with previous studies in other locations for both natural and polluted sediments (Rashid and Leonard, 1972; Nissenbaum and Swaine, 1976; Gross, 1976; MSRC, 1978).

Metal-Mud Content Correlation. The degree of association of the metals with mud content of dredged material sediment follows the sequence: Fe>Mn>Cu=Pb>Hg>Ag=Cd. Compared to metal-organic matter correlations, the metal versus mud content correlations (Figure 46) are significantly weaker for each pair indicating that the organic matter, rather than mud content has significant control over the distributions of Fe, Mn, Pb, Cu, Cd, Hg, and Ag in the dredged material sediments.

Because of the highly organic rich nature of much of the dredged sediment, the mud fraction of the sediment does not appear to be the controlling factor with respect to the distribution of metals. Sewage-related materials may add large quantities of metals and organic matter without substantially altering the grain size of the samples.

From the results obtained, it is only possible to make certain generalizations. It appears that organic matter plays the most significant role in the distribution of metals in the dredged material sediments. Iron and manganese hydrous oxide phases may also control the metal distributions especially of Cu and Pb.

#### 4.6.5 Depositional Record of Metal Inputs

We calculated the inputs of certain metals (Fe, Mn, Pb, Cu, Cd, Ag, Hg) and organic matter from estimated sedimentation rates at each station for the periods 1936-73 and 1973-78 and the observed depth distributions of metals in each core (Table 19). The arithmetical averages of metal concentrations in upper and lower units of each core, above the basement, corresponding to 1973-78 and 1936-73 accumulations, respectively, were used for the calculations of pre- and post-1973 metal inputs. A value of  $2.6 \text{ gm/cm}^3$  was assumed for the density of the solid phases and 31% as the average water content of deposited dredged material.

The wide distribution of coring stations in the study area provides information about the inputs of metals deposited in different parts of the dumpsite over a period of time. For example, the highest metal input values are obtained for the apex stations (cores 3 and 6)

Table 19. Anthropogenic inputs of metals and organic matter associated with dredged materials dumped in New York Bight during the periods 1936-73 and 1973-78.<sup>1</sup>

Core No.	Station Location	ANTHROPOGENIC INPUTS (g/m <sup>2</sup> /yr)															
		Period 1973-78								Period 1936-73							
		Fe <sup>2</sup>	Mn	Pb	Cu	Cd	Ag	Hg	Organic Matter <sup>2</sup>	Fe <sup>2</sup>	Mn	Pb	Cu	Cd	Ag	Hg	Organic Matter <sup>2</sup>
2	Top of southeast slope	13.9	185	64.9	73.1	1.48	1.84	1.12	14.6	6.0	67.7	30.3	29.9	0.52	1.03	0.55	18.2
3	Pile apex	12.4	145.6	47.5	66.7	0.89	1.28	0.67	35.1	18.3	196	150	181	1.70	2.50	1.77	48.6
4	Base of southeast slope	3.5	73.1	5.7	6.8	0.20	0.14	0.21	12.4	1.61	16.4	1.34	1.34	0.025	0.032	0.024	3.34
5	Middle of southeast slope	15.0	201	58.2	58.4	1.34	2.88	0.99	35.7	3.11	30.1	5.04	8.76	0.17	0.22	0.17	7.11
6	Pile apex	17.5	284	25.5	24.9	0.55	0.52	0.48	34.4	18.5	201	82.1	75.2	1.57	1.80	1.67	39.95
8	Base of northwest slope	3.9	47.7	24.9	25.4	0.65	0.81	0.55	13.5	2.79	26.4	14.9	11.9	0.17	0.29	0.26	7.52
9	Top of northwest slope	5.0	114	19.4	21.0	0.48	0.63	0.44	12.5	6.3	71.1	33.3	31.8	2.41	0.54	0.55	18.2

<sup>1</sup>In these estimates, a value of 2.6 gm/cm<sup>3</sup> was used for the density of the solid phases present in dredged materials and an average water content of 31% by weight.

<sup>2</sup> ×10<sup>3</sup> g/m<sup>2</sup>/yr

for the period 1936-73. As expected, the lowest metal inputs are recorded in cores taken at the downslope stations (cores 4 and 8). Other stations, located on the top and middle of the slopes (cores 2, 5, and 9), exhibit intermediate input rates; the upslope cores showing higher values than the downslope cores.

For the period 1973-78, however, highest input values for some trace metals are obtained for the upslope cores 2 and 5, lying on the southeast slope of the pile. The pile apex cores (3 and 6) exhibit relatively low inputs. This can be explained by the recent dumping that took place at a site to the southeast of the designated dumpsite used before 1973. Overall the southeast slope stations exhibit higher metal inputs than those located on the northwest slope.

For the period 1936-73, the inputs of Pb and Cu at the apex and downslope stations (cores 3 and 4, respectively) vary by more than two orders of magnitude; Cd, Ag, and Hg by one to two orders of magnitude. The Pb and Cu inputs in each core are very similar as well as the inputs of Cd, Ag, and Hg. The organic matter and Fe inputs are also comparable. Mn input is slightly higher than those for Pb and Cu. In a given core, input rates among the metals vary in proportion to their average concentrations in the deposit. For most cores, the order is organic matter >Fe>>Mn>Pb=Cu>>Ag>Cd=Hg.

For the period 1973-78, the input values for the trace metals vary over a smaller range, the maxima being relatively lower and the minima higher than the corresponding values for the 1936-73 period. The general order of the magnitude of the metal inputs is the same as above.

To put the calculated input values in the right perspective, it is best to compare these values with the anthropogenic inputs of metals in naturally deposited coastal sediments of other areas such as the California Basin, the Baltic Sea, and the Naragansett Bay (Table 16). The compilation in Table 20 shows that Pb, Cu, Cd, and Ag inputs to the New York Bight, through dredged material dumping, are generally much larger; up to two to three orders of magnitude higher than those for the other sites. This is particularly true in the central areas of the dredged material deposit. Relative to the Pb and Cu inputs to the Naragansett Bay sediments, these metals are depositing on the apex of the pile, as a result of dumping, at rates higher by factors of 40-80 and 30-70, respectively. Inputs of Pb and Cu at the downslope stations on the deposit are comparable to those reported for the Naragansett Bay. As reported by Goldberg *et al.* (1977), the Cu and Pb inputs to the Naragansett Bay sediments are two orders of magnitude higher than those from the Baltic Sea and the California Basins.

Anthropogenic inputs of Fe and Mn to the sediments of the California Basins, the Baltic Sea, and the Naragansett Bay are reported to be negligible (Bruland *et al.*, 1974; Erlenkeuser *et al.*, 1974; Goldberg *et al.*, 1977). However, Table 14 shows large anthropogenic enrichments of Fe and Mn in New York Bight dredged material as compared to the underlying natural sediment. This leads to a strong anthropogenic input of these metals, via dredged material dumping, to the New York Bight (Table 16). Bruland *et al.* (1974) reported average values of natural inputs of Fe and Mn for the California Basin deposits to be

Table 20. Interstitial concentrations of iron, manganese, and zinc in cores 4I, 6I, 8I and 9I.

Core No.	Core Description	Sample Interval (cm)	Iron (ppm)	Manganese (ppm)	Zinc (ppb)
4I	black sandy mud	0 - 4	76.7	6.85	81
	black sandy mud	4 - 8	89.8	6.92	76
	black muddy sand	8 - 12	60.2	2.18	77
	brown muddy sand	12 - 15.5	28.5	1.70	34
	black mud, brown sand	15.5 - 19.0	26.3	1.94	31
	black mud	19.0 - 22.5	26.3	2.21	41
	black sandy mud	22.5 - 29.5 <sup>1</sup>	-	-	-
	black sandy mud	29.5 - 33.0	5.5	1.01	76
6I	brown sand	0 - 15 <sup>1</sup>	-	-	-
	black sandy mud	15 - 19	1.6	1.43	13
	black sandy mud	20 - 24	44.9	2.44	20
	black sandy mud	25 - 29	58.0	2.61	25
	black sandy mud	30 - 34	60.8	2.58	28
	black sandy mud	35 - 39	66.3	2.56	59
	black mud	40 - 44	76.7	2.46	22
	black mud	45 - 49	79.4	2.34	37
8I	black mud	0 - 4	6.0	1.44	9
	black mud	7 - 11	10.4	2.02	7
	black mud	14 - 18	21.9	2.21	21
	black mud	21 - 25	21.9	1.86	60
	black mud, coal fragments	28 - 32	11.5	1.35	48
	black mud, some gravel	35 - 39	5.5	1.36	27
	black mud, some gravel	42 - 46	8.2	1.74	12
	black sandy mud, gravel	49 - 53	31.8	1.95	48
	black mud	56 - 60	7.7	1.65	12
	black mud	61 - 67	6.0	1.62	25
9I	black sandy mud	0 - 3	0.7	0.77	6
	black sandy mud	3 - 6	b.d. <sup>2</sup>	0.35	5
	black sandy mud	6 - 9	0.2	0.34	12
	black sandy mud	9 - 12	3.8	0.98	6
	black sandy mud	12 - 15	8.8	1.21	12
	black sandy mud	15 - 18	9.9	1.53	27
	black mud, red clay	18 - 21	14.8	2.03	25
	red clay	21 - 24	41.1	2.43	13
	black sandy mud	24 - 27	49.8	2.58	6
	black sandy mud	27 - 30	44.4	2.46	28

<sup>1</sup>Since the sediment was relatively coarse-grained, no interstitial water could be extracted.

<sup>2</sup>Dissolved Fe concentrations below 0.16 ppm were undetectable.

18 g/m<sup>2</sup>/yr and 0.15 g/m<sup>2</sup>/yr, respectively. The Mn and Fe inputs to the New York Bight through disposal of dredged material are more than two to three orders of magnitude higher than the natural weathering rates recorded in the California Basin sediments.

#### 4.6.6 Interstitial Water Chemistry

The dissolved Fe, Mn, and Zn concentration profiles for each core are displayed in Figure 47 and the results of the analysis are given in Table 20. The interstitial concentrations of Fe, Mn, and Zn in sediment cores at the study site exhibit highly variable concentration levels and distribution profiles. The minimum and maximum values observed for dissolved Fe, Mn, and Zn in the four cores were <0.2-90 ppm, 0.3-6.9 ppm, and 5-81 ppb, respectively. The interstitial waters were also analyzed for dissolved Cu, Cd, and Hg; their concentrations were below 6 ppb for Cu, 1 ppb for Hg, and 2 ppb for Cd for all samples.

In core 4I shown in Figure 47a, Fe and Mn profiles display maxima just below the core top, the concentrations decreasing down the core until minimum values are observed at ≈33 cm near the core bottom. The Zn profile is similar to the Fe and Mn profiles except that the minimum is reached at ≈18 cm. Zn concentrations increase below this depth approaching those observed at the core top. Maxima and minimum concentrations for Fe, Mn, and Zn observed in this core were 89.8 and 5.5 ppm, 6.9 and 1.0 ppm, and 81 and 31 ppb, respectively. The pore water presented in the 22.5 to 29.5 cm section of the core could not be extracted because of high sand content.

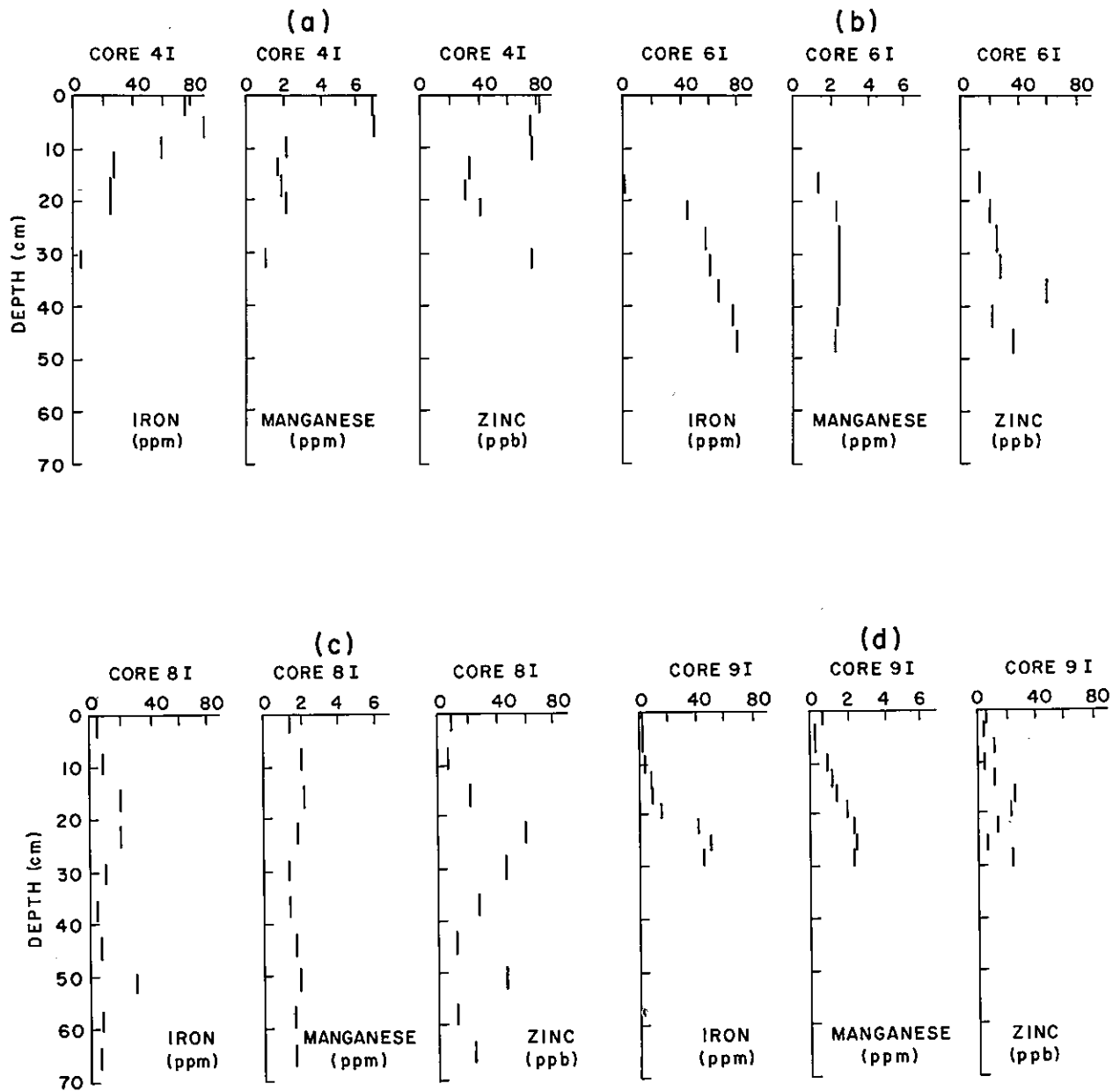


Figure 47. Depth distributions of interstitial iron, manganese, and zinc in dredged material deposit cores: (a) core 4I; (b) core 6I; (c) core 8I; and (d) core 9I.

The Fe, Mn, and Zn profiles for core 6I (Figure 47b) are mirror images of those observed in core 4I, the minima being at 15-19 cm depth. The pore water present in the top 0-15 cm of core 6I, could not be extracted because the sediment was predominantly sand. The Fe profile exhibits a systematic increase with depth, approaching a maximum of 79.4 ppm in the bottom-most section of the core. This concentration is comparable to the maximum observed at the top of core 4I. The Zn profile is similar to that for Fe, increasing down the core to a maximum of 59 ppb at ≈35 cm, but decreasing somewhat in the lower sections. Mn concentrations show little variability in this core, remaining relatively constant below 20 cm at about 2.5 ppm.

Depth distributions of Fe, Mn, and Zn in core 8I (Figure 47c) are completely different from those observed in other cores taken in the study area. The profiles of all three metals are similar for this core, exhibiting two maxima at approximately 20 cm and 50 cm; however, the relative variability in concentrations differs among the metals. Minimum values for the three metals were found near the sediment-water interface.

The interstitial Fe and Mn profiles in core 9I display minima at the core top (0-9 cm) where a strong H<sub>2</sub>S odor was present (Figure 47d). The concentrations increase systematically with depth until maxima are reached for both metals at 24-30 cm. These profiles are similar to those observed in core 6I where the distributions are shifted down to a greater depth in the core as a result of the sandy horizon at 0-15 cm. The Zn profile in core 9I shown in Figure 48d is also similar to that

in core 6I but the range in concentrations is smaller. The maximum in the Zn profile again occurs higher in the core ( $\approx 18$  cm) than those for Fe and Mn. Like Fe and Mn, the Zn minimum occurs near the core top. The interpretation of the observed interstitial metal profiles is given below.

Mn Profiles. As discussed, significant differences exist between the Mn profiles at different stations. The highest interstitial Mn concentration was observed in core 4I just below the sediment/water interface (4-8 cm). This indicates rapid removal of oxygen from the interstitial waters and transformation of solid oxide Mn phases into dissolved  $Mn^{2+}$ . Below the maximum in core 4I, manganese concentrations drop rapidly and this must reflect removal of  $Mn^{2+}$  into a solid phase, probably rhodochrosite ( $MnCO_3$ ). In contrast to core 4I, the dissolved Mn maxima in cores 6I, 8I, and 9I are recorded at greater depths, indicating that the oxic/anoxic boundary may be located deeper in these cores.

The interstitial Mn profiles described above can be represented qualitatively as a two-layer system where the boundary between the upper unit and lower unit corresponds to the observed maximum in the profile; a depth where maximal Mn remobilization occurs (Elderfield, 1979; Calvert and Price, 1972; Li *et al.*, 1969). This boundary probably corresponds to the transition zone from oxic to anoxic sediment. The upward decrease in manganese concentration above the boundary is related to the vertical migration of Mn by diffusion and advection, resulting from a concentration gradient and burial compaction, respectively. The decreasing concentration of Mn with depth, below the boundary, probably results from a diffusion gradient caused by dissolution

and precipitation of solid Mn phases, such as oxides and carbonates, respectively (Calvert and Price, 1972; Elderfield, 1979).

In areas of high sedimentation rate, such as those examined here, the surface sediment is oxidized while the sub-surface sediment is reduced. As sedimentation proceeds, the surface sediment, containing both Fe and Mn oxide phases, is buried and microbial oxidation of sedimentary organic matter results in the reduction and dissolution of the oxide phases at depth. With compaction, the dissolved Mn migrates toward the sediment-water interface.

Using the average bottom water manganese levels reported by Segar and Cantillo (1976) as concentrations at the sediment/water interface, the concentration gradients, above the maxima, vary by an order of magnitude:  $0.09 \mu\text{g}/\text{cm}^4$  in core 9I to  $0.86 \mu\text{g}/\text{cm}^4$  in core 4I. Compared with cores 6I and 9I, the rather steep concentration gradient in core 4I results mainly from the location of the concentration maximum close to the core top.

Fe Profiles. The interstitial Fe profiles closely resemble the dissolved Mn profiles. However, the concentration gradients calculated for dissolved iron are greater than those observed for dissolved manganese.

It has been reported that Fe concentrations in anoxic interstitial waters are controlled by the solubilities of various iron sulfide minerals such as greigite and mackinawite and amorphous sulfides (Berner, 1971). More recently, several workers have reported the precipitation of vivianite,  $\text{Fe}_3(\text{PO}_4)_2 \cdot 8\text{H}_2\text{O}$ , as the controlling factor

for dissolved Fe concentration in reducing sediments containing high concentrations of dissolved phosphate (Bray *et al.*, 1973; Emerson, 1976; Martens *et al.*, 1978).

Since the dissolved Fe profiles closely follow the dissolved Mn profiles, it seems likely that processes similar to those described above for Mn also control the dissolved Fe concentrations. That is, the observed maxima in the profiles correspond to the zones of maximal Fe remobilization. Decreasing concentrations towards the core top, above the maxima, indicate diffusive and/or advective transport of dissolved Fe to the oxic sediment and/or the overlying water column. Like the interstitial Mn profiles, the decline in Fe concentrations below the maxima with depth indicate a diffusion gradient resulting from the dissolution and precipitation of solid Fe mineral phases such as oxides, and sulfides and phosphates, respectively.

The observed concentration gradients for  $\text{Fe}^{2+}$  display the same pattern as those observed for  $\text{Mn}^{2+}$ . The values range from 1.84  $\mu\text{g}/\text{cm}^4$  in core 9I to 11.23  $\mu\text{g}/\text{cm}^4$  in core 4I. The concentration gradients for  $\text{Fe}^{2+}$  are greater by more than an order of magnitude than those for  $\text{Mn}^{2+}$ . This implies a greater rate for the remobilization of  $\text{Fe}^{2+}$  than for  $\text{Mn}^{2+}$ . However, since the iron concentrations of bulk sediment are two orders of magnitude greater than those for manganese, the sediments may serve as a relatively more efficient trap for remobilized  $\text{Fe}^{2+}$  as compared with  $\text{Mn}^{2+}$ .

Zn Profiles. Although some divergences were observed, particularly at the core bottoms, the interstitial Zn profiles follow similar trends to those for Fe and Mn. It is expected that similar sedimentary processes control the dissolution and precipitation of Fe, Mn, and Zn. Coprecipitation (and dissolution) of Zn with Mn and Fe oxyhydroxides may be partly responsible for the similarity in the distributions of these three metals.

In reducing sediments, sulfide precipitation is generally thought to control interstitial Zn concentrations. However, dissolved silica and  $\text{CO}_3^-$  species have been postulated as possible controlling factors in natural systems (Hem, 1972; Willey, 1977). Chelation by dissolved organic matter in sediments may also reduce the activity of free  $\text{Zn}^{2+}$  ions in interstitial water solutions and thereby maintain higher total dissolved Zn levels than theoretically predicted based on saturation equilibrium calculations.

Segar and Cantillo (1976) found a wide range of concentrations for dissolved Zn present in the bottom water of the New York Bight Apex with an average value determined to be 32 ppb. This is close to the average concentration of 30 ppb found in this study for interstitial waters in sediments from the dredged material deposit. These data indicate that the dredged material deposit may be a diffusional source of dissolved Zn to overlying waters in some areas (e.g., Core 4I) and a sink in other areas (e.g., Cores 6I, 8I, and 9I) of the deposit depending upon the concentrations ambient in the sediments and the overlying water at the time. However, since concentrations

in both water and sediments appear to be relatively similar, it is unlikely that diffusional transport of dissolved Zn is significant in any case.

Cu, Cd and Hg Profiles. Dissolved Cu, Cd, and Hg in all interstitial water samples were found to be below 6 ppb, 2 ppb, and 1 ppb, respectively. It is generally believed that in reducing sediments the dissolved concentrations of these trace elements reach saturation with respect to their sulphide phases resulting in the precipitation of authigenic metal sulphides. However, higher than equilibrium saturation concentrations have been reported for interstitial trace elements for other areas (MSRC, 1978; Elderfield and Hepworth, 1975; Lindberg and Harris, 1974; Presley *et al.*, 1972; Brooks *et al.*, 1968). In these cases, like interstitial Zn discussed above, processes other than metal sulphide precipitation are believed to control the dissolved Cd, Cu, and Hg concentrations.

In contrast to the relatively high concentrations of interstitial  $\text{Fe}^{2+}$  and  $\text{Mn}^{2+}$  observed in the sediment cores, the dissolved Cu, Cd, and Hg concentrations are extremely low, indicating that these elements are practically immobile in the dissolved state and retained by the sediments most effectively.

Benthic Fluxes of Dissolved Fe, Mn, and Zn. The net fluxes of dissolved Mn, Fe, and Zn from sediment to the overlying water column can be calculated from the observed concentration gradients recorded above the maxima in the profiles of Fe, Mn, and Zn. The profiles, below the maxima, reflect dissolution and precipitation reactions and

can be ignored in the flux calculations. The interstitial waters, however, are not significantly enriched in zinc relative to its concentration in the overlying water. Therefore, the zinc diffusional flux is considered to be negligible and not calculated here.

The upward flux can be calculated using the equation:

$$J(\text{Fe,Mn}) = -D \frac{dc}{dz} - \omega c \quad (3)$$

where  $D$  is the apparent molecular diffusion coefficient of  $\text{Fe}^{2+}$  or  $\text{Mn}^{2+}$ ,  $c$  is the concentration of  $\text{Fe}^{2+}$  or  $\text{Mn}^{2+}$  in the interstitial water, and  $dc/dz$  their concentration gradients,  $z$  is depth in the core ( $z = 0$  at the core top;  $z = \lambda$  at the depth of maximum concentration), and  $\omega$  is the rate of sedimentation, used here as an advective velocity term.

To obtain maximum flux values, we assume a linear concentration gradient. The concentrations of dissolved Fe and Mn at depth,  $z = 0$  are 12 and 8 ppb, respectively, as reported by Segar and Cantillo (1976) for bottom water sampled in the dredged material dumpsite area. For estimating advective fluxes of Fe, Mn and Zn average values of their concentrations above the observed maxima were used for  $c$ .

Assuming negligible interaction between  $\text{Fe}^{2+}$  and  $\text{Mn}^{2+}$  ions and the sediment host particles, a value of  $1.06 \times 10^{-6}$   $\text{cm}^2/\text{sec}$  is used for the apparent diffusion coefficient for both  $\text{Fe}^{2+}$  and  $\text{Mn}^{2+}$  at  $4^\circ\text{C}$  as reported by Manheim (1976). Sediment tortuosity and porosity corrections have been made in the  $D$  value given above. Rates of sedimentation, assumed to be constant over a period of time, are used to calculate the advective flux term.

Table 21 gives the observed concentration gradients for  $\text{Fe}^{2+}$  and  $\text{Mn}^{2+}$ , the concentration maxima depths, the sedimentation rates at each station, and the calculated diffusive, advective, and total fluxes of  $\text{Fe}^{2+}$  and  $\text{Mn}^{2+}$  at each station. Also included in Table 21 are the advective flux values for Zn. It is clear that the advective process dominates the net benthic flux of  $\text{Fe}^{2+}$ ,  $\text{Mn}^{2+}$ , and  $\text{Zn}^{2+}$ . This is to be expected considering the high sedimentation rates in the area. The effect is most pronounced at station 6I, where the calculated sedimentation rate was found to be approximately 60 cm/year. The diffusive flux of  $\text{Fe}^{+}$  or  $\text{Mn}^{+}$  is a small fraction of their total benthic flux. Some precipitation of dissolved Fe and Mn will likely occur as these migrating ions encounter the oxidizing zone at the sediment/water interface. Therefore, the calculated flux values may reflect a liberal estimate.

In order to evaluate the effect of high sedimentation rate on the interstitial water profiles, it is important to determine the time scale of the diffusional process. The time required for an interstitial water profile to adjust to equilibrium conditions by diffusion is given by

$$t = \frac{x^2}{D} \quad (4)$$

where  $t$  is the time scale of diffusion;  $x$  is the length of the diffusion path, and  $D$  is the diffusion coefficient for  $\text{Fe}^{2+}$  or  $\text{Mn}^{2+}$ .

Using a value of 8 cm for  $x$  and  $\sim 10^{-6}$   $\text{cm}^2/\text{sec}$  for  $D_{\text{Fe,Mn}}$  in equation (2), a value of  $\sim 2$  years is obtained for  $t$ . This is approximately the time required for the dissolved  $\text{Fe}^{2+}$  or  $\text{Mn}^{2+}$  to diffuse

Table 21. Estimates of the diagenetic flux of dissolved Fe, Mn, and Zn in dredged material sediments, New York Bight.

Core No.	Metal	Concentration <sup>1</sup> Gradient ( $\mu\text{g}/\text{cm}^4$ )	Depth of Maximum Concentration, $z$ (cm)	Sedimentation <sup>2</sup> Rate, $\omega$ (cm/yr)	Calculated Flux ( $\text{g}/\text{m}^2/\text{yr}$ )		
					Diffusive Term	Advective Term <sup>3</sup>	Total
4I	Mn	0.86	8	20	0.288	1.38	1.67
	Fe	11.23	8	20	3.75	16.65	20.40
	Zn	-	12	20	-	0.016	0.016
6I	Mn	0.17	29	60	0.060	0.974	1.03
	Fe	2.27	49	60	0.759	29.08	29.84
	Zn	-	49	60	-	0.015	0.015
9I	Mn	0.09	27	11	0.030	0.149	0.179
	Fe	1.84	27	11	0.615	1.48	2.09
	Zn	-	18	11	-	0.001	0.001

<sup>1</sup>Bottom water concentrations of Fe = 12 ppb and Mn = 8 ppb, reported by Segar and Cantillo (1976), are used to estimate concentration gradients.

<sup>2</sup>Sedimentation rates are those estimated for the period 1973-78.

<sup>3</sup>Average values of dissolved Fe, Mn, and Zn concentrations, above the maxima, are used to calculate the advective flux term.

through 8 cm of sediment in core 4I. Assuming a constant sedimentation rate, the time scale of sedimentation at this station is comparable to that of diffusion, indicating that diffusion may be an important process at this station.

In other cores, however, the characteristic time scale of diffusion ( $t$ ) was found to range from 13 years for core 6I to 23 years for core 9I. This implies that the time scale of sedimentation is too fast at these stations as compared with diffusion. In other words, diffusion is not a significant process at these stations.

In our calculations of benthic fluxes, we have assumed that the sedimentation rate is constant over a period of time at the New York Bight dredged material disposal site. In reality, however, it is not constant but episodic; each episode corresponds to a dump event or a number of events having variable frequency and mass loads. During dump events, the impact of the load on the bottom may result in sediment compaction. Thus, in turn, will enhance the upward flow of interstitial water, resulting in a greater advective transfer of dissolved Fe, Zn, and Mn across sediment-water interface to the overlying water. This episodic dumping may contribute more interstitial Fe, Zn, and Mn to the overlying water than that calculated above for the advective term.

Sediment resuspension may also contribute to the benthic fluxes of metals. For example, the impact of individual dump events may result in resuspension of bottom sediments. This and other turbulent sediment resuspension processes, such as storm events, can result in

the release of dissolved Mn or Fe and other metals to the overlying water column. Lindberg and Harris (1974), Bricker and Troup (1975), and Sanders (1978) report that remobilization of metals during sediment resuspension can be a significant process contributing metals to overlying waters.

Additionally, a dump or a storm event may replace the metal-rich interstitial water with metal-depleted bottom water, resulting in a net flux via flushing. This process would operate at a faster rate than molecular diffusion. The importance of this process is a function of the depth to which flushing takes place, the frequency of individual events, and the extent of metal enrichment in the pore waters. The potential flux of interstitial metals due to a dump event can be estimated by taking cores before and after the event. The amount of metals transferred to overlying waters, as a result of a dump or storm, can be estimated from the difference in the interstitial metal profiles. Elderfield (1978) found lower zinc concentrations in pore waters of Conway estuary sediment, following a storm event. Using the difference in the concentration gradients of interstitial Zn, before and after the storm event, he was able to calculate a flux via flushing for the one-day storm. Similar observations were reported by Sanders (1978) for interstitial Mn in sediments of Calico Creek, North Carolina.

Although bioturbation, as a benthic process, is known to enhance the flux of interstitial metals to overlying waters, it is unlikely that it is an important mechanism in the study area considering the high sedimentation rates. Pearce *et al.* (1976) have reported that

the dredged material dumpsite sediments are practically devoid of benthic organisms. The absence of benthic organisms is also indicated by our sampling.

#### 4.6.7 Stratigraphy

The stratigraphy of the dredged material deposit has been established using sediment texture and metal data from the cores collected in the study area.

The stratigraphic sections of the deposit based on sediment texture and metal data are shown in Figures 48 and 49. The ten cores taken at the dumpsite are arranged in sequence. In Figures 48 and 49, cores 1 and 6 represent the end points of the northwest transect whereas the end points of the southeast transect are represented by cores 3 and 10. Cores 3 and 6 lie on the apex of the deposit where the two transects intersect. The vertical relationship of each of the cores is based on the tide corrected soundings taken at the time of the coring. The horizontal scale gives the relative distances between cores.

Textural Stratigraphy. The sediment types chosen for stratigraphic correlation were distinctive in texture and generally were easily visually identifiable. Grain size and organic content were then used to ascertain the similarity of the sediment. The greensand layer provides the only natural sub-bottom horizon. In cores 5, 2, and 9 the greensand must have been exposed as an erosional surface because it comprises the top of the natural sediment, being directly overlain by dredged material. In other cores where the natural sediment was

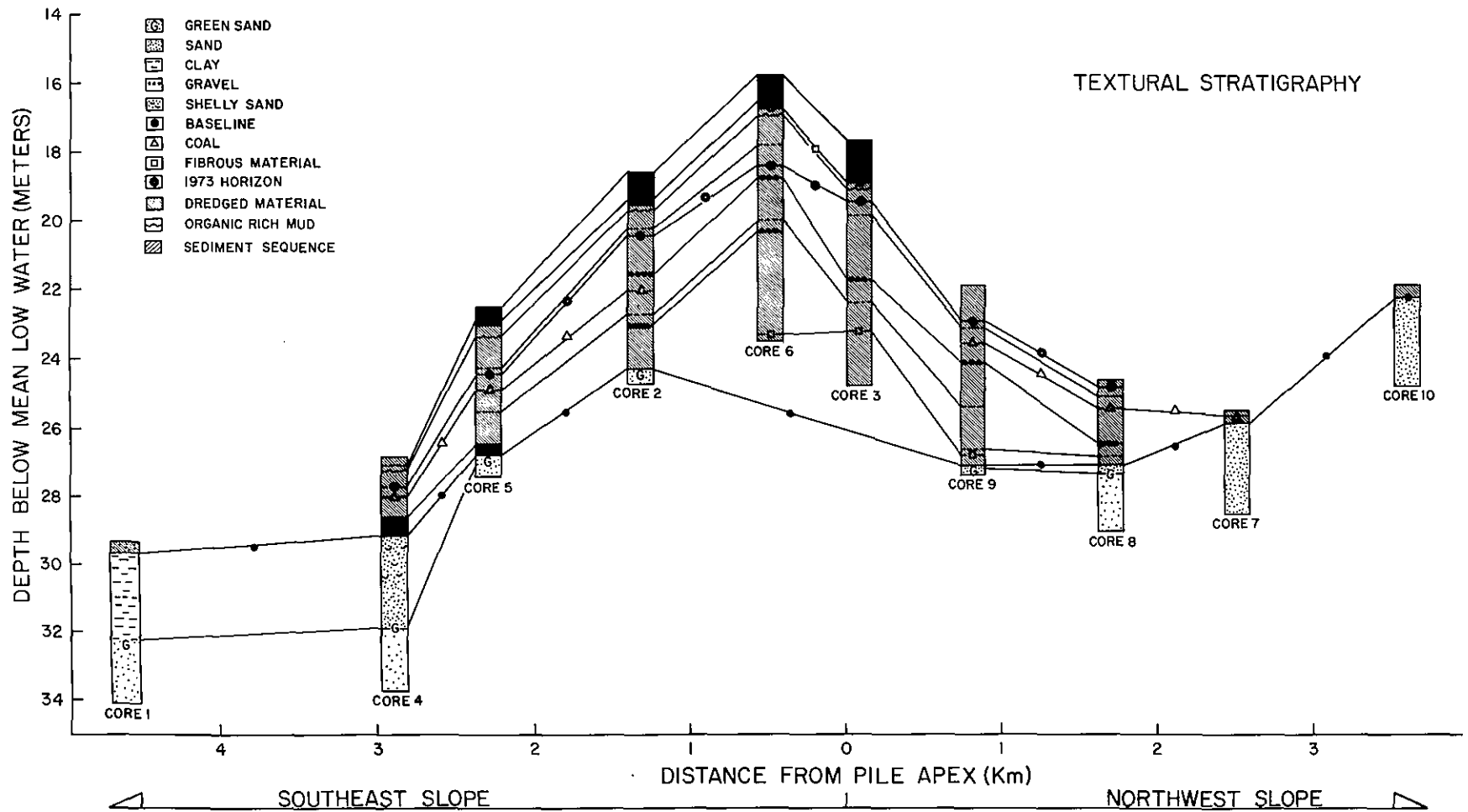


Figure 48. Cross-sectional profile of the deposit along the northwest-southeast transects, showing the textural stratigraphy.

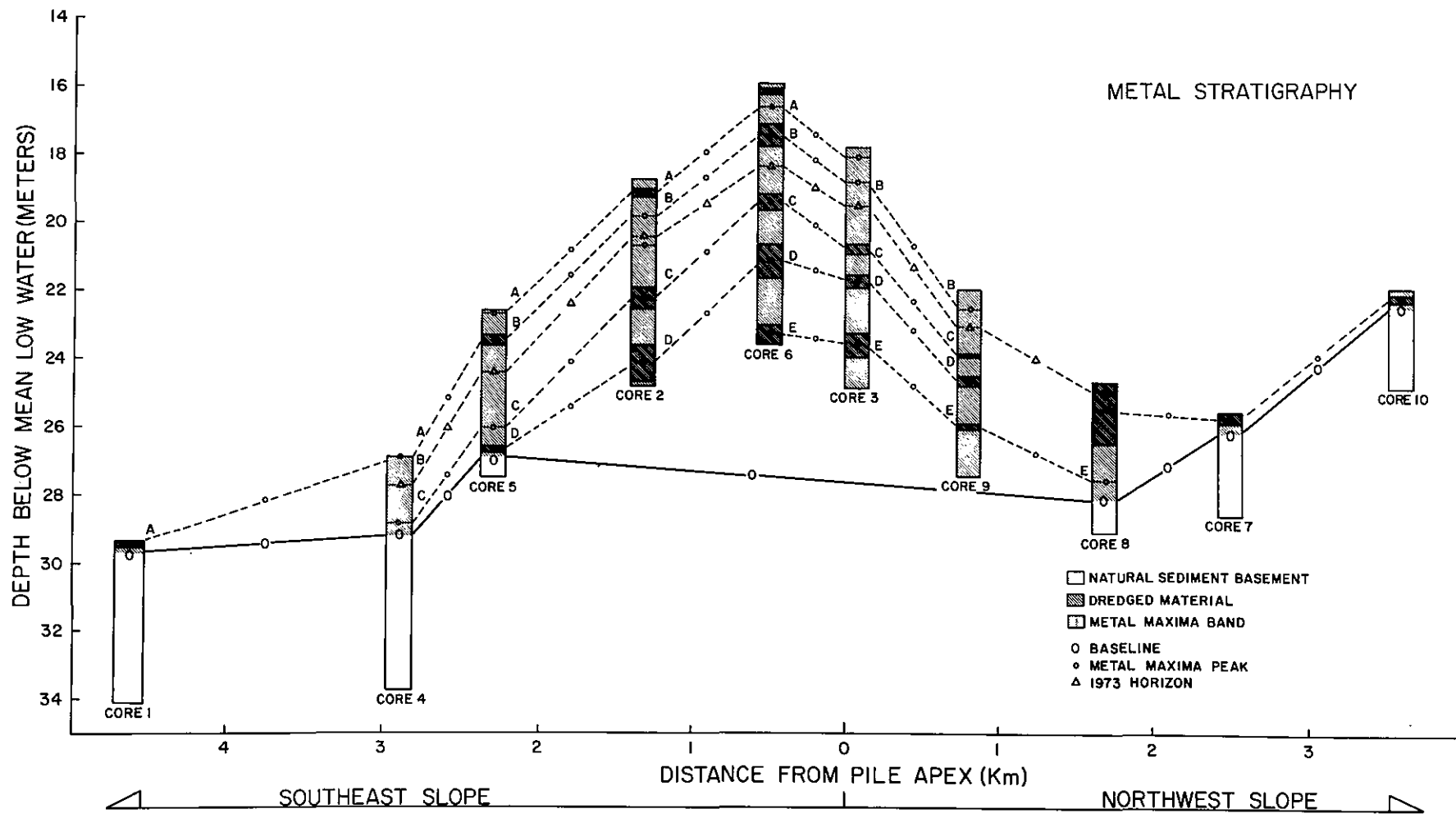


Figure 49. Cross-sectional profile of the deposit along the northwest-southeast transects, showing the metal stratigraphy.

sampled, the material underlying the dredged material was medium to coarse grained white or gray sand. The profile of the basement horizon conforms roughly to the 1936 bathymetry. The lithology is shown for the natural sediment in Figure 48 while the dredged material is simply shown by shading.

The dark cross-hatched areas at the tops of cores 2, 3, 5, and 6 represent a thick bed of sand/mud/sand sequence. A similar sequence of sediment types was present in the basal units of dredged materials, overlying the natural sediment, in cores 4 and 5. The other horizons indicated on Figure 48 represent discrete beds of coal, gravel, mud, clay and fibrous organic material.

The coal beds were present in two horizons. In cores 2, 4, and 5 coal was observed at depths of 3.4, 1.1, and 2.3 m, respectively. Coal was also found at 1.6 m in core 9, and at 0.9 m depth in core 8 and throughout the 60 cm thick bed of dredged material at the top of core 7. The relative positions of occurrence of this material in the cores suggest that these beds may belong to the same horizon with gaps present in cores 3 and 6. The coal was generally angular anthracite of pebble size, associated with wood fragments.

From the depth of the beds and the average sedimentation rates for each core it has been determined that the coal beds were deposited between 1962 and 1967. Gross (1976) reported that the annual dumping of coal ash peaked at  $0.18 \times 10^6$  tons in 1963. The two coal beds may therefore have been associated with this dumping.

The red clay horizons were the most extensive. This material was found in a variety of forms, primarily in beds and in galls. The upper horizon was found in the top meter of cores 2, 3, 4, 5, and 6 occasionally mixed with the mud of the sediment sequence shown in Figure 48. A second horizon was found, just above the 1973 bathymetry horizon, in cores 2, 5, and 6. A third was observed just below the 1973 horizon in cores 3, 8, and 9. The fourth red clay horizon was found throughout the deposit in cores 2, 3, 5, 6, and 9. The lower-most clay horizon was found above the natural sediment basement in cores 8 and 9. It is believed that this clay type represents sediment derived from Newark Bay (D. Suskowski, personal communication). Thus, the red clay horizons observed in the deposit may reflect dumping of material dredged from that area.

While muds are ubiquitous in the dumpsite there were certain distinct beds of organic rich mud which were recognizable by the particularly high organic content and very low gravel and sand percentages. A horizon of this material was present in the top portions of cores 2, 3, 4, 5, and 6. The presence of this horizon may represent dumping of large amounts of sewage sludge at the site in late 1971 (Conner *et al.*, 1979). This horizon has been correlated with horizon B of the metal stratigraphy discussed later.

The 1973 horizon was established from the 1973 bathymetric survey (Freeland and Merrill, 1977), based on interpolation between station locations. Note that the strike-lines for this horizon are generally parallel to those for the textural stratigraphy. This

indicates that there is good agreement between the two methods. Further, a sufficient number of horizons have been identified to demonstrate that individual dumping projects may be distinguished in the sedimentary record.

In Figure 48, it may be seen that the stratigraphy of the northwest slope is less developed than for the central and southeastern sections of the deposit, particularly at the core tops. Above the 1973 horizon, there are no well defined strata in this part of the deposit.

As expected, the dredged material deposit thins out towards the edges. Much of this spread is believed to be due to post-depositional dispersion of dumped material. Statistical tests applied to the percentages of gravel and mud in samples from each core provide clear evidence that there is significantly more mud found in the peripheral cores than in those taken at the apex of the deposit. This indicates that fine grained sediment is winnowed from the crest of the site and re-deposited downslope. As a result of this sedimentary process, the stratigraphic record is rather tenuous along the fringes of the deposit. A similar observation has been made, in general, for bedding forms. Toward the fringes of the deposit the discrete beds of sediment that are seen in the central cores are less frequent, a result of the above mentioned processes.

Metal Stratigraphy. A schematic representation of the stratigraphy of the dredged material deposit as deduced from the observed maxima in heavy metal concentration profiles of each core is displayed

in Figure 49. The metals used for this purpose were Ag, Pb, Cu, Cd, and Hg. The portion of each core that is composed of dredged material is shown by light shading. The sections of the cores that represent natural sediment are left unshaded. The surface of the dredged material deposit as it was indicated by the 1973 survey (Freeland and Merrill, 1977) is represented by the horizon marked with a triangle. The horizons indicated by black circles are maxima in the metal profiles of the sample stations.

The strike lines between the cores join segments of beds that apparently were synchronously deposited and reflect the same source material and dumping project. The maxima occur in two forms; (1) as thick beds of sediment having similar metal concentrations and depicted as darkly shaded sections of the cores marked with a dark circle; and (2) as discrete metal-rich layers represented by a single line also marked by a dark circle. To further differentiate these metal horizons, letters A, B, C, D, and E have been used in the stratigraphy (Figure 49).

The basement of the deposit is represented by a horizon marked with open circles. It was defined as the depth where the metal profiles exhibited a sharp drop in concentrations to lower and less variable values. Cores 2, 3, 6, and 9 did not penetrate to this depth.

Cores 1, 7, and 10 are peripheral to the dredged material deposit. These stations show only background levels of metals with slight

elevation of metal content in the top half meter of the cores. They do not contribute to defining any stratigraphic metal horizons but do indicate the surficial spread of the dumped material. Of interest is the observation that these stations show little delineation of any strata within the dredged material. Rather, they are relatively homogeneous in their contaminated surficial material. This is in marked contrast to the cores taken from the center of the deposit which show frequent stratigraphic relationships.

The correlation of horizons in Figure 49 is, in general, good for the five central cores. This correlation also agrees with the horizon based on the 1973 bathymetric survey.

Cores 2 and 3 exhibit a spike of metal concentrations, just below the 1973 horizon. This is absent in station 6 presumably as a result of wide sampling intervals in the core. The bottom-most horizon of cores 3, 6, 8, and 9, does not appear in cores 2, 4, or 5 indicating that dumping started on the southeastern slope more recently than it did elsewhere on the deposit. This is also seen in the cross-sectional profile of the pile (Figure 24).

All of the metal maxima comprising horizon B (Figure 49) lie above the 1973 horizon in the cores. Therefore, the material overlying this horizon was dumped between 1973 and 1978. From the position of horizon B relative to the 1973 horizon, a reasonable estimate for the time of deposition of the metal rich sediment is 1975. Horizon B is also seen in the textural stratigraphy represented by a bed of highly organic mud.

Horizon C is seen throughout the dredged material pile. At station 3, 6, and 9 this horizon is found 1 meter below the 1973 stratum. Further to the south horizon C is found deeper in the cores, indicating that this area on the southern flank has only recently been subject to heavy dumping. This is also evident from the estimated sedimentation rates for the period 1973-78 and the net bathymetric change profile for this period.

It is believed that horizon C represents the first massive input of sewage sludge to the dumpsite prior to 1973. According to Conner *et al.* (1979), approximately  $4.4 \times 10^6$  m<sup>3</sup> of sewage sludge were dumped at the site during the period October-December, 1971. Textural stratigraphy exhibits the presence of an organic rich stratum at this depth in the deposit. Sewage sludge is known to be enriched in organic matter and certain heavy metals (Gross, 1970). The stratum, represented by horizon C, does indeed exhibit these characteristics.

The correlation between the textural stratigraphy and metal stratigraphy is generally very good. The location of the metal horizons agreed well with those based on sediment texture. In addition, the slopes of the strike-lines between adjacent cores are usually similar for the two stratigraphic profiles. Thus, the spatial distribution of metals over a period of time in the dredged material deposit is basically controlled by the character and distribution of different sediment types in the deposit. This, in turn, is related to the nature and mass of the dredged material, the frequency of individual dump events, and the pre- and post-depositional sedimentary processes.

## 5. MASS BALANCE OF DREDGED MATERIAL AND ASSOCIATED METALS

### 5.1 Dredged Material

Based on Tables 6 and 10, Table 22 has been compiled to provide a comparison of the amount of dredged material dumped with the amount of material actually found in the deposit for the period 1936-78. Estimates are also given for the periods 1936-73 and 1973-78.

The total volume dumped during the period is estimated to be  $208 \times 10^6 \text{ m}^3$ . The estimated volume of material present in the deposit for the same time period is reported to be  $120 \times 10^6 \text{ m}^3$ . This figure corresponds to approximately 58% of the volume that was actually dumped. The bulk mass estimates, however, show that 82% of the mass of material dumped during the period 1936-78 is present in the deposit. This difference can be attributed to post-depositional compaction of dredged material in the deposit as indicated by the bulk density values of  $1.2 \text{ g/cm}^3$  for harbor sediments and  $1.7 \text{ g/cm}^3$  for dredged material in the deposit. Some of the compaction observed in our samples could have resulted during the vibracoring process.

The dry mass of material was estimated from its water content. Table 22 shows that a total dry mass of  $125 \times 10^{12} \text{ g}$  of material was removed from the dredging sites during the period 1936-78. A value of  $141 \times 10^{12} \text{ g}$  was obtained for the total dry mass of material present in the deposit, indicating that approximately 10% more sediment is present in the deposit than the total mass dumped during the period 1936-78. This mass imbalance may be due to the deposition of sand

Table 22. Estimates of dredged material dumped during the period 1936-78<sup>1</sup> and material present in the deposit<sup>2</sup>.

Dumping Period	Estimates of Dredged Material Dumped				Estimates of Material in the Deposit			
	Bulk Volume (10 <sup>6</sup> m <sup>3</sup> )	Bulk Mass (10 <sup>12</sup> g)	Dry Mass (10 <sup>12</sup> g)	Input Rate (10 <sup>12</sup> g/yr)	Bulk Volume (10 <sup>6</sup> m <sup>3</sup> )	Bulk Mass (10 <sup>12</sup> g)	Dry Mass (10 <sup>12</sup> g)	Input Rate (10 <sup>12</sup> g/yr)
1973-78 (5 years)	52.0	62.4	31.2	6.3	27.0	45.9	31.7	6.3
1936-73 (37 years)	156.0	187.2	93.6	2.6	93.0	158.1	109.1	2.9
1936-78 (42 years)	208.0	249.6	124.8	2.9	120.0	204.0	140.8	3.4

<sup>1</sup>Based on dredged material dumping records for the period 1936-78.

<sup>2</sup>Based on the 1936, 1973, and 1978 bathymetric surveys.

on the dumpsite from surrounding areas. As discussed earlier, we believe that as much as 8% of the total volume of material present in the deposit is sand, derived from surrounding areas, transported onto the dumpsite by natural processes such as storm events.

However, considering the uncertainties in the data compiled in Table 22, it is quite conceivable that the discrepancy discussed above is not significant. It is interesting to note that for the short-time period 1973-78, the period for which the available data are most reliable, the mass of material dumped approaches 98% of that present in the deposit.

Therefore, in terms of mass balance, it appears that the mass of material dumped at the site over a period of time is conserved within the deposit. However, the differences in the volume estimates are significant and can be attributed to compaction of dredged material in the deposit.

## 5.2 Trace Metals

The average metal concentrations of sediment sampled from the New York Harbor and from the dredge hoppers are given in Table 23. Also given in Table 23 are the average concentrations of metals observed in the dredged material deposit core sections corresponding to the dumping period 1973-78.

Comparison of the mass of metals associated with dredged material dumping during the period 1973-78 with the mass of metals deposited at the dumpsite during the same dumping period is given in Table 24.

Table 23. Average metal concentrations of dredged material derived from the source areas and from the deposit.

Metal	New York Harbor and Hopper Sediments (ppm) <sup>1</sup>	Dredged Material Deposit Sediments (ppm) <sup>2</sup>
		1973-78
Fe	35000	19900
Mn	420	261
Cu	180	76
Pb	134	68
Cd	3.6	1.6
Hg	4.5	1.6

<sup>1</sup>Metal data reported by Williams *et al.* (1978) and Conner *et al.* (1979)

<sup>2</sup>This study.

Table 24. Comparison of mass and rates of metal inputs associated with dredged material dumping during 1973-78 with the metal inputs based on the depositional record.

Metal	Dredged Material Dumping		Dredged Material Deposit		Metal Remaining in Deposit (%)
	Total Metal Inputs (g) <sup>1</sup>	Annual Metal Inputs (g/yr)	Total Metal Inputs (g) <sup>2</sup>	Annual Metal Inputs (g/yr)	
Fe	$1.18 \times 10^{12}$	$23.60 \times 10^{10}$	$0.63 \times 10^{12}$	$12.60 \times 10^{10}$	53
Mn	$1.42 \times 10^{10}$	$28.40 \times 10^8$	$0.83 \times 10^{10}$	$16.60 \times 10^8$	58
Cu	$6.1 \times 10^9$	$12.20 \times 10^8$	$2.40 \times 10^9$	$4.80 \times 10^8$	39
Pb	$4.50 \times 10^9$	$9.00 \times 10^8$	$2.20 \times 10^9$	$4.40 \times 10^8$	49
Hg	$1.52 \times 10^8$	$30.40 \times 10^6$	$0.50 \times 10^8$	$10.00 \times 10^6$	33
Cd	$1.22 \times 10^8$	$24.40 \times 10^6$	$0.50 \times 10^8$	$10.00 \times 10^6$	41

<sup>1</sup>Based on the dumping records for the period 1973-78 and average metal concentrations of dredged material sampled from dredging sites.

<sup>2</sup>Based on net accumulation of material in the deposit during the period 1973-78 and average metal concentrations of dredged material in the deposit cores.

The estimates given in Table 24 are compiled based on the information presented in Tables 6, 7, 8, 10, 22, and 23. Table 24 also includes estimates of annual metal inputs to the dumpsite based on the depositional record and the available data on dredged material derived from source areas. The last column in Table 24 gives the percentages of metals retained in the deposit relative to the mass of metals dumped during the period 1973-78.

The total inputs of metals to the dumpsite during the period 1973-78, via dumping, vary from  $1.2 \times 10^8$  g for Cd to  $11800 \times 10^8$  g for Fe. The Hg and Pb estimates are similar to those of Cd and Cu, respectively; the sequence of decreasing inputs of metals being: Fe > Mn > Cu > Pb > Hg > Cd. The total metal inputs for the same dumping period, based on the depositional record, are consistently lower for each metal, varying from  $0.50 \times 10^8$  g for Cd to  $6300 \times 10^8$  g for Fe. Approximately, 53 and 58% of the iron and manganese deposited at the dumpsite, via dredged material dumping during the period 1973-78, are found in the deposit. Other metals exhibit much greater loss from the deposit than iron and manganese.

We believe that the lower metal estimates for the deposit may be due to the following processes:

1. Transport of finer grained, metal rich material away from the center outside the perimeter of the deposit. As discussed earlier, preferential transport of fine grained material to the fringes of the pile can occur during descent of the material in the water column. Erosion of the fine grained component of deposited dredged material by storm events is known to occur in this area (Freeland and Merrill, 1977). This agrees with our observation that the apex and upslope

cores contain, on the average, more sand than the downslope cores. Stubblefield *et al.* (1977) also reported the presence of fine grained sediment in the outlying areas surrounding the deposit.

2. Possible desorption of certain metals during descent of dumped dredged material in the water column. Oxidation of metal sulphides present in reducing dredged material can also result in the loss of metals during descent in the water column.

3. Metal data for dredging source areas, compiled in Table 7, are based upon limited sampling and, therefore, may not be representative of all dredging sites.

4. As reported earlier, the transport of sand onto the dumpsite from surrounding areas may be a significant factor. The presence of this relatively uncontaminated sand can result in a dilution effect, giving rise to lower metal estimates.

## 6. GEOCHEMICAL CONSEQUENCES OF DREDGED MATERIAL DUMPING

Considering the magnitude of the process of dredged material dumping in the New York Bight, it is important to evaluate its effect on the regional geochemical systems.

Relative to other metal inputs to the New York Bight, dredged material dumping is the major contributor, accounting for 24 to 80% of the total input (Mueller *et al.*, 1976). Atmospheric metal inputs to the Bight, as reported by Duce *et al.* (1976) vary from 1.5% for Cd to 13% for Pb of the total metal inputs. Secondary inputs, related to wastewater discharges, land runoff, and sewage sludge dumping, are also significant.

Comparison of metal enrichments and inputs as recorded in the dredged material deposit with those reported for other coastal deposits shows clearly the impact of dredged material dumping in the New York Bight for the last 100 years or so.

A mass balance of total inputs via dredged material dumping with the inputs estimated from the depositional record for the period 1973-78 indicates that, although most of the dredged material dumped is found in the deposit, all metals studied are lost from the system in varying degrees, either during the dumping process or following deposition.

## 7. CONCLUSIONS

The sediments of the dredged material deposit are comprised of a wide variety of sediment types, which can be classified as quartz and glauconitic sands, muds, sandy muds, gravel intermixed with muds, and artifact material such as coal and fly ash, wood, slag, metal flakes, glass, etc. Fine grained, black sandy mud is characteristic of dumped dredged material. Glauconitic sand and gravelly quartzose sand are typical of the natural sediment underlying the deposit and in surrounding areas.

The spatial distributions of heavy metals such as Pb, Cu, Ag, Hg, Cd, Fe, and Mn in the dredged material deposit exhibit highly variable and considerably elevated concentrations over those observed in sediment outside the deposit and in underlying natural sediment. Compared to metal enrichments reported for other coastal deposits, the degree of metal enrichment observed in dredged material sediments are orders of magnitude greater.

Organic matter appears to play a significant role in the distribution of metals in the dredged material sediments. Iron and manganese hydrous oxide phases also appear to control the trace metal distributions, especially for Cu and Pb.

The estimated rates and magnitudes of metal inputs to the New York Bight, based on the depositional record, are found to be orders of magnitude higher than those reported for other naturally deposited coastal sediments. On a regional scale, it appears that dumping of dredged material affects the metal depositional record in the New York Bight.

A mass balance of total inputs to the dumpsite via dredged material dumping with inputs estimated from the depositional record for the period 1973-78 indicates that, although most of the dumped material is present in the deposit, most metals are lost from the system in varying degrees either during the dumping process or following deposition of the dumped material.

Pore water data indicate a sediment derived flux of dissolved Fe, Mn, and Zn to overlying water column due to diagenetic remobilization of these metals in the dredged material. Because of the high sedimentation rates, the advective component dominates the benthic flux. Other metals like Cd, Cu, or Hg are present at extremely low concentrations in the pore waters, indicating that their flux is very small or practically negligible. Other processes, such as sediment resuspension or flushing action of metal-rich pore water by metal-poor bottom water due to dump events, storms, and tidal action can enhance the flux of interstitial metals.

Statistically significant differences in the mud content of peripheral cores relative to centrally located cores have ascertained that large scale differentiation of sediment takes place at the dumpsite. Laminated sediments and discrete beds of variable thickness are typical of the central part of the deposit which receives the bulk of direct dumping. Relatively undifferentiated, fine grained sediments are characteristic of the fringes of the deposit. We believe that most of the material deposited on the periphery of the deposit is the result of the movement of fine grained sediment after dumping. This material, settling slowly, is carried either by tidal currents or by the outward pulse generated by individual dumping events to be deposited away from the center of dumping activity.

There is not only movement of fine grained material away from dumping centers, but there is movement of sand onto the edges of the dumpsite deposit. Flaser-like bed forms composed of greensand, typical of erosion windows of the shelf proximal to the deposit, represent as much as 8% of the entire deposit. This sand, derived from surrounding areas, has been brought to the site as storm entrained sediment.

An overall stratigraphy of the deposit, defining the natural sediment basement and the various horizons of anthropogenic materials, has been developed. Sedimentation rates of various horizons have yielded ages that agree within a few percent of estimated times of deposition derived from dumping records.

## 8. ACKNOWLEDGEMENTS

We gratefully acknowledge the assistance of the officers and crew of the R/V ATLANTIC TWIN and R/V KELEZ during the sediment sampling and pore water chemistry cruises. We also thank H. Bokuniewicz and A.E. Cok for participating in the seismic reflection profiling and sediment sampling cruises, respectively. We thank W. O'Brien, N. Mohéban, B. Subramaniam, and R.J. Wilke for their help in the laboratory. We are particularly indebted to E. Quinn for typing this report and M.A. Lau for typing the first draft.

At Brookhaven National Laboratory, A. Beckwith, J.J. Fuhrmann, T.C. Kycia, and R. Lorenz assisted in the x-radiographic analysis of the sediment cores. We thank them for their help.

This work was supported by a research grant No. 0478B013 from the Marine Ecosystem Analysis Program of the National Oceanic and Atmospheric Administration and the New York District Office of the Army Corps of Engineers to R. Dayal and I.W. Duedall at the Marine Sciences Research Center, State University of New York at Stony Brook. We thank D. Goodrich and D. Suskowski for their comments. We also thank H. Stanford for his help in the completion of the project and G. Chu for proofreading the final report.

## 9. REFERENCES

- Anderson, J. (1974): A study of the digestion of sediment by the  $\text{HNO}_3\text{-H}_2\text{SO}_4$  and  $\text{HNO}_3\text{-HCl}$  procedures. *Atomic Absorption Newsletter*, 13:31-32.
- Berner, R.A. (1971): *Principles of Chemical Sedimentology*, McGraw-Hill, New York, 240 pp.
- Bouma, A.H. (1969): *Methods in the Study of Sedimentary Structures*, Wiley-Interscience, New York, 458 pp.
- Boyer, P.S., E.A. Guinness, M.A. Lynch-Blosse, and R.A. Stoleman (1977): Greensand fecal pellets from New Jersey. *Journal of Sedimentary Petrology*; 47:267-280.
- Bray, J.R., O.P. Bricker, and B.N. Troup (1973): Phosphate in interstitial water of anoxic sediments; oxidation effects during sampling procedure. *Science*, 180:1302-1364.
- Bricker, O.P., and B.N. Troup (1975): Sediment-water exchange in Chesapeake Bay. In: *Estuary Research 1, Chemistry, Biology and the Estuarine System*, (ed. L.E. Cronin), Academic Press, 3-27.
- Brooks, R.R., B.J. Presley, and I.R. Kaplan (1968): Trace elements in the interstitial waters of marine sediments. *Geochemica et Cosmochimica Acta*, 32:397-414.
- Bruland, K.W., K. Bertine, M. Koide, and E.D. Goldberg (1974): History of metal pollution in southern California coastal zone. *Environmental Science and Technology*, 5:425-432.
- Calvert, S.E. and N.B. Price (1972): Diffusion and reaction profiles of dissolved manganese in the pore water of marine sediments, *Earth and Planetary Science Letters*, 16:245-249.
- Carmody, D.J., J.B. Pearce, and W.B. Yasso (1973): Trace metals in sediments of New York Bight. *Marine Pollution Bulletin*, 4:132-135.
- Conner, W.G., D. Aurand, M. Leslie, J. Slaughter, A. Amir, and F.I. Rovenscroft (1979): Disposal of dredged material within the New York District: Volume 1, present practices and candidate alternatives. MITRE Tech. Report MTR-7808, The MITRE Corporation, McLean, Virginia.
- Duce, R.A., G.T. Wallace, and B.J. Ray (1976): Atmospheric trace metals over the New York Bight, NOAA Tech. Report ERL 361-MESA 4:17 pp.

- Elderfield, H. (1979): Manganese fluxes to the oceans. *Marine Chemistry*, 4:103-132.
- Elderfield, H. (1978): Chemical variability in estuaries. In: *Bio-geochemistry of Estuarine Sediments*, Proceedings of a UNESCO/SCOR workshop held in Melreux, Belgium, 171-178.
- Elderfield, H., and A. Hepworth (1975): Diagenesis, metals and pollution in estuaries. *Marine Pollution Bulletin*, 6:85-87.
- Emerson, S. (1976): Early diagenesis in anaerobic lake sediments: chemical equilibria in interstitial waters. *Geochimica et Cosmochimica Acta*, 40:925-934.
- Erlenkeuser, H., E. Seuss, and H. Willkomm (1974): Industrialization affects heavy metal and carbon isotope concentrations in recent Baltic Sea sediments. *Geochimica et Cosmochimica Acta*, 38-823-842.
- Folk, R.L. (1974): *Petrology of Sedimentary Rocks*, Hemphill's Publishing Company, Austin, Texas, 170 pp.
- Folk, R.L., and W.C. Ward (1957): Brazos River bar: a study in the significance of grain size parameters. *Journal of Sedimentary Petrology*, 27:3-27.
- Freeland, G.L., D.J.P. Swift, and R.A. Young (1979): Mud deposits near the New York Bight dumpsites: origin and behavior. In: *Ocean Dumping and Marine Pollution*, (eds. H.D. Palmer, and M.G. Gross), Dowden, Hutchinson and Ross, Stroudsburg, PA., 73-96.
- Freeland, G.L., and D.J.P. Swift (1978): *Surficial Sediments*. New York Bight Atlas Monograph 10, New York Sea Grant Institute, 93 pp.
- Freeland, G.L., and G.F. Merrill (1977): The 1973 bathymetric survey in the New York Bight apex: maps and geological implications. NOAA Tech. Memo. No. 19, ERL, MESA, Boulder, Colorado, 20 pp.
- Friedman, G.M. (1969): Address of the retiring president of the international association of sedimentologists: differences in size distributions of populations of particles among sands of various origins. *Sedimentology*, 26:3-32.
- Fuhrmann, M. (1980): Sedimentology of the New York Bight dredged material dumpsite deposit. M.S. Thesis, Adelphi University, 160 pp.
- Goldberg, E.D., E. Gamble, J.J. Griffin, and M. Koide (1977): Pollution history of Narragansett Bay as recorded in its sediments. *Estuarine and Coastal Marine Science*, 5:549-561.

- Gross, M.G. (1976): Sources of urban waste. In: *Middle Atlantic Continental shelf and the New York Bight*, (ed. M.G. Gross), American Society of Limnology and Oceanography, Special Symposium 2:150-161.
- Gross, M.G. (1976): *Waste Disposal*. New York Bight Atlas Monograph 26, New York Sea Grant Institute, Albany, New York, 32 pp.
- Gross, M.G. (1972): Geologic aspects of waste solids and marine waste deposits, New York metropolitan region. *Geological Society of America Bulletin*, 83:3163-3176.
- Gross, M.G. (1971): Carbon Determination. In: *Procedures in Sedimentary Petrology*, (ed. R.E. Carver), Wiley-Interscience, New York.
- Gross, M.G. (1970): Preliminary analysis of urban waste, New York metropolitan region. Tech. Report Series No. 5, Marine Sciences Research Center, State University of New York, Stony Brook, 33 pp.
- Heaton, M.G. (1978): Chemical aspects of hydraulic dredging and open-water pipeline disposal in estuaries. M.S. Thesis, Marine Sciences Research Center, State University of New York, Stony Brook, 127-128.
- Hem, J.D. (1972): Chemistry and occurrence of Cd and Zn in surface water and ground water. *Water Resources Research*, 8:661-679.
- Hoover, W.L., J.R. Melton, and P.A. Howard (1971): Determination of trace amounts of mercury in foods by flameless atomic absorption. *Journal Assoc. Official Anal. Chemists*, 54:860-865.
- Jackson, M.L. (1958): *Soil Chemical Analysis*, Prentice-Hall, Englewood Cliffs, New Jersey, 498 pp.
- Jones, C.R., C.T. Fray, and J.R. Schubel (1979): Textural properties of the surficial sediments of the lower bay of New York harbor. Marine Sciences Research Center, State University of New York, Stony Brook, Special Report 21: 113 pp.
- Li, Y.H., J. Bischoff, and G. Mathieu (1969): The migration of manganese in the Arctic Basin sediment. *Earth and Planetary Science Letters*, 7:265-270.
- Lindberg, S.E., and R.C. Harris (1974): Mercury-organic matter associations in estuarine sediments and interstitial water. *Environmental Science and Technology*, 8:459-462.
- Manheim, F.T. (1976): Interstitial waters of marine sediment. In: *Chemical Oceanography*, Volume 6, (eds. J.P. Riley and R. Chester), Academic Press, N.Y., 115-178.

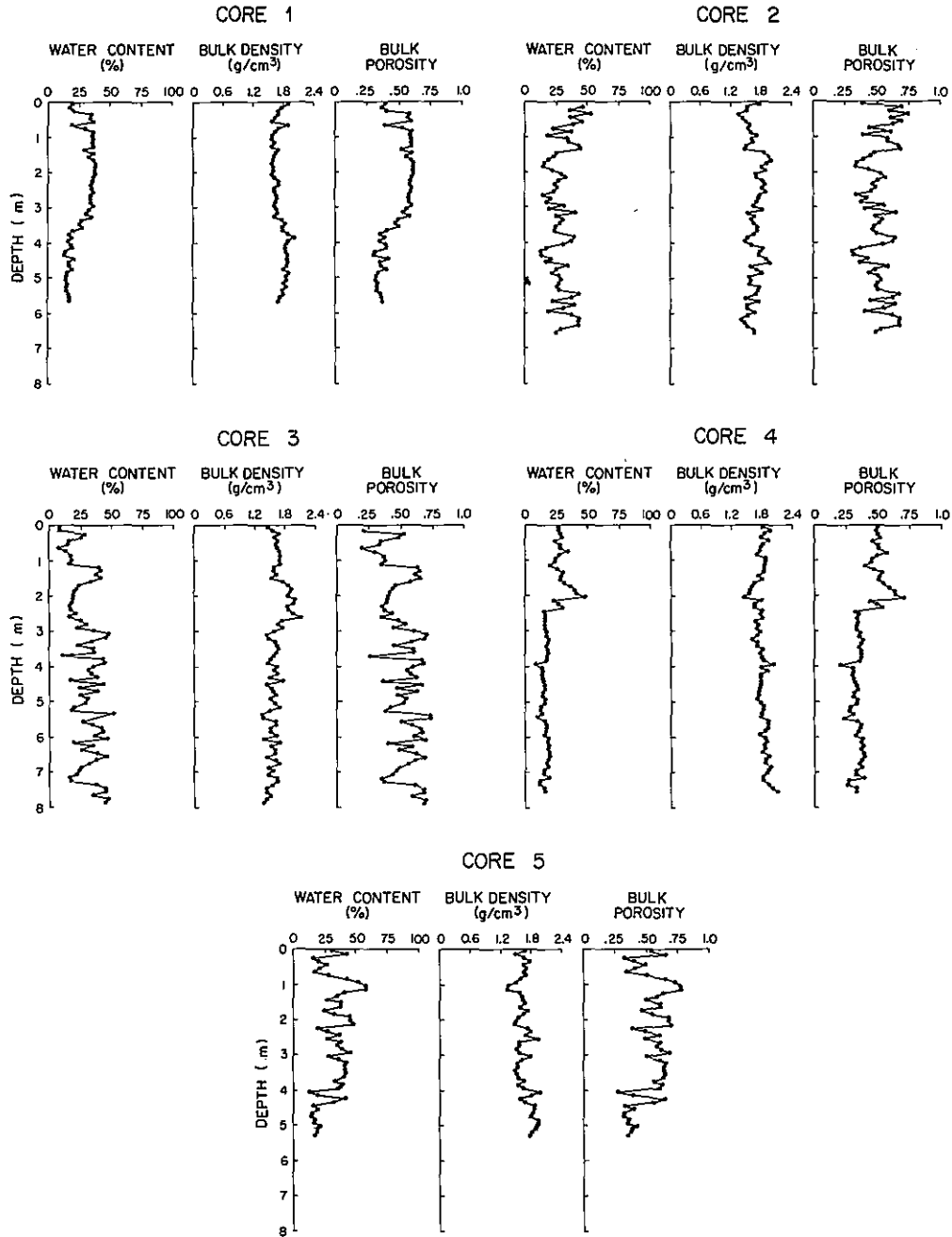
- Marine Sciences Research Center (1978): Aquatic disposal field investigations Eaton's Neck disposal sites Long Island Sound. Army Corps of Engineers Dredged Material Research Program, Tech. Report D-77-6: 322 pp.
- Martens, C.S., R.A. Berner, and J.K. Rosenfeld (1978): Interstitial water chemistry of anoxic Long Island Sound sediment, 2. Nutrient regeneration and phosphate removal. *Limnology and Oceanography*, 23:605-617.
- McCrone, A.W. (1967): The Hudson River Estuary: sedimentary and geochemical properties between Kingston and Haverstraw, New York. *Journal of Sedimentary Petrology*, 37:475-486.
- Meade, R.H. (1972): Sources and sinks of suspended matter on continental shelves. In: *Shelf Sediment Transport: Processes and Patterns*, (ed. D.J. Swift), Dowden, Hutchinson and Ross, Inc., Stroudsburg, Pa., 249-262.
- Mueller, J.A., J.S. Jeris, A.R. Anderson, and C.F. Hughes (1976): Contaminant inputs to the New York Bight. NOAA Tech. Memo. No. 6, MESA, Boulder, Colorado, 347 pp.
- Nissenbaum, A., and D.J. Swaine (1976): Organic Matter-metal interactions in recent sediments: the role of humic substances. *Geochimica et Cosmochimica Acta*, 40:809-816.
- Oertel, G.F. (1973): Examination of textures and structures of mud in layered sediments at the entrance of a Georgia tidal inlet, *Journal of Sedimentary Petrology*, 43:33-41.
- Olsen, C.R., H.J. Simpson, R.F. Bopp, S.C. Williams, T.H. Peng, and B.L. Deck (1978): A geochemical analysis of the sediments and sedimentation in the Hudson Estuary. *Journal of Sedimentary Petrology*, 2:401-418.
- Panuzio, F.L. (1965): Lower Hudson River siltation. In: *Proceedings of the Federal Interagency Sedimentation Conference*, Agricultural Research Service Miscellaneous Report 970: 512-550.
- Pearce, J., J. Caracciolo, M. Halsey, and L. Rogers (1976): Temporal and spatial distributions of benthic macro-invertebrates in the New York Bight. In: *Middle Atlantic Continental Shelf and the New York Bight*. (ed. M.G. Gross), American Society of Limnology and Oceanography, Special Symposium 2: 394-403.
- Perkin Elmer Corporation (1978): Analytical methods using the MHS mercury/hydride system, Perkin Elmer Corp., Überlingen, West Germany.

- Presley, B.J., Y. Kolodny, A. Nissenbaum, and I.R. Kaplan (1972): Early diagenesis in a reducing fjord, Saanich Inlet, British Columbia, 1. Trace element distribution in interstitial water and sediment. *Geochimica et Cosmochimica Acta*, 36:1073-1090.
- Proni, J.R., R. Murkerji, D. Kester, and D. Hansen (1980): Acoustical observations of dumped dredged material dispersion in the New York Bight. Presented at 2nd International Ocean Dumping Symposium, Woods Hole, Mass., April, 1980.
- Rashid, M.A. and J.D. Leonard (1972): Modifications in the solubility and precipitation behavior of various metals as result of their interaction with sedimentary humic acid. *Chemical Geology*, 11:89-97.
- Reeburgh, W.S. (1967): An improved interstitial water sampler. *Limnology and Oceanography*, 12:163-167.
- Reimers, R.S., W.D. Burrows, and P.A. Krenke (1973): Total mercury analysis: review and critique, *Journal of Water Pollution Control Federation*, 1:814-828.
- Reineck, H.E. and I.B. Singh (1973): *Depositional Sedimentary Environments*. Springer-Verlag, New York, 439 pp.
- Ries, H., H.B. Kimmel, and G.M. Knapp (1904): The clays and clay industries of New Jersey. Volume VI of the final report of the state geologist, Geological Survey of New Jersey, Trenton, N.J., 569 pp.
- Royse, C.F. (1970): *An Introduction to Sediment Analysis*, Arizona State University, 112 pp.
- Sanders, J.G. (1978): The sources of dissolved manganese to Calico Creek, North Carolina. *Estuarine and Coastal Marine Science*, 6:231-238.
- Segar, D.A. and A. Cantillo (1976): Trace metals in the New York Bight. In: *Middle Atlantic Continental Shelf and the New York Bight*, (ed. M.G. Gross), American Society of Limnology and Oceanography, Special Symposium 2:171-198.
- Stubblefield, W.L. R.W. Permenter, and D.J.P. Swift (1977): Time and space variation in the surficial sediments of the New York Bight apex. *Estuarine and Coastal Marine Science*, 5:597-607.
- Swift, D.J., G.L. Freeland, P.E. Gadd, G. Han, J.W. Lavelle, and W.L. Stubblefield (1976): Morphologic evolution and coastal sand transport, New York-New Jersey shelf. In: *Middle Atlantic Continental Shelf and the New York Bight*, (ed. M.G. Gross), American Society of Limnology and Oceanography, Special Symposium 2:69-89.

- Troup, B.N., O.P. Bricker, and J.T. Bray (1974): Oxidation effects on the analysis of iron in interstitial water of recent anoxic sediments. *Nature*, 249:237-239.
- Ure, A.M. and C.A. Shand (1974): The determination of mercury in soils and related materials by cold vapour atomic absorption spectrometry. *Analytica Chimica Acta*, 72:63-67.
- Willey, J.D. (1977) Coprecipitation of zinc with silica in seawater and in distilled water. *Marine Chemistry*, 5:267-290.
- Williams, S.J. and D.B. Duane (1974): Geomorphology and sediments of the inner New York Bight continental shelf. Tech. Memo. No. 45, U.S. Army Corps Eng. Coastal Eng. Res. Center, 81 pp.
- Williams, S.J., H.J. Simpson, C.R. Olsen, and R.F. Bopp (1978): Sources of heavy metals in sediments of the Hudson River Estuary. *Marine Chemistry*, 6:195-213.

APPENDIX A

A-1. DEPTH PROFILES OF WATER CONTENT, BULK DENSITY, AND BULK POROSITY  
IN CORES 1, 2, 3, 4, AND 5.



A-2. DEPTH PROFILES OF WATER CONTENT, BULK DENSITY, AND BULK POROSITY  
IN CORES 6, 7, 8, 9, AND 10.

